Evolution of circumstellar disks and planet formation

Wladimir (Wlad) Lyra
Sagan Fellow

Caltech - JPL

João Alves (Vienna), Axel Brandenburg (Stockholm), Mario Flock (Paris), Saavik Ford (NYC), Sebastien Fromang (Paris), Bengt Gustafsson (Uppsala), Anders Johansen (Lund), Tobias Heinemann (KITP), Hubert Klahr (Heidelberg), Marc Kuchner (Goddard), Min-Kai Lin (CITA), Mordecai Mac Low (AMNH), Barry McKernan (NYC), Colin McNally (NBI), Sijme-Jan Paardekooper (Cambridge), Bob Pappalardo (JPL), Nikolai Piskunov (Uppsala), Natalie Raettig (Heidelberg), Zsolt Sándor (Budapest), Leo Sattler (Berkeley/UFRJ), Neal Turner (JPL), Steve Vance (JPL), Andras Zsom (MIT).

California State Uniiversity Northridge (CSUN)
Feb 13th, 2015

Outline

- Part I: Primordial disks
    - Turbulence and accretion: “active” and “dead” zones
    - Planet formation
    - Observational constraints

- Part II: Debris disks
    - Photoelectric instability

Protoplanetary Disks

PP disk fact sheet

Density: $10^{13} – 10^{15}$ cm^{-3}
(Air: 10^{21} cm^{-3})

Temperature: 10-1000 K

Scale: 0.1-100AU
(1 AU = 1.49×10^{13} cm)

Mass: $10^{-3} – 10^{-1}$ M_{sun}
(1 M_{sun} = 2×10^{33} g)

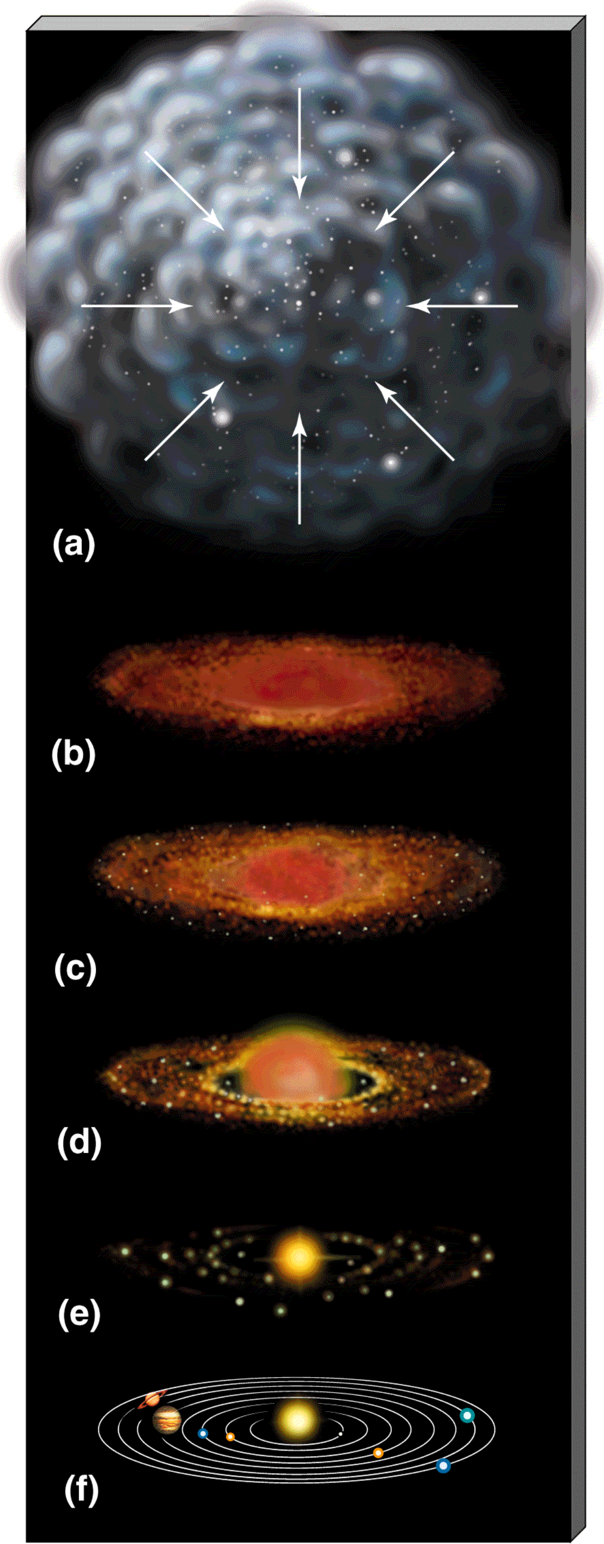

A disk life story

Gas-rich phase (< 10 Myr)
Primordial Disks

Thinning phase (~10 Myr)
Transitional Disks

Gas-poor phase (>10 Myr)
Debris Disks

Accretion in disks occurs via turbulent viscosity

Turbulence in disks is enabled by
the Magneto-Rotational Instability

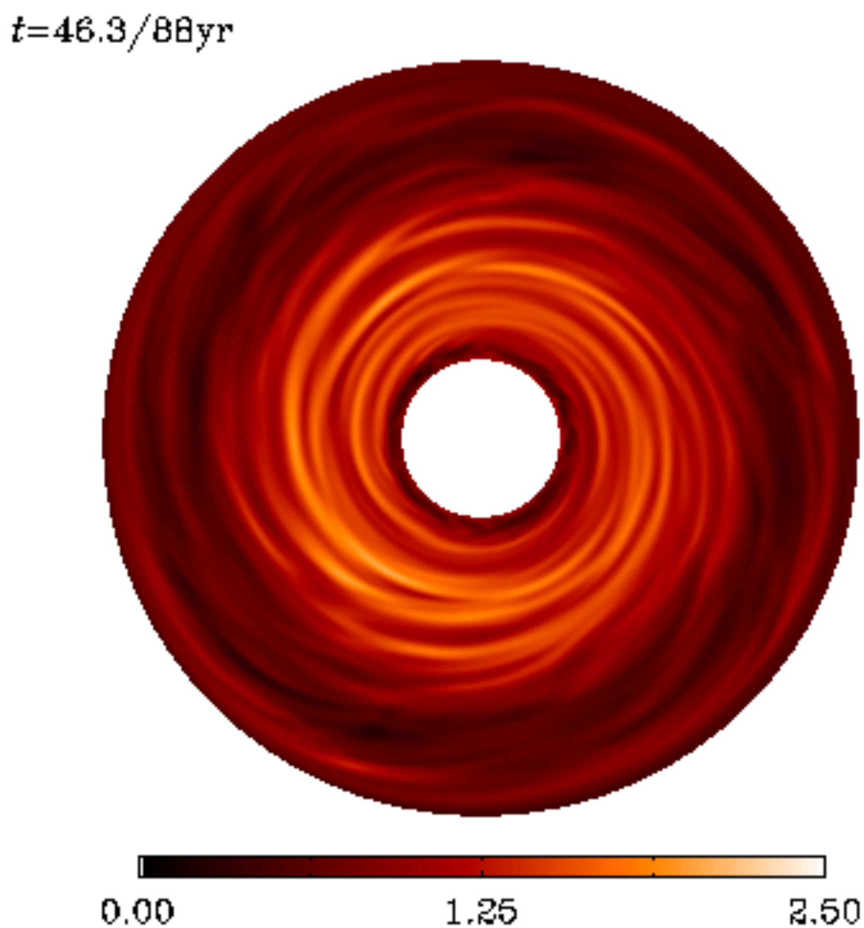

Magnetized disk
Lyra et al. (2008a)

MRI sketch

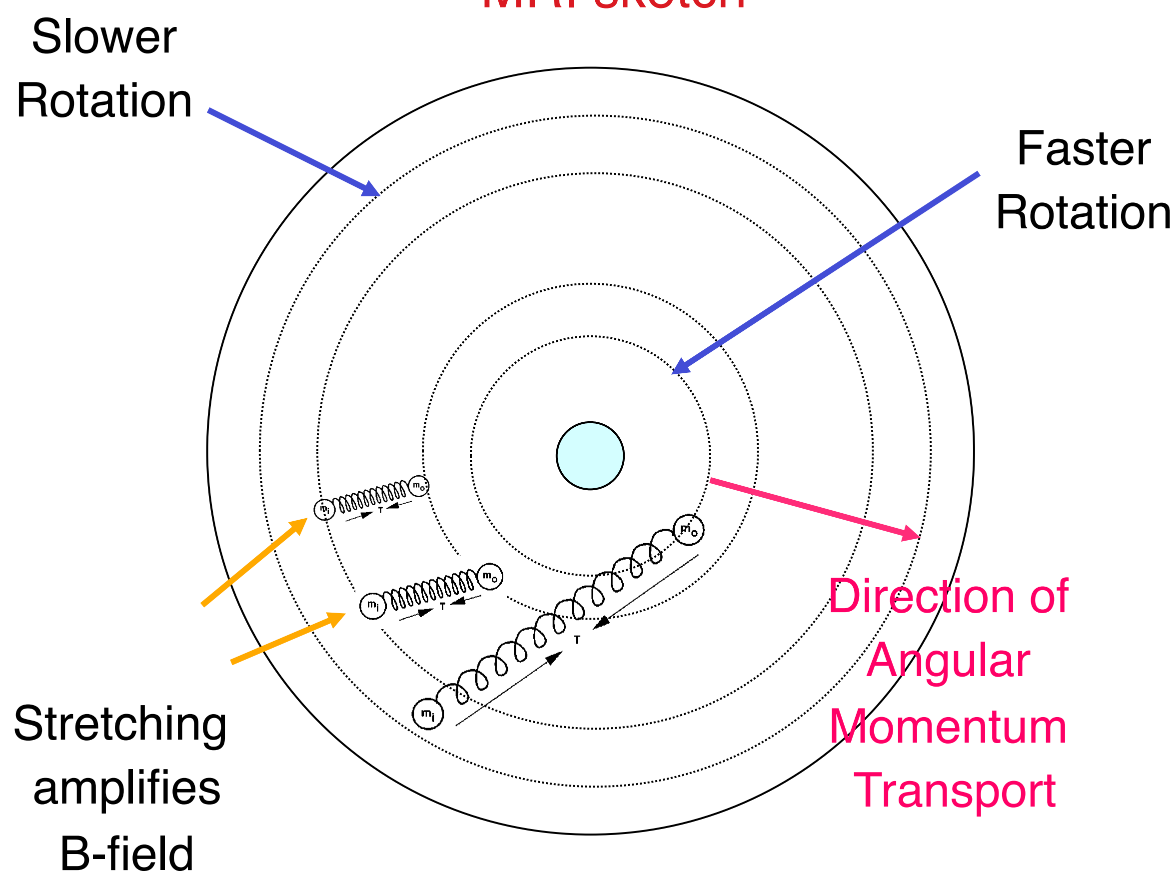

Unstable if angular velocity decreases outward

Accretion in disks occurs via turbulent viscosity

Turbulence in disks is enabled by
the Magneto-Rotational Instability

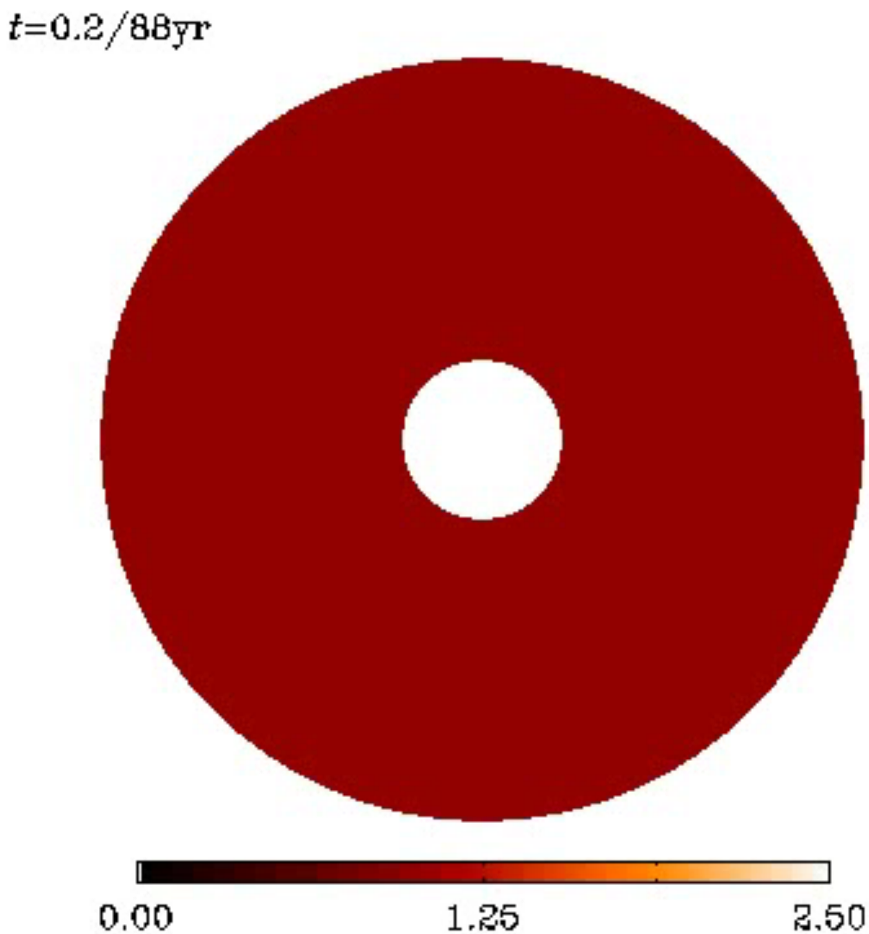

Magnetized disk
Lyra et al. (2008a)

MRI sketch

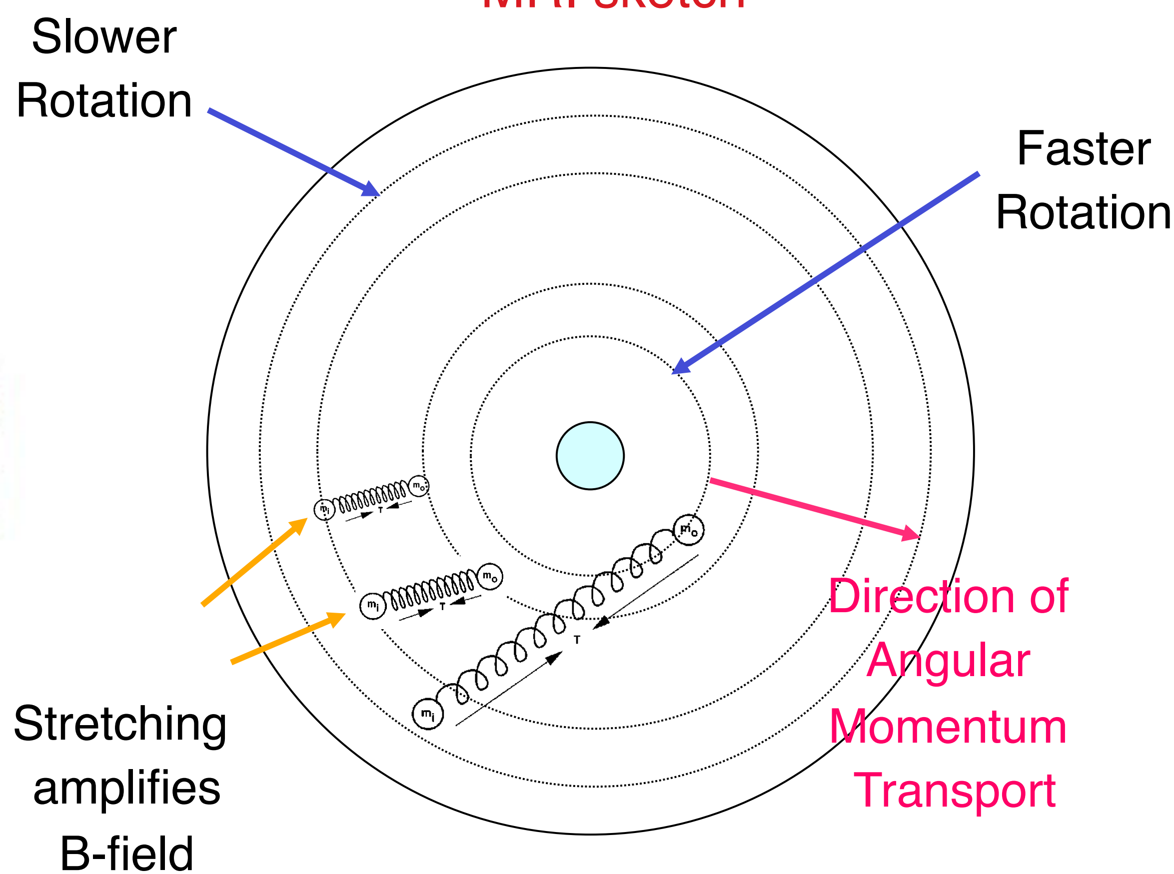

Unstable if angular
velocity decreases
outward

Particle drift

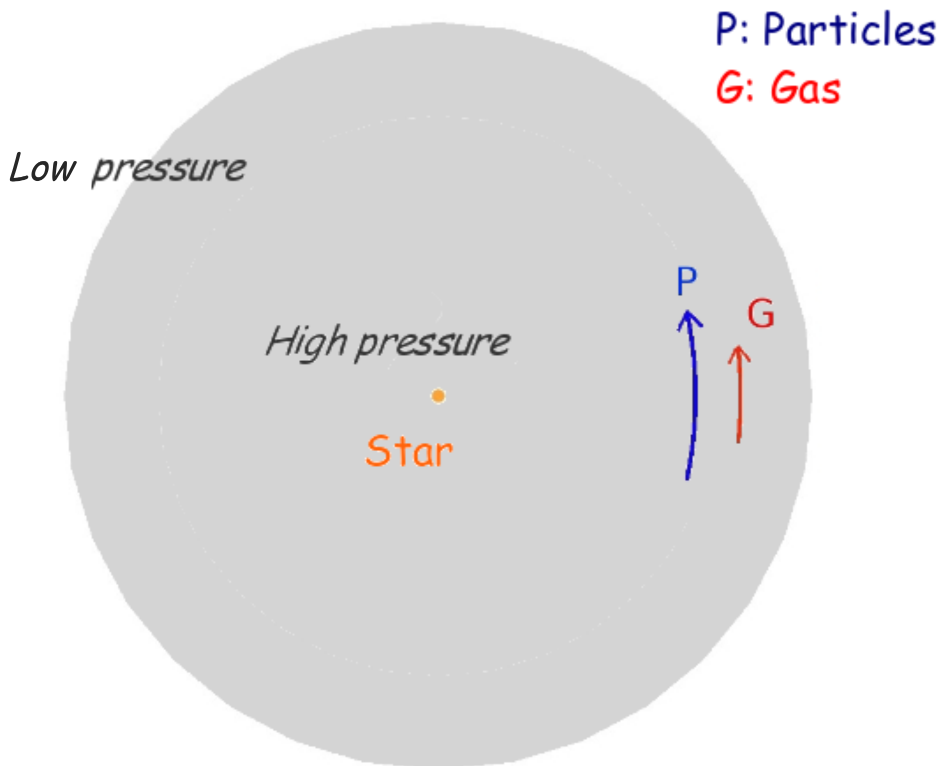

Adapted from Whipple (1972)

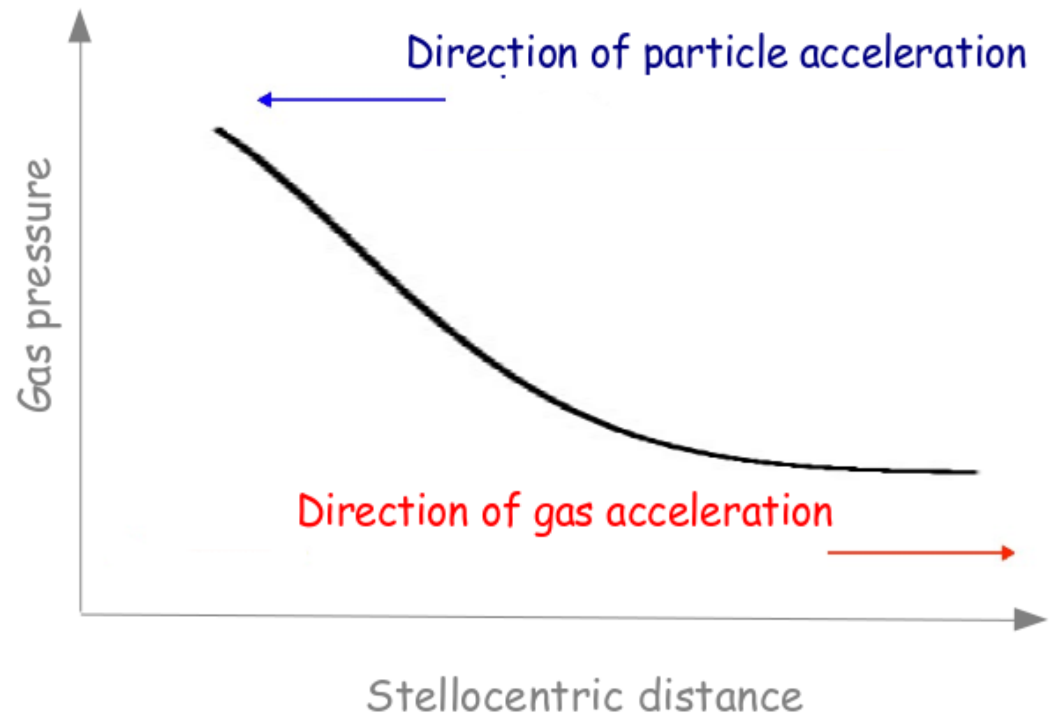

Pressure Trap

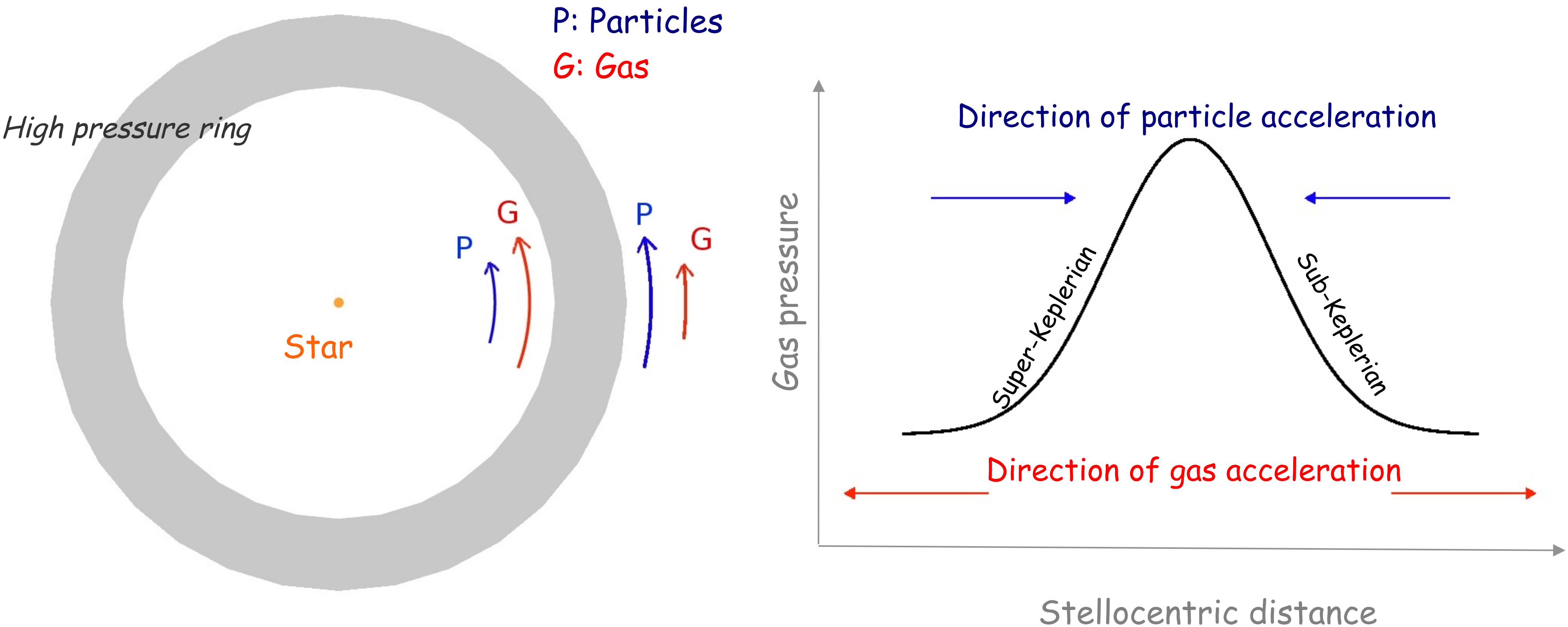

Adapted from Whipple (1972)

Pressure Trap

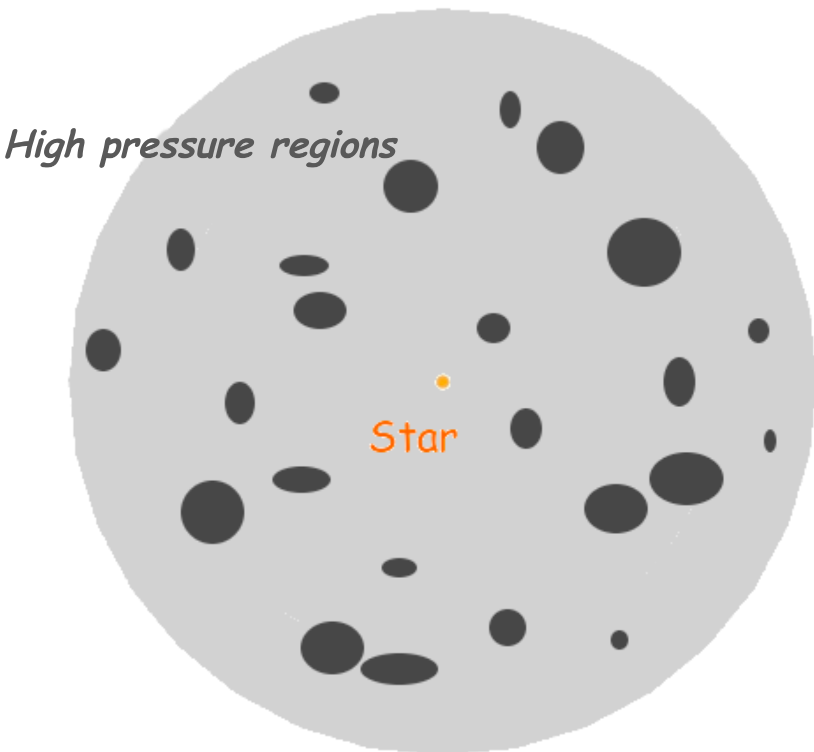

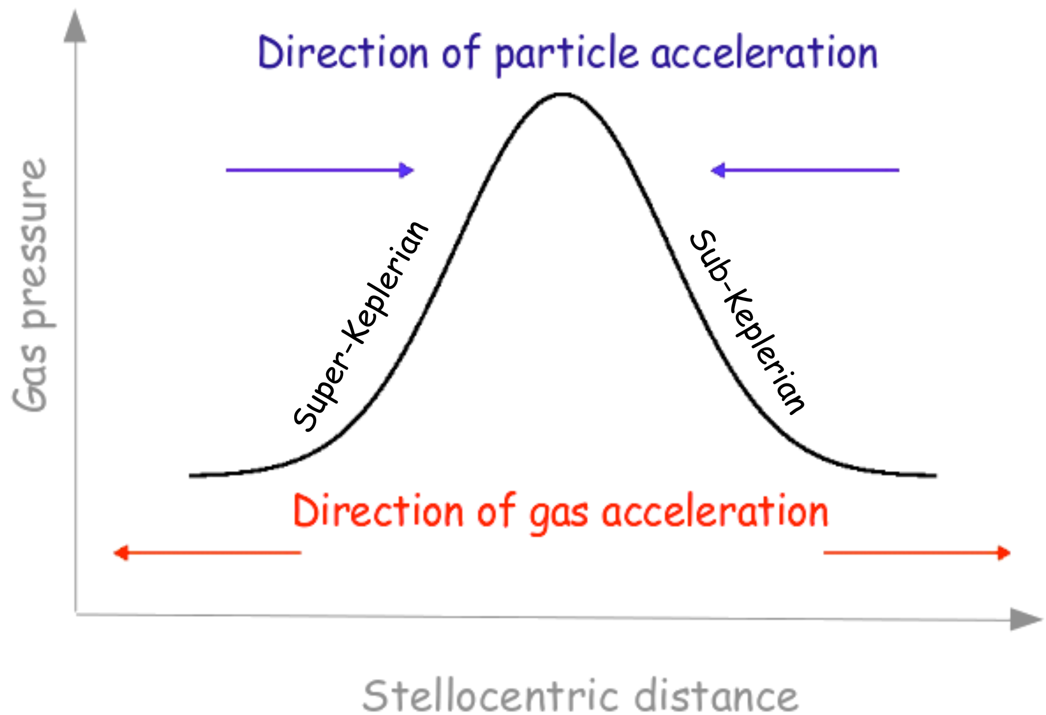

Turbulence concentrates solids mechanically in pressure maxima

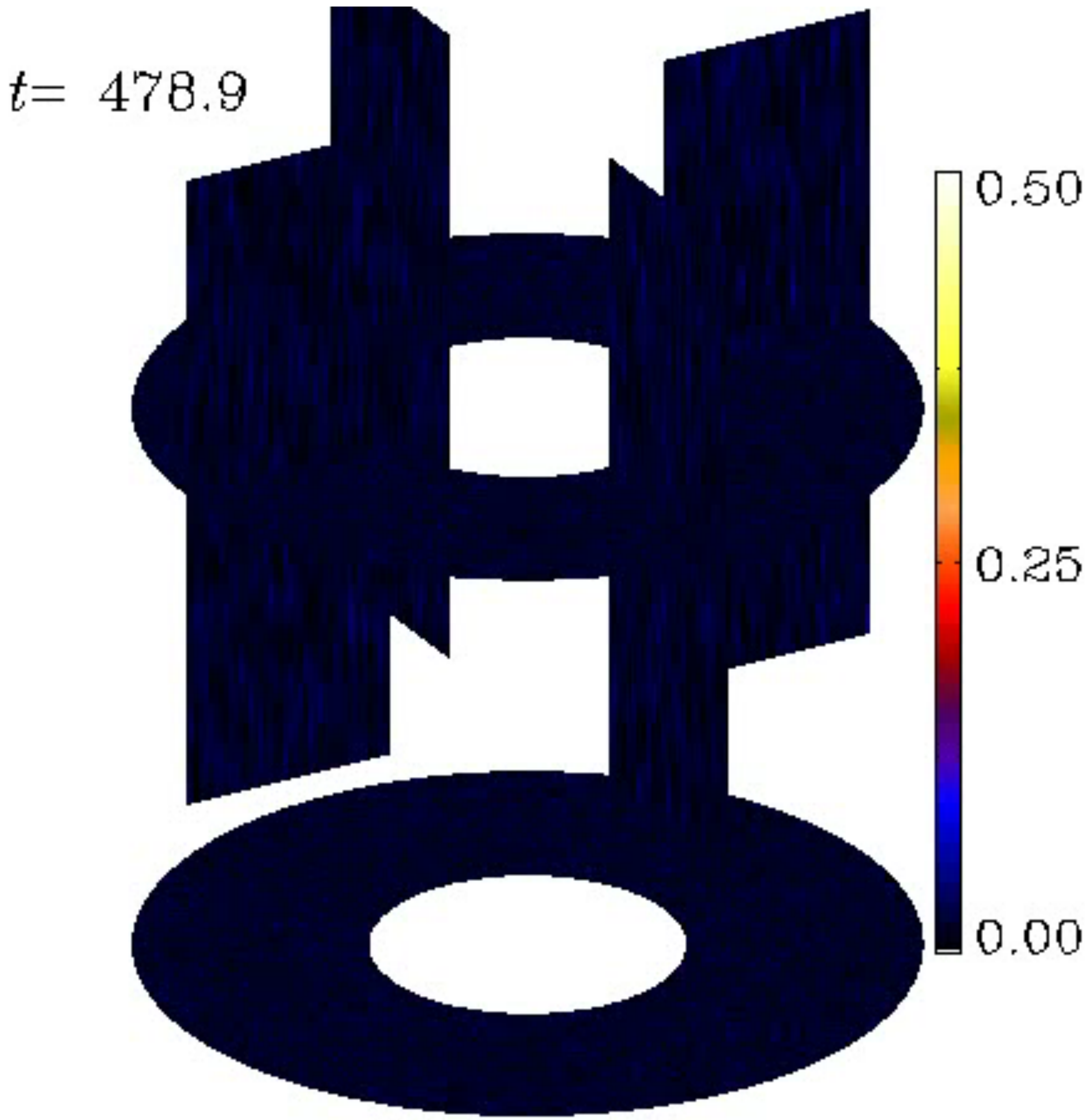

Lyra et al. (2008a)

Gravitational collapse into asteroid-mass objects

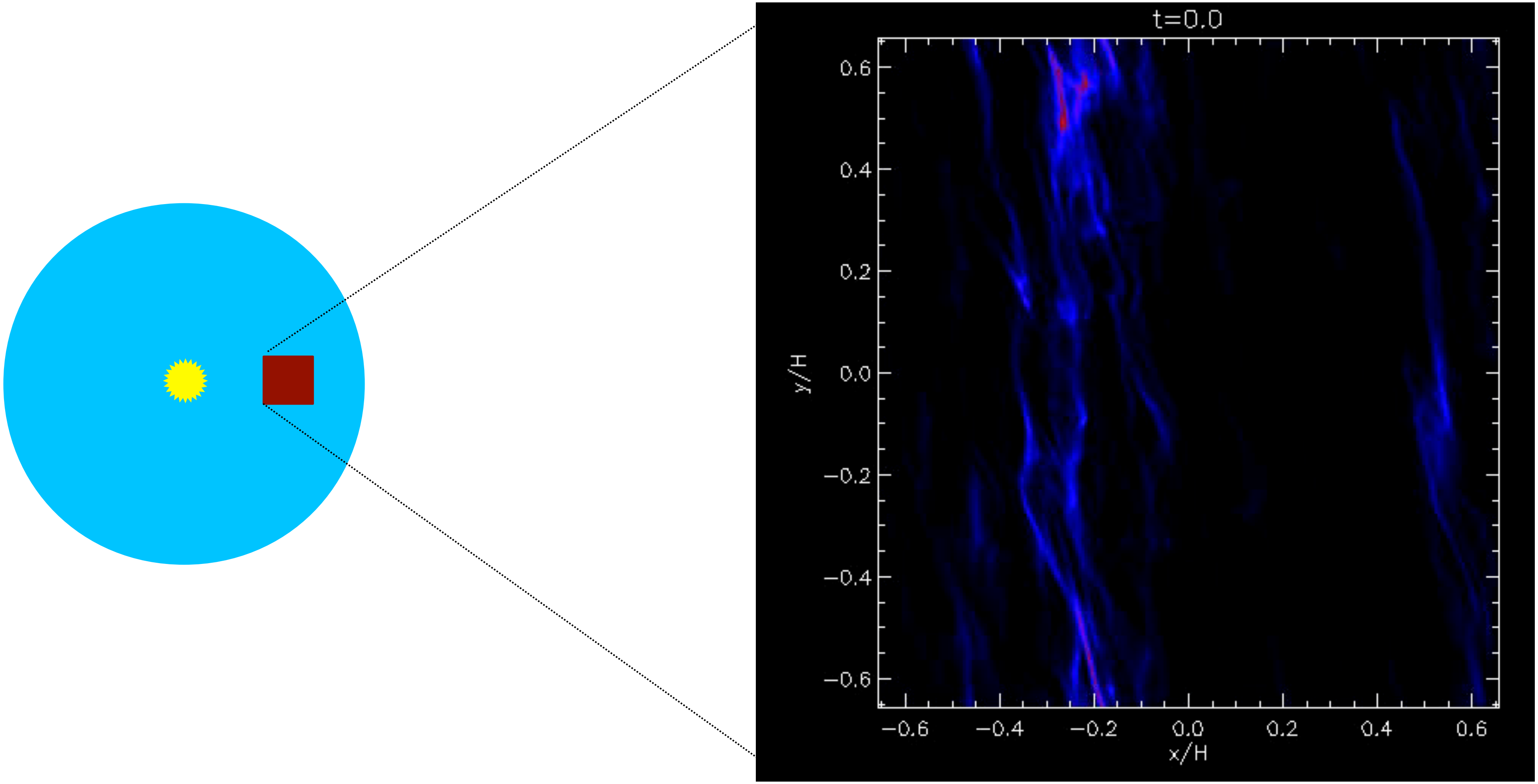

Johansen et al. (2007)

Dead zones are robust features of protoplanetary disks

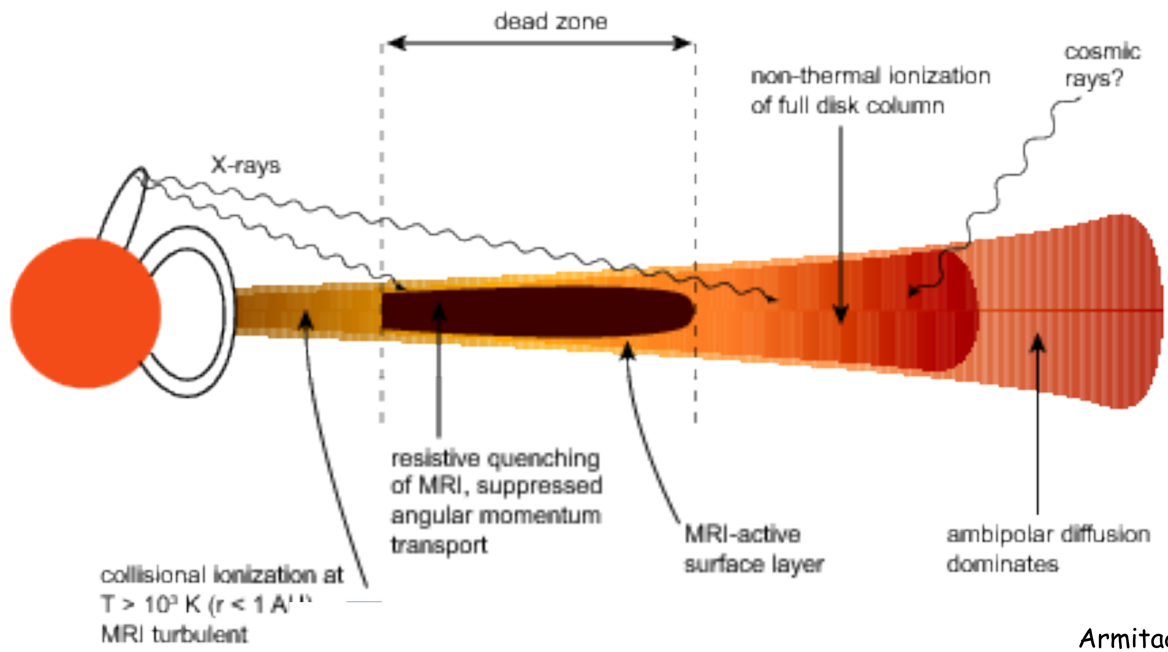

Armitage (2010)

Disks are cold and thus poorly ionized
(Blaes & Balbus 1994)

Therefore, accretion is **layered**
(Gammie 1996)

There should be a **magnetized, active zone**,
and a **non-magnetic, dead zone.**

Inner Active/Dead zone boundary

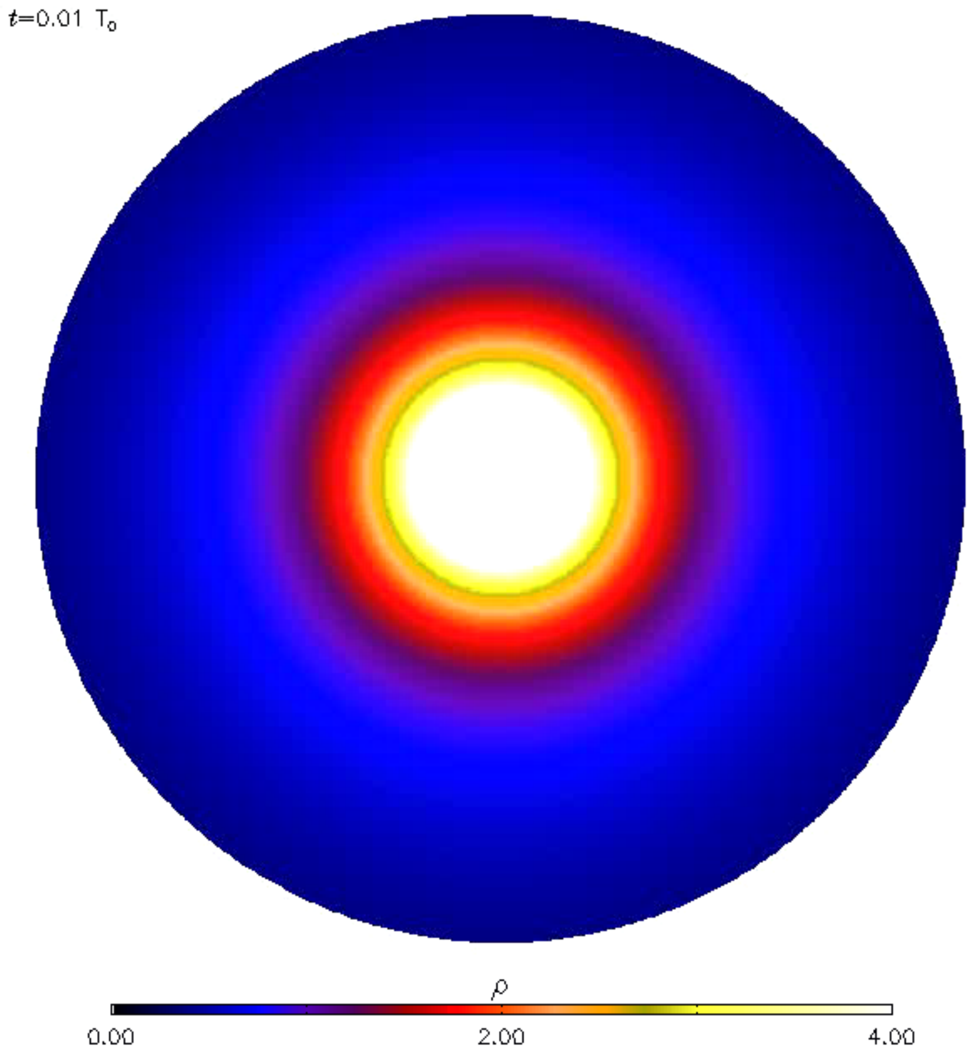

Magnetized inner disk + resistive outer disk

Lyra & Mac Low (2012)

Outer Dead/Active zone transition

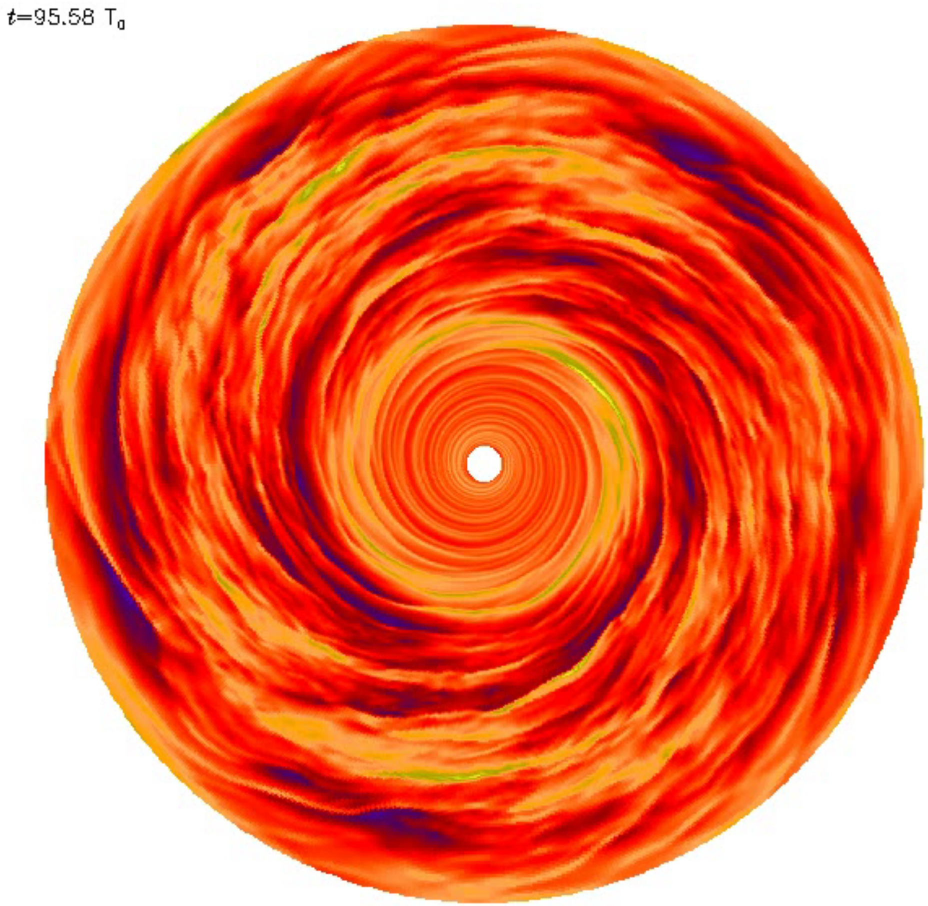

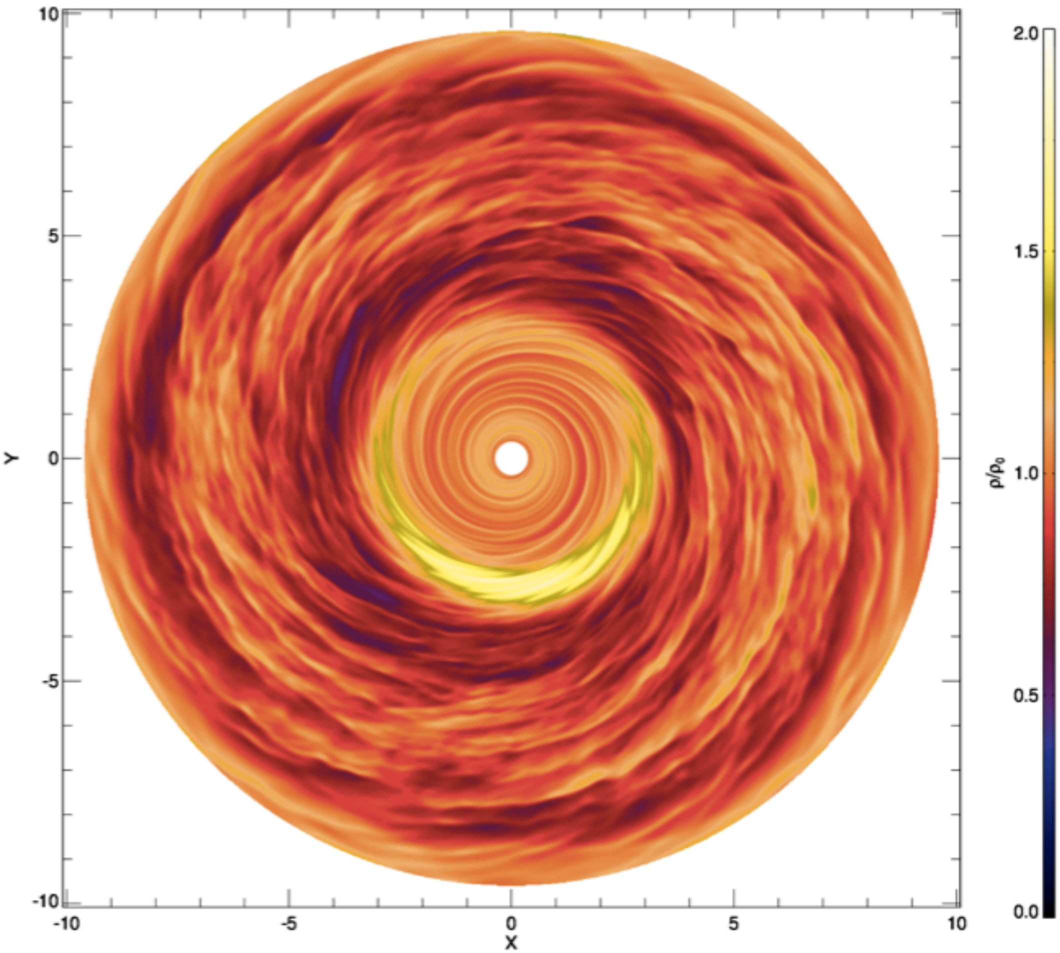

Resistive inner disk + magnetized outer disk

Lyra et al (2015)

Vortices – an ubiquitous fluid mechanics phenomenon

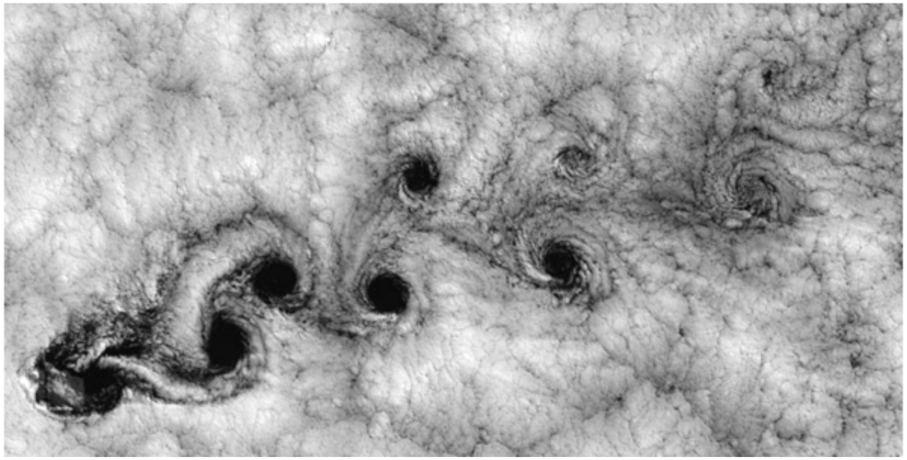

Vortices – an ubiquitous fluid mechanics phenomenon

Von Kármán *vortex street*

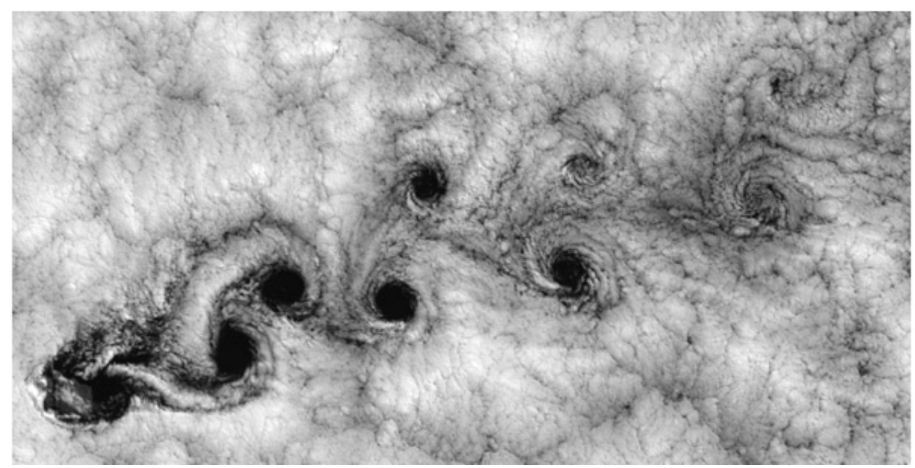

Rossby Wave Instability
(or.... Kelvin-Helmholtz in rotating disks)

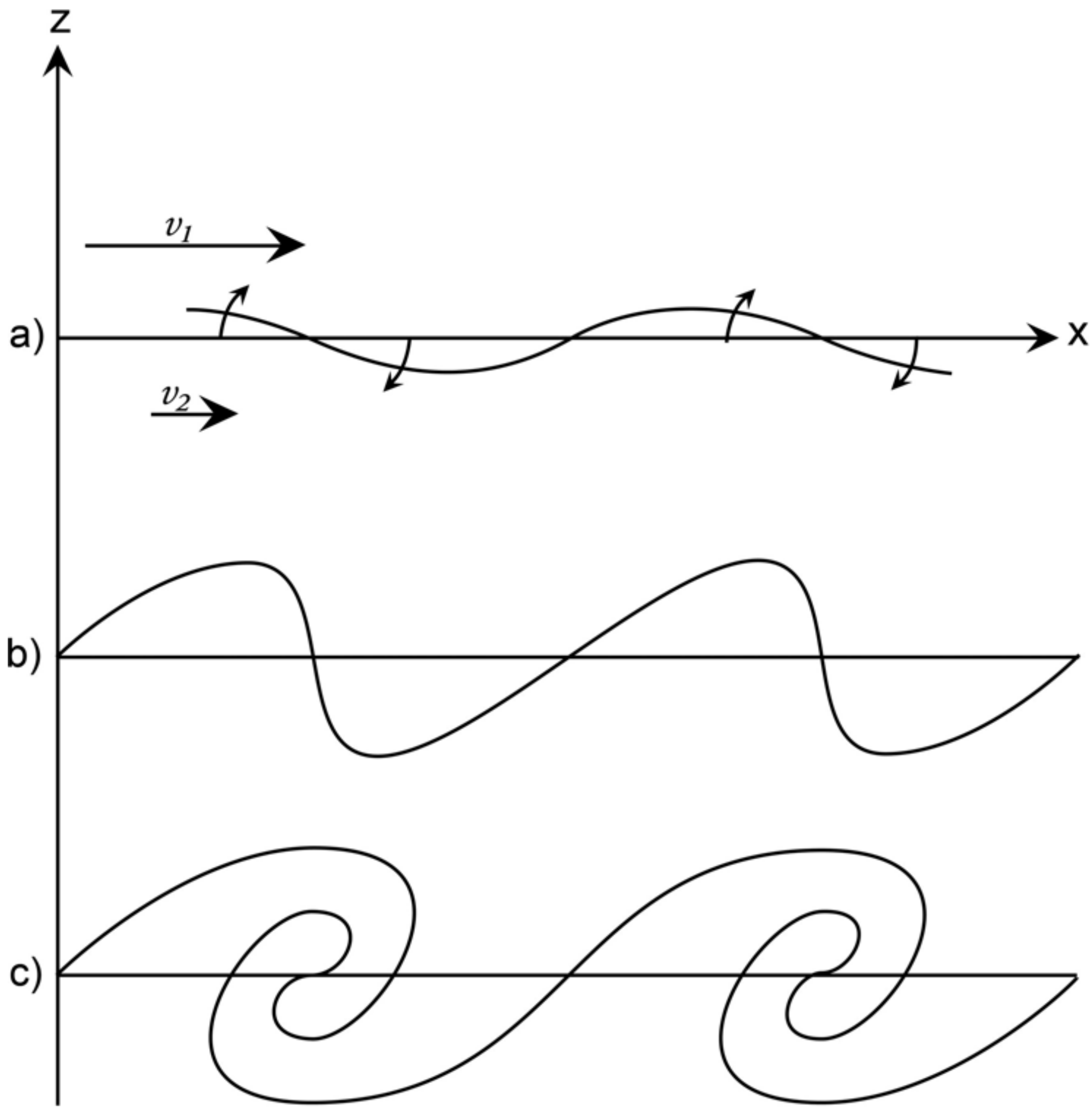

Active/dead zone boundary

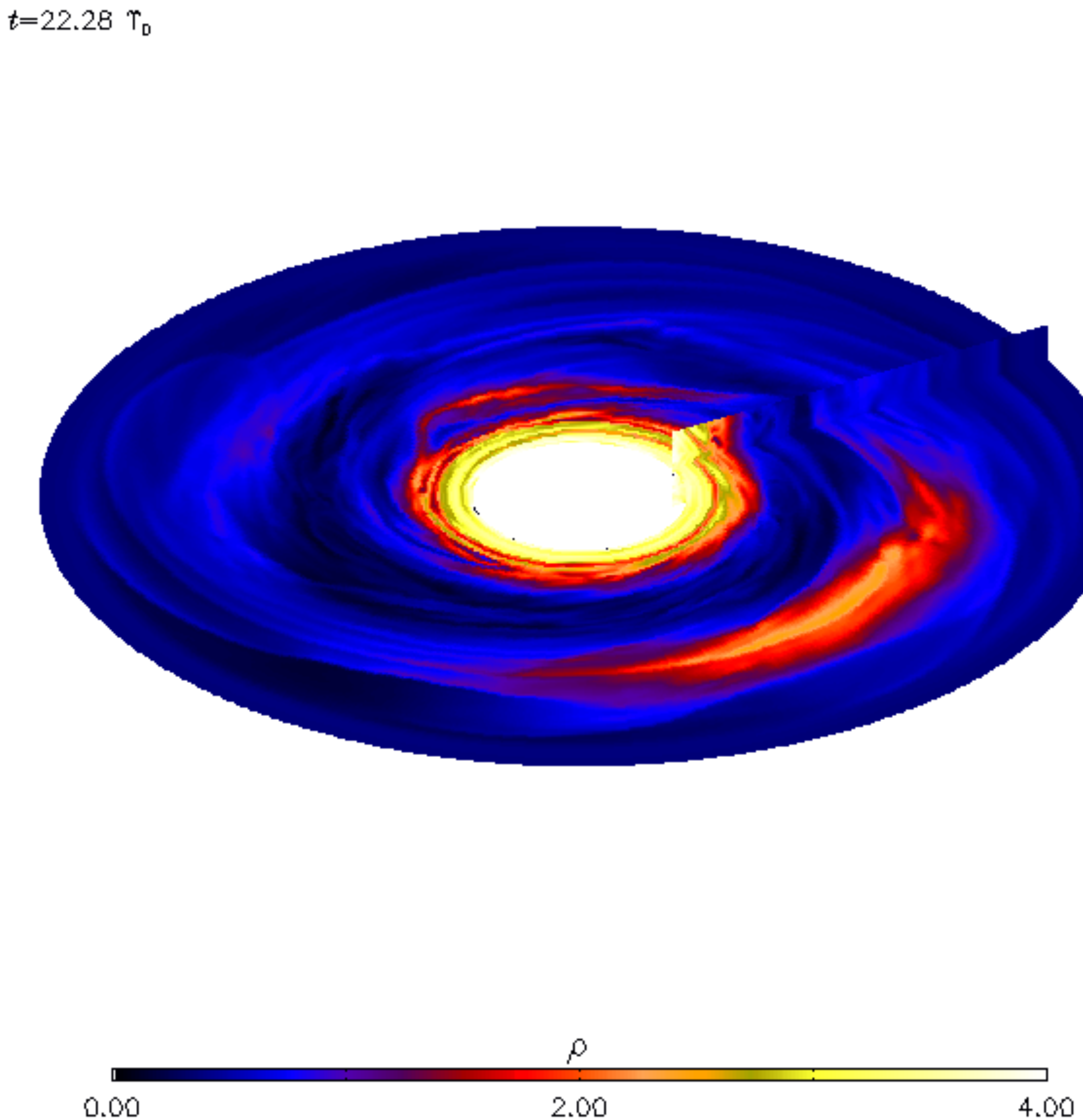

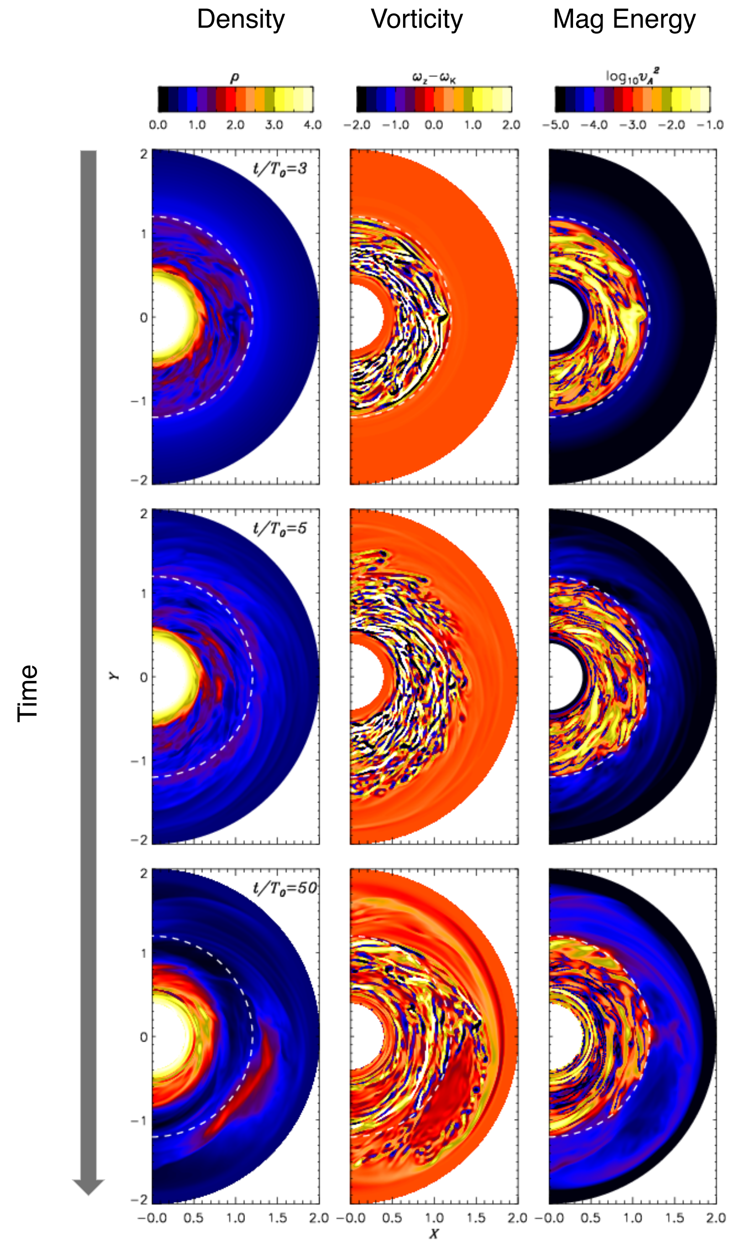

Magnetized inner disk + resistive outer disk

Lyra & Mac Low (2012)

The Tea-Leaf effect

Geostrophic balance:

$$2\Omega \times \boldsymbol{u} = -\rho^{-1} \nabla p$$

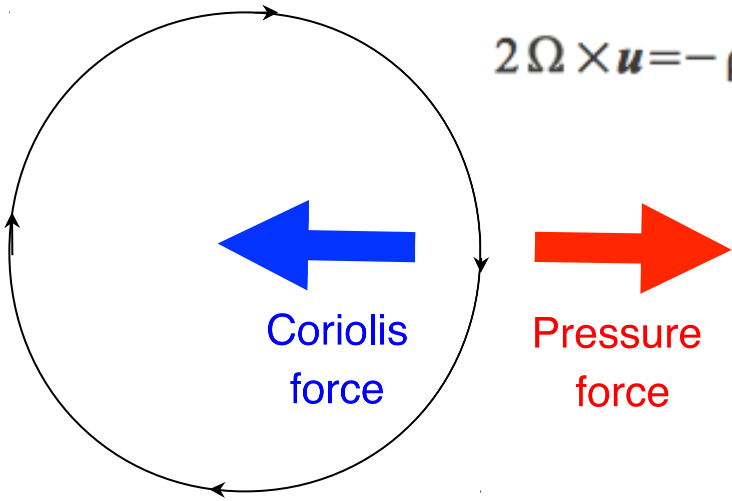

Vortex
streamline

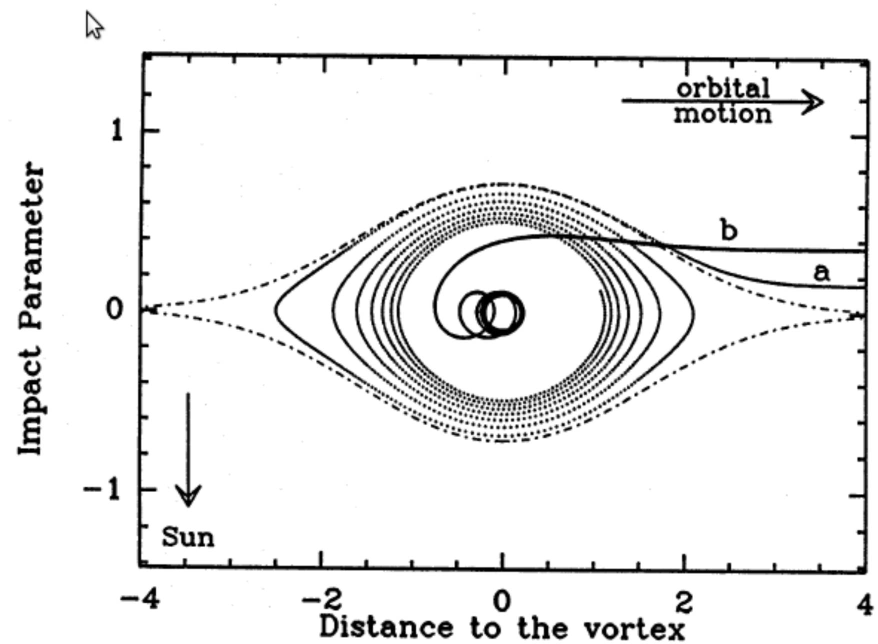

Barge & Sommeria (1995)

Particles do not feel the pressure gradient.
They sink towards the center, where they accumulate.

Aid to planet formation

(Barge & Sommeria 1995, Adams & Watkins 1996, Tanga et al. 1996)

Speed up planet formation enormously

(Lyra et al. 2008b, 2009ab, Raettig et al. 2012)

The Tea-Leaf effect

Geostrophic balance:

$$2\Omega \times \boldsymbol{u} = -\rho^{-1}\nabla p$$

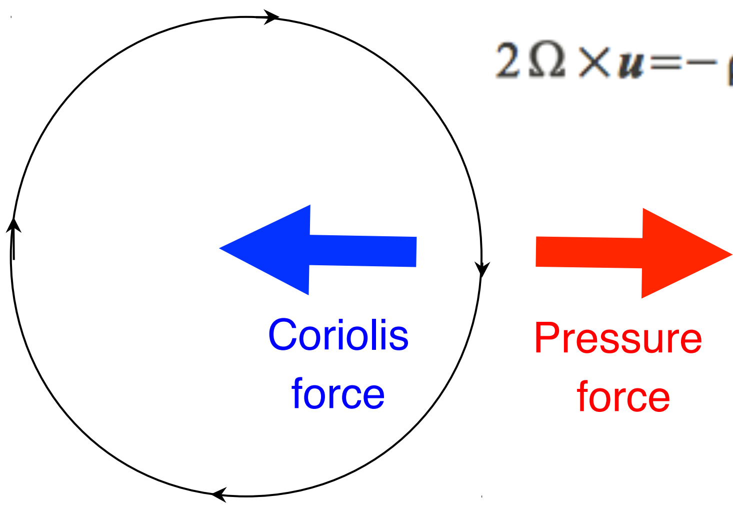

Vortex streamline

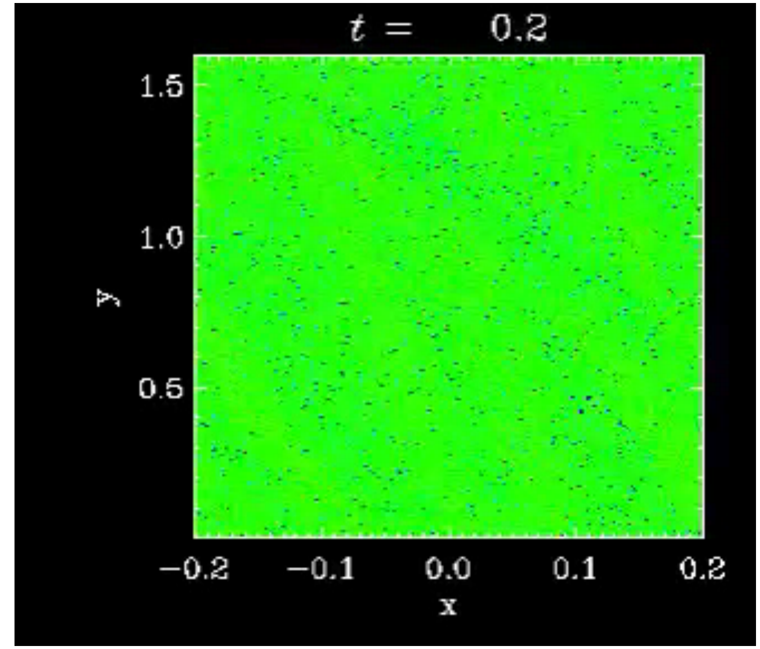

Raettig et al. (2012, 2015)

Particles do not feel the pressure gradient.
They sink towards the center, where they accumulate.

Aid to planet formation

(Barge & Sommeria 1995, Adams & Watkins 1996, Tanga et al. 1996)

Speed up planet formation enormously

(Lyra et al. 2008b, 2009ab, Raettig et al. 2012, 2015)

Vortices and Planet Formation

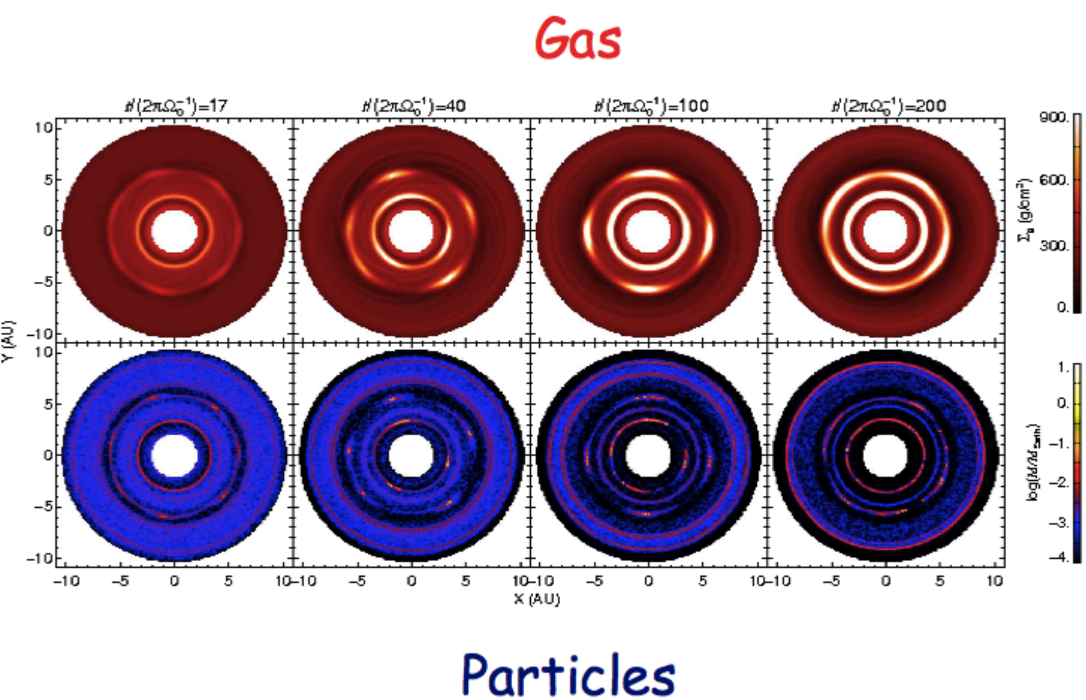

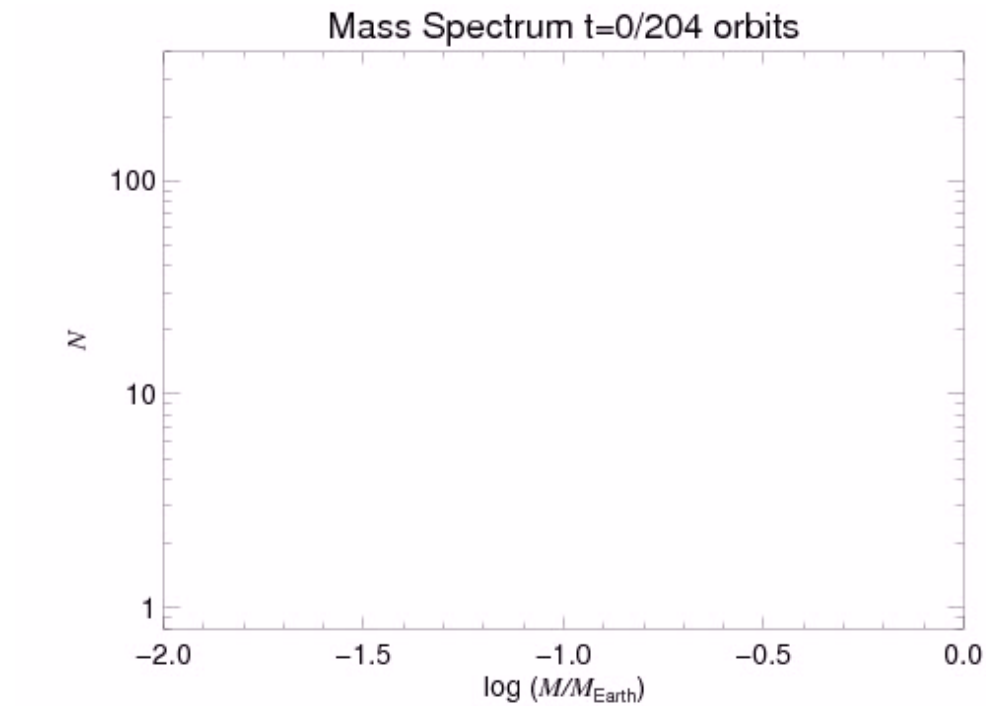

Collapse into Mars mass objects

(Lyra et al. 2008b, 2009a,
see also Lambrechts & Johansen 2012)

Vortices and Planet Formation

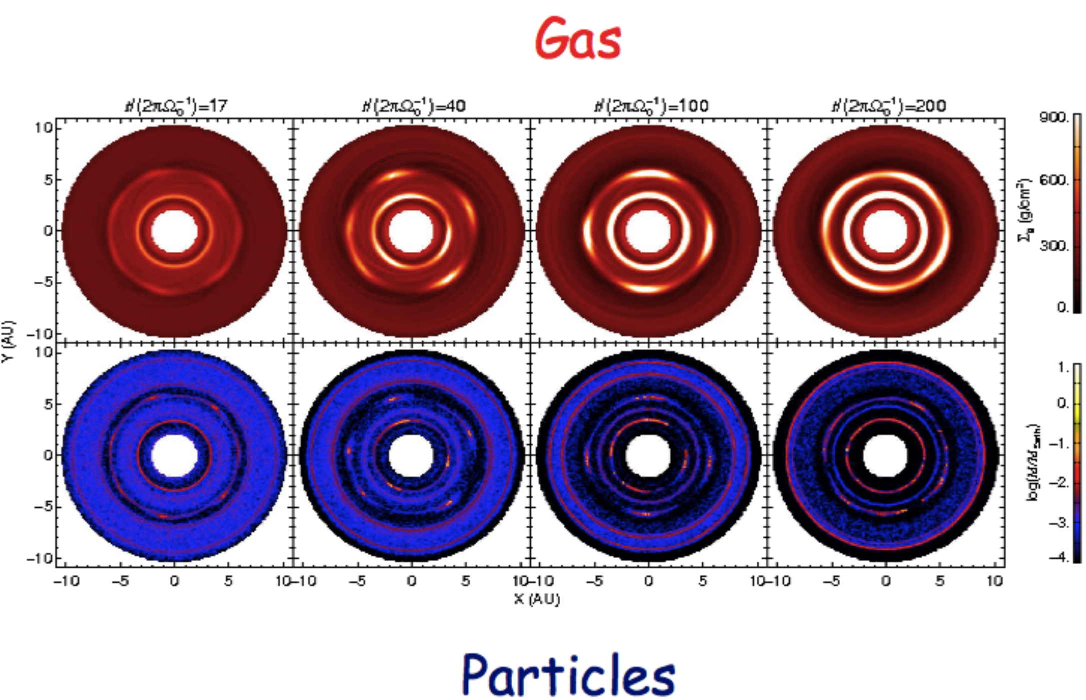

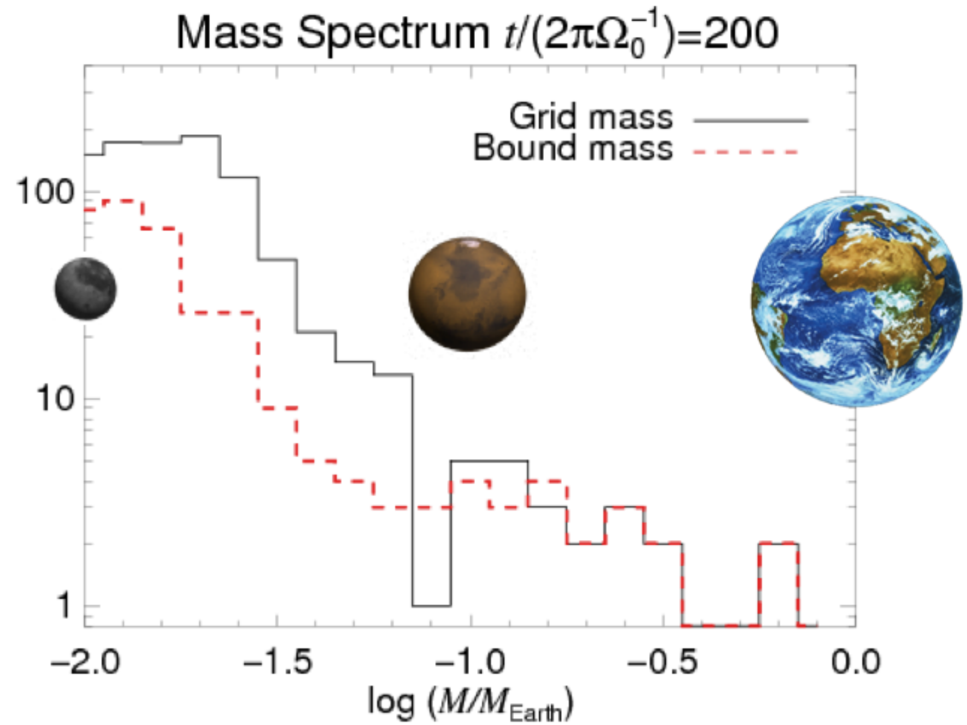

Collapse into Mars mass objects

(Lyra et al. 2008b, 2009a,
see also Lambrechts & Johansen 2012)

Rapid formation of planetary cores

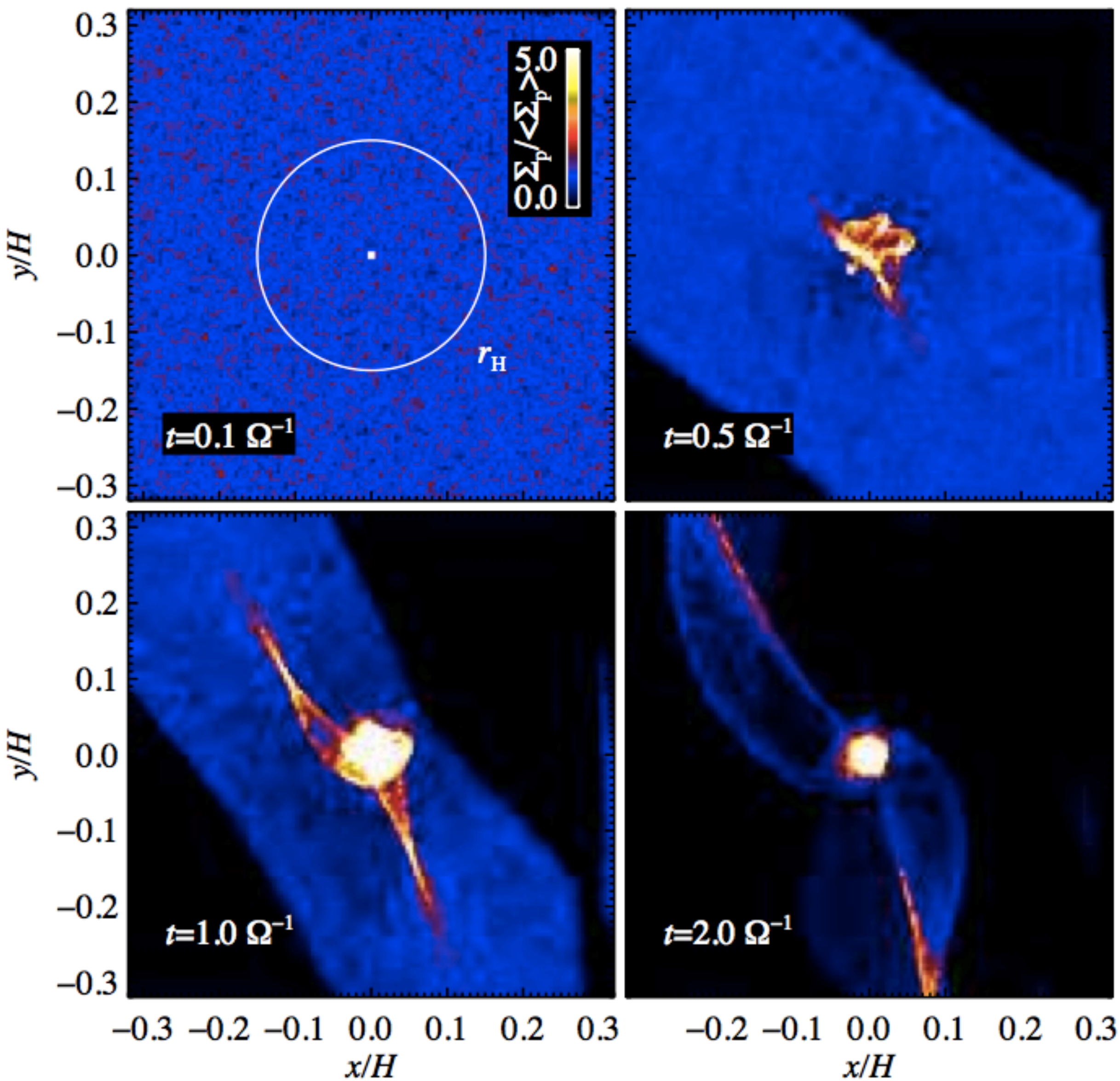

Lambrechts & Johansen (2012)

Baroclinic Instability – Excitation and self-sustenance of vortices

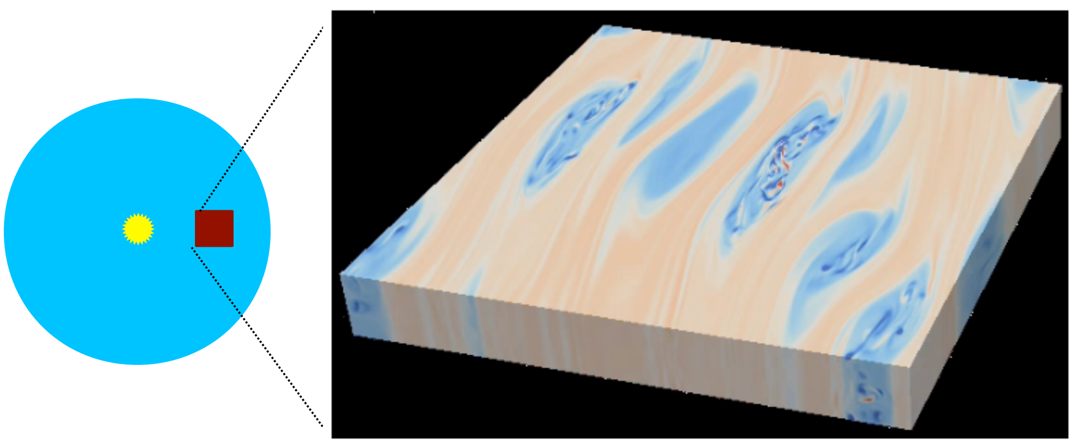

Lesur & Papaloizou (2010)

Sketch of the
Baroclinic Instability

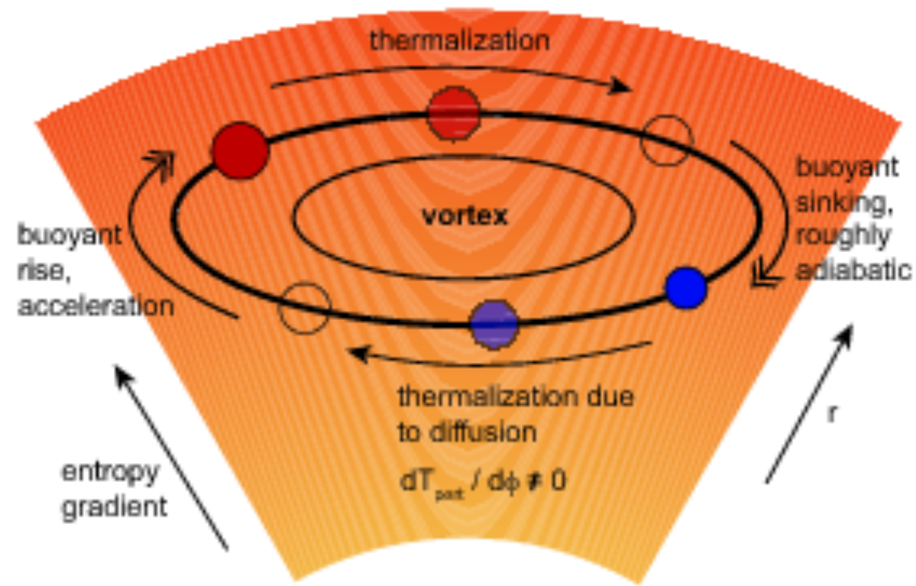

Armitage (2010)

$$\frac{\partial \omega}{\partial t} = \underbrace{-(\boldsymbol{u}\cdot\nabla)\omega}_{\text{advection}} \underbrace{-\,\omega(\nabla\cdot\boldsymbol{u})}_{\text{compression}} + \underbrace{(\omega\cdot\nabla)\boldsymbol{u}}_{\text{stretching}} + \underbrace{\frac{1}{\rho^2}\nabla\rho\times\nabla p}_{\text{baroclinicity}} + \underbrace{\nu\nabla^2\omega}_{\text{dissipation}}$$

Baroclinic Instability – Excitation and self-sustenance of vortices

1. *Radial entropy gradient*
2. *Thermal diffusion*

Sketch of the
Baroclinic Instability

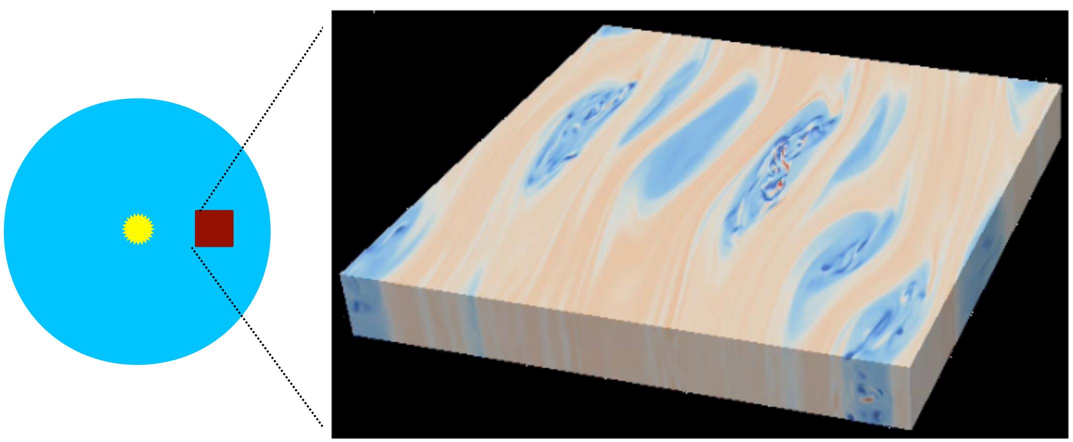

Lesur & Papaloizou (2010)

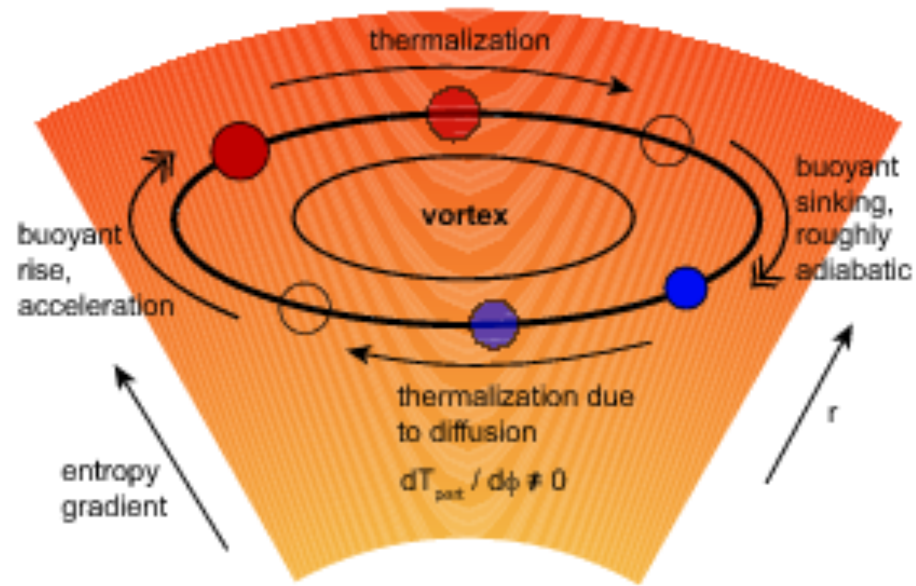

Armitage (2010)

$$\frac{\partial \omega}{\partial t} = \underbrace{-(\boldsymbol{u}\cdot\nabla)\omega}_{\text{advection}} \underbrace{-\,\omega(\nabla\cdot\boldsymbol{u})}_{\text{compression}} + \underbrace{(\omega\cdot\nabla)\boldsymbol{u}}_{\text{stretching}} + \underbrace{\frac{1}{\rho^2}\nabla\rho\times\nabla p}_{\text{baroclinicity}} + \underbrace{\nu\nabla^2\omega}_{\text{dissipation}}$$

Baroclinic Instability – Excitation and self-sustenance of vortices

1. Radial entropy gradient

2. Thermal diffusion

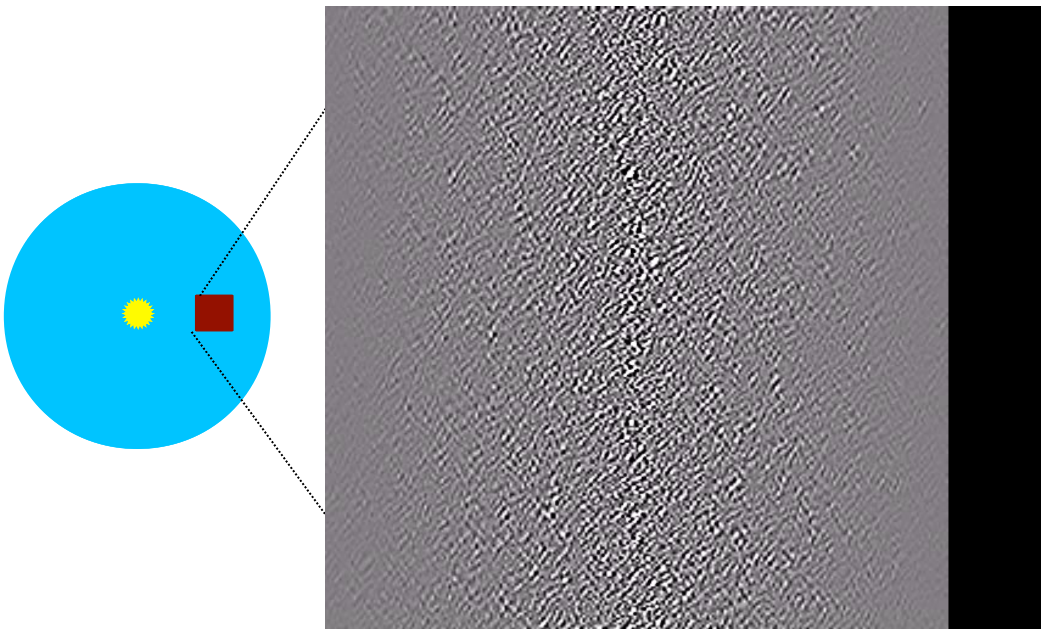

Lyra & Klahr (2011)

Sketch of the Baroclinic Instability

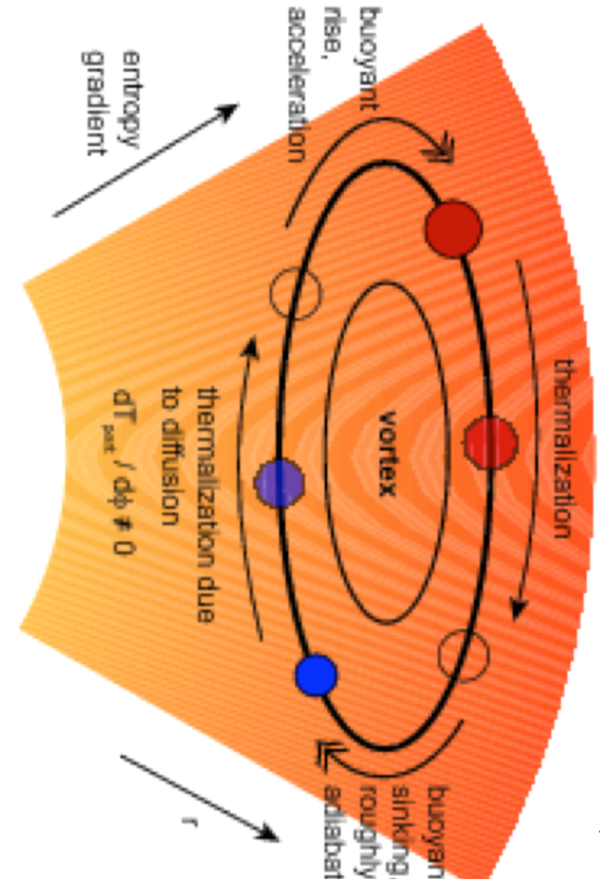

Armitage (2010

$$\frac{\partial \omega}{\partial t} = \underbrace{-(\boldsymbol{u}\cdot\nabla)\omega}_{\text{advection}} \underbrace{-\,\omega(\nabla\cdot\boldsymbol{u})}_{\text{compression}} + \underbrace{(\omega\cdot\nabla)\boldsymbol{u}}_{\text{stretching}} + \underbrace{\frac{1}{\rho^2}\nabla\rho\times\nabla p}_{\text{baroclinicity}} + \underbrace{\nu\nabla^2\omega}_{\text{dissipation}}$$

Baroclinic instability and layered accretion

What happens when the vortex is magnetized?

Hydro

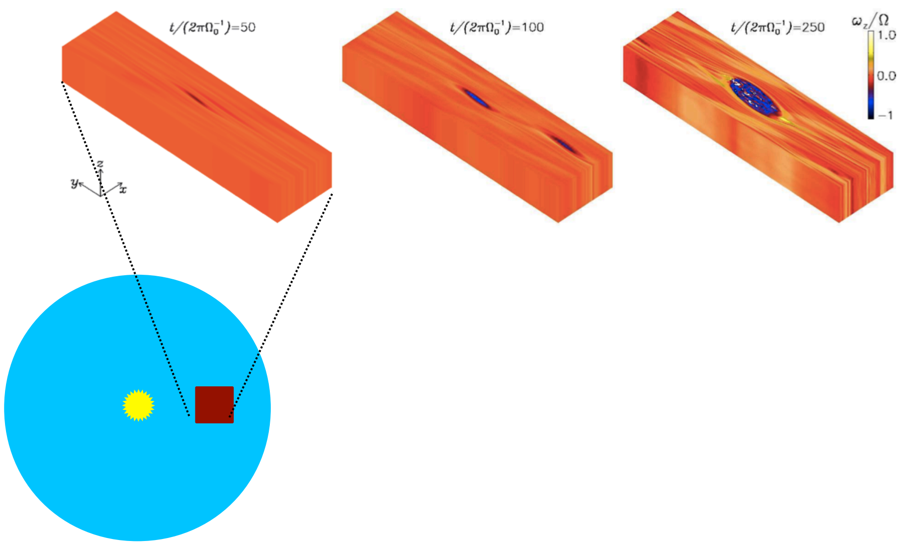

MHD

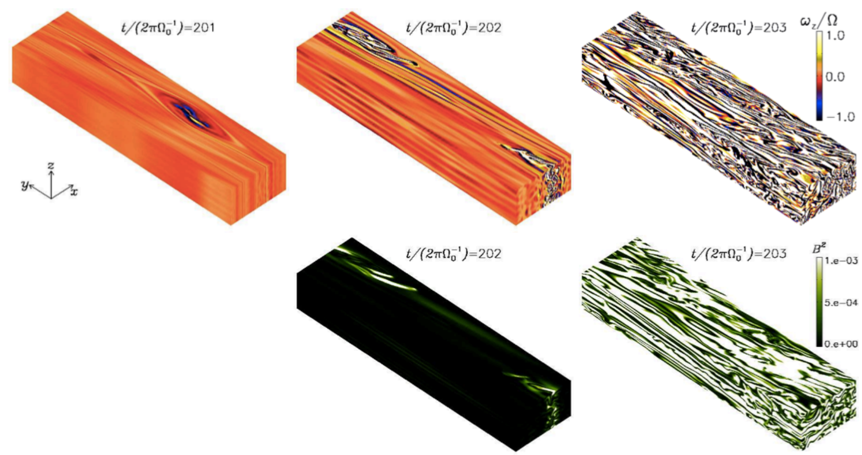

Vorticity

Mag. Energy

Lyra & Klahr (2011)

Baroclinic instability and layered accretion

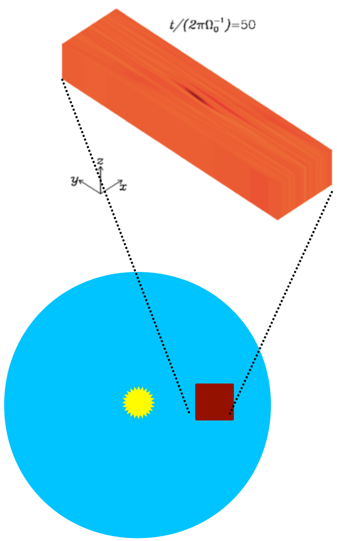

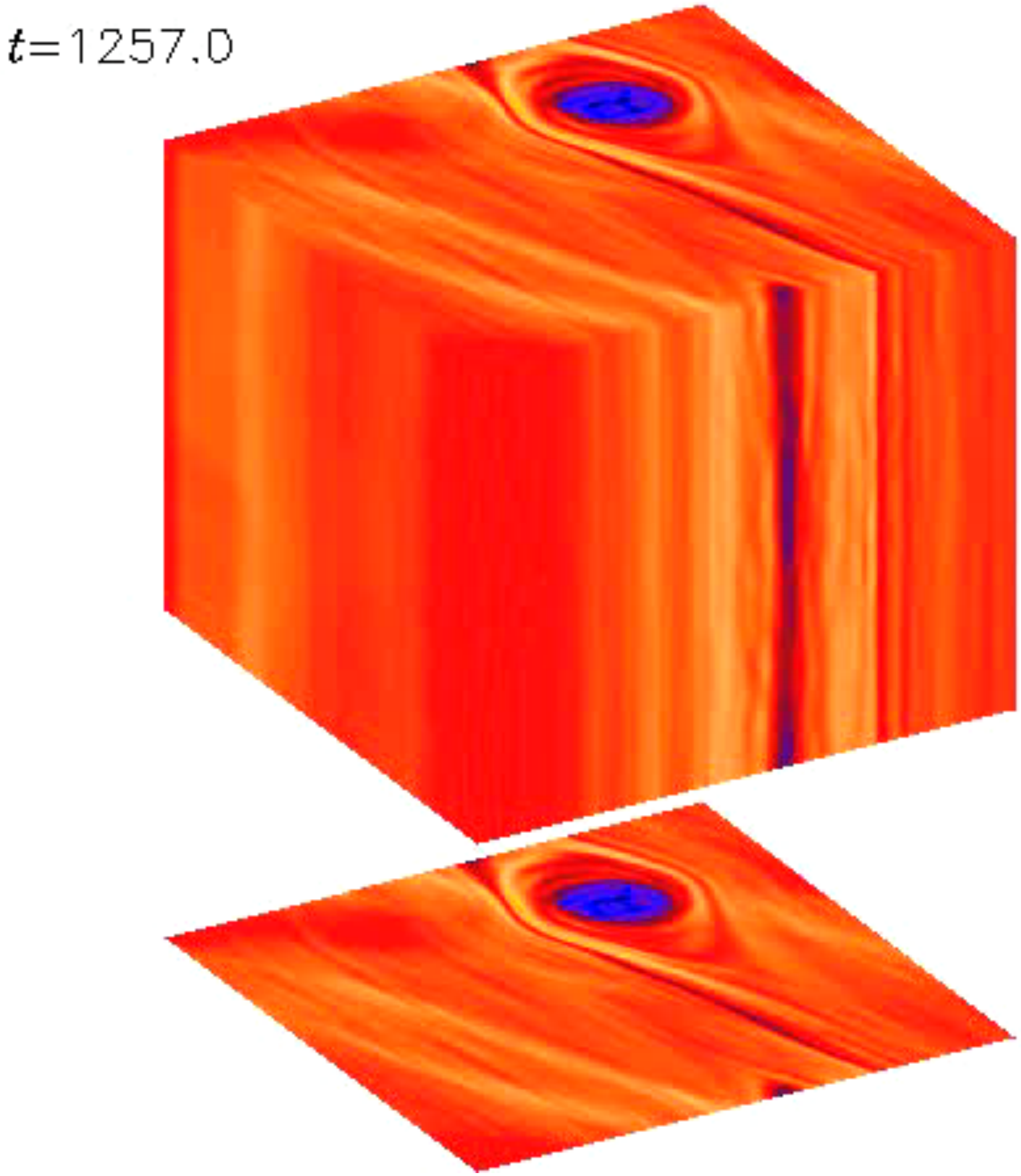

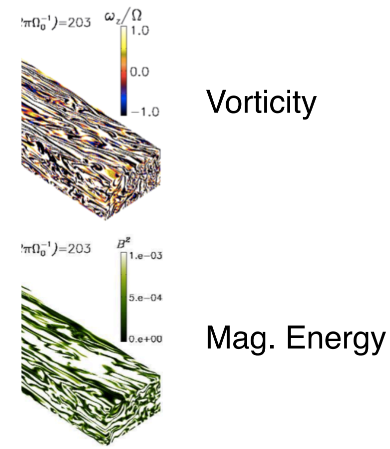

Baroclinic instability and layered accretion

What happens when the vortex is magnetized?

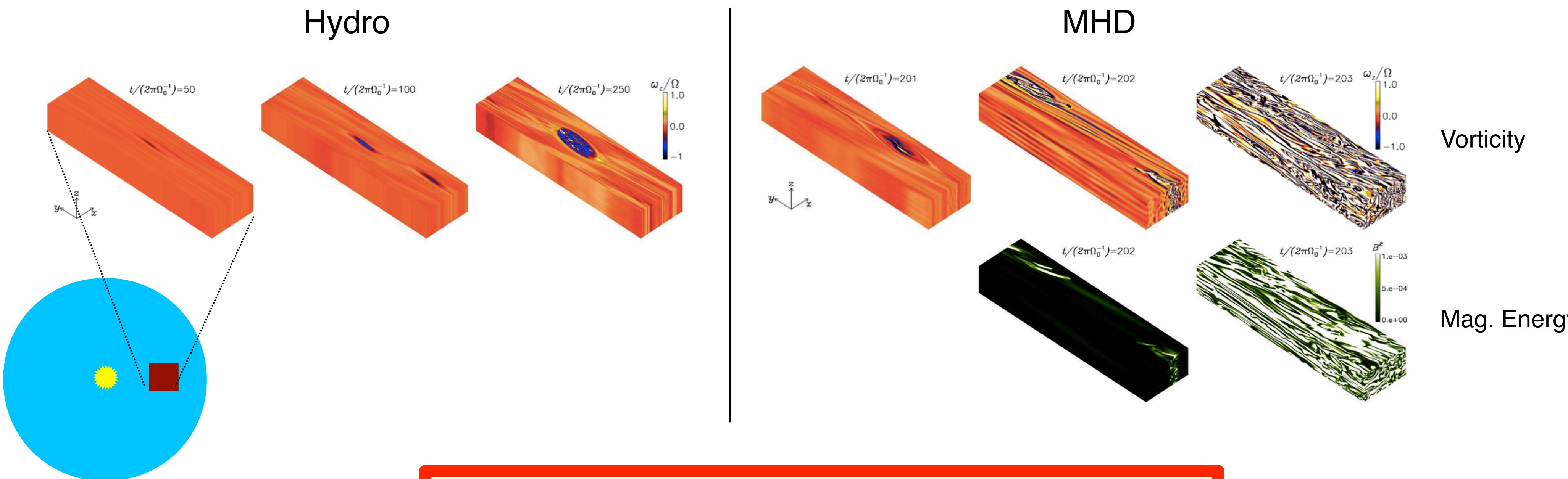

Baroclinic vortices
do ***not*** survive magnetization

Lyra & Klahr (2011)

A possible detection of vortices in disks?

Observations

Brown et al. (2009)

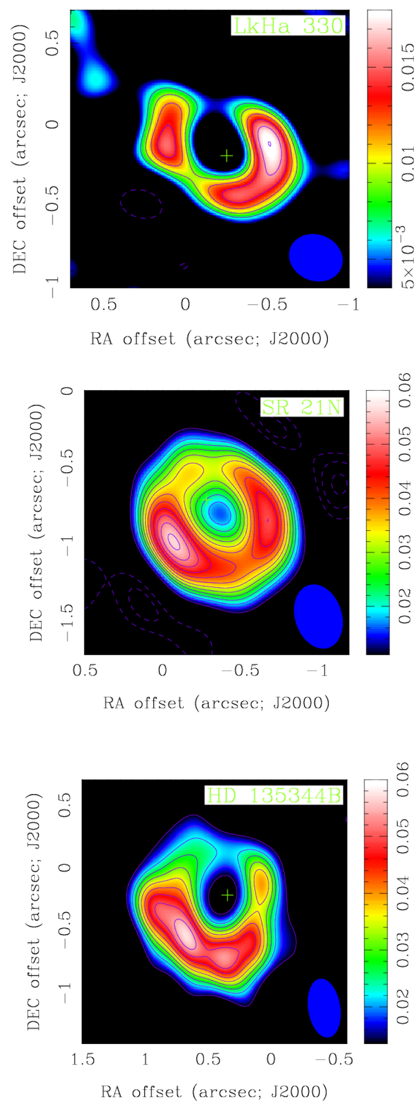

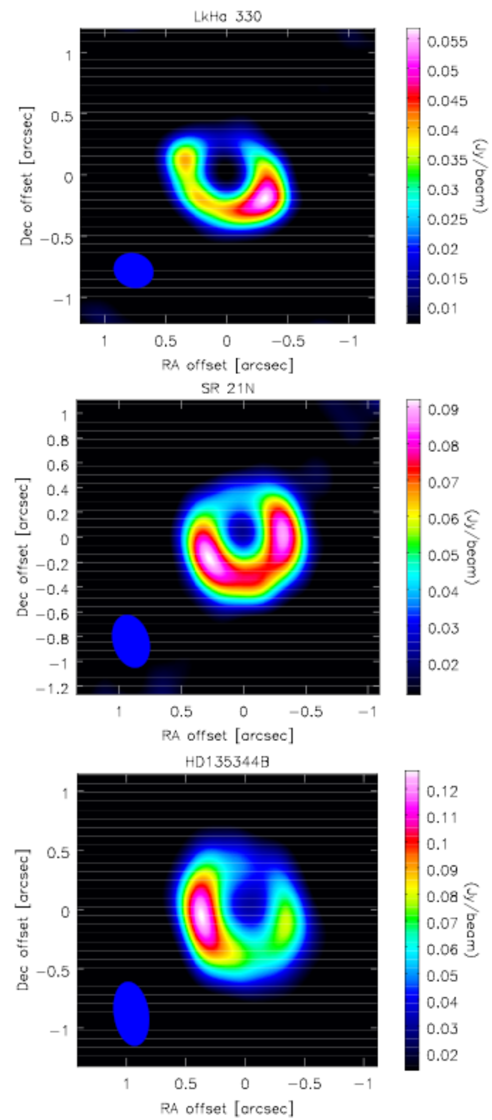

Models

Simulated observations of Rossby vortices

Regaly et al. (2012)

Oph IRS 48

A Major Asymmetric Dust Trap in a Transition Disk

Nienke van der Marel,[1]* Ewine F. van Dishoeck,[1,2] Simon Bruderer,[2] Til Birnstiel,[3] Paola Pinilla,[4] Cornelis P. Dullemond,[4] Tim A. van Kempen,[1,5] Markus Schmalzl,[1] Joanna M. Brown,[3] Gregory J. Herczeg,[6] Geoffrey S. Mathews,[1] Vincent Geers[7]

The statistics of discovered exoplanets suggest that planets form efficiently. However, there are fundamental unsolved problems, such as excessive inward drift of particles in protoplanetary disks during planet formation. Recent theories invoke dust traps to overcome this problem. We report the detection of a dust trap in the disk around the star Oph IRS 48 using observations from the Atacama Large Millimeter/submillimeter Array (ALMA). The 0.44-millimeter–wavelength continuum map shows high-contrast crescent-shaped emission on one side of the star, originating from millimeter-sized grains, whereas both the mid-infrared image (micrometer-sized dust) and the gas traced by the carbon monoxide 6-5 rotational line suggest rings centered on the star. The difference in distribution of big grains versus small grains/gas can be modeled with a vortex-shaped dust trap triggered by a companion.

Although the ubiquity of planets is confirmed almost daily by detections of new exoplanets (*1*), the exact formation mechanism of planetary systems in disks of gas and dust around young stars remains a long-standing problem in astrophysics (*2*). In

iencemag.org SCIENCE VOL 340 7 JUNE 2013 1199

van der Marel et al. 2013

A possible huge vortex observed with ALMA

The Oph IRS 48 “dust trap”

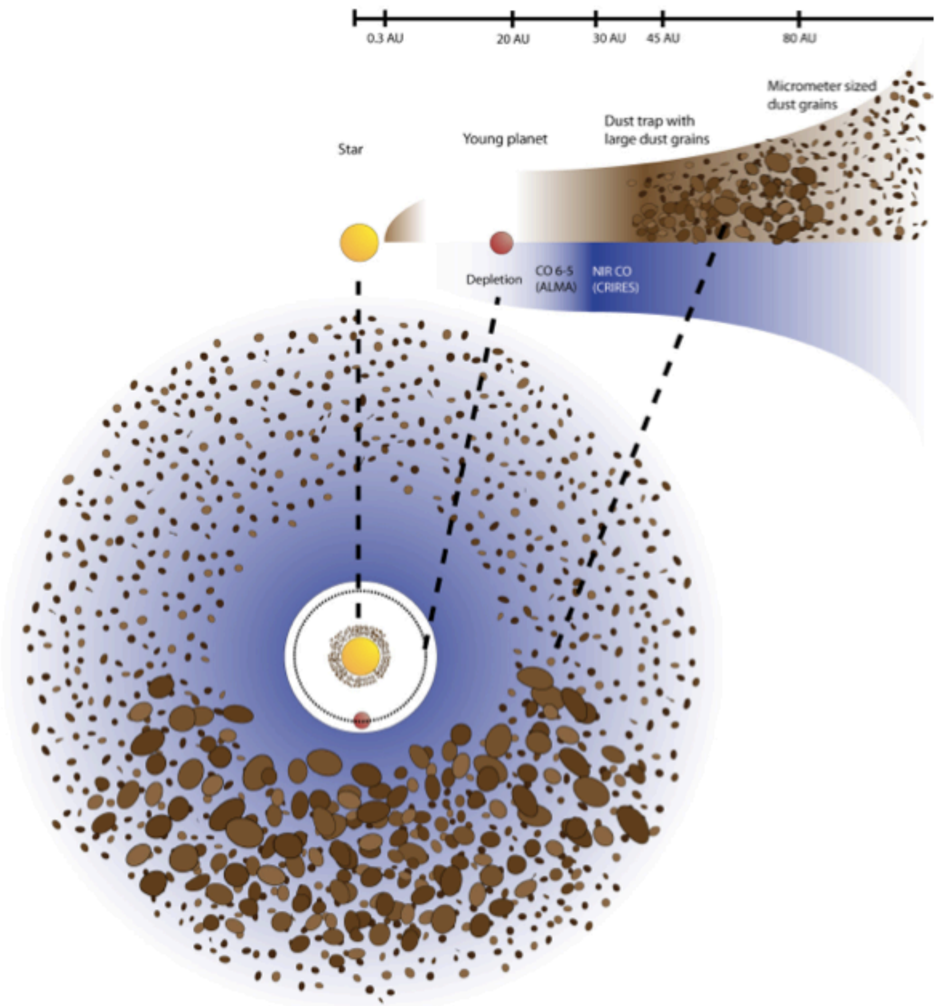

van der Marel et al. (2013)

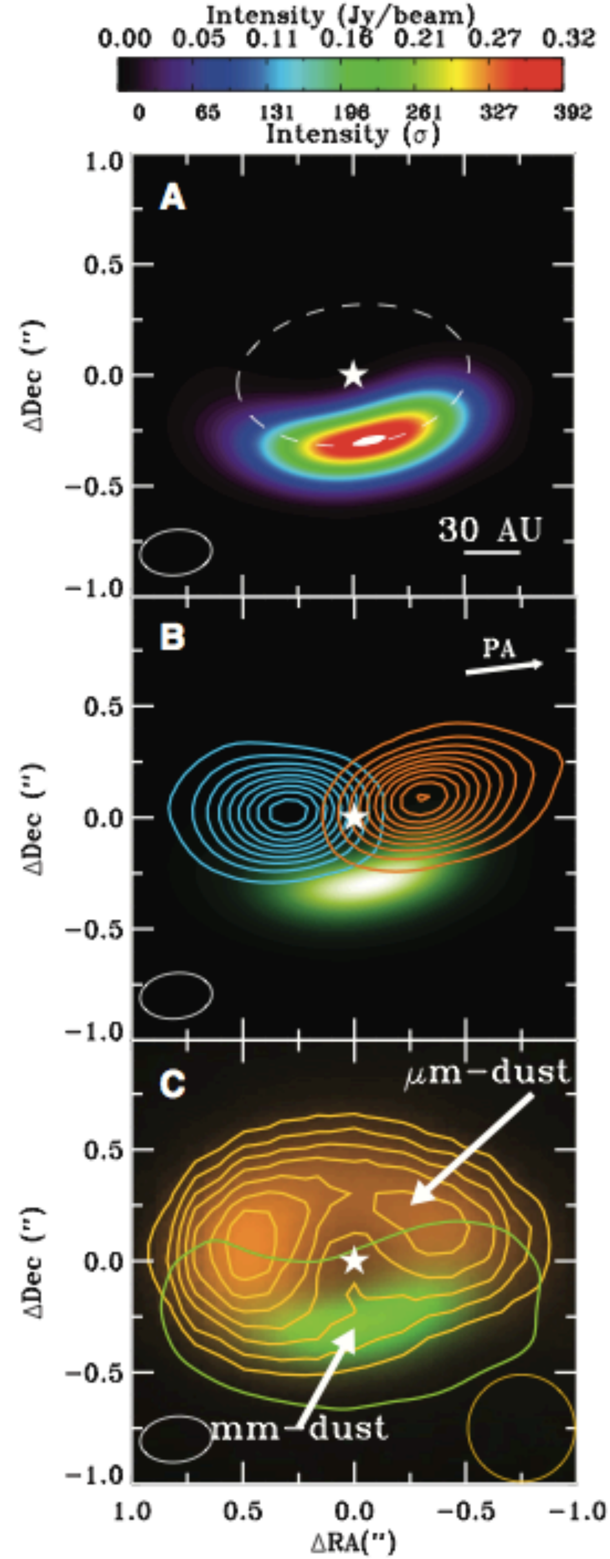

asymmetric mm dust at 63 AU

Gas detection: Keplerian rotation

Micron-sized dust follows gas

Dust Trapping

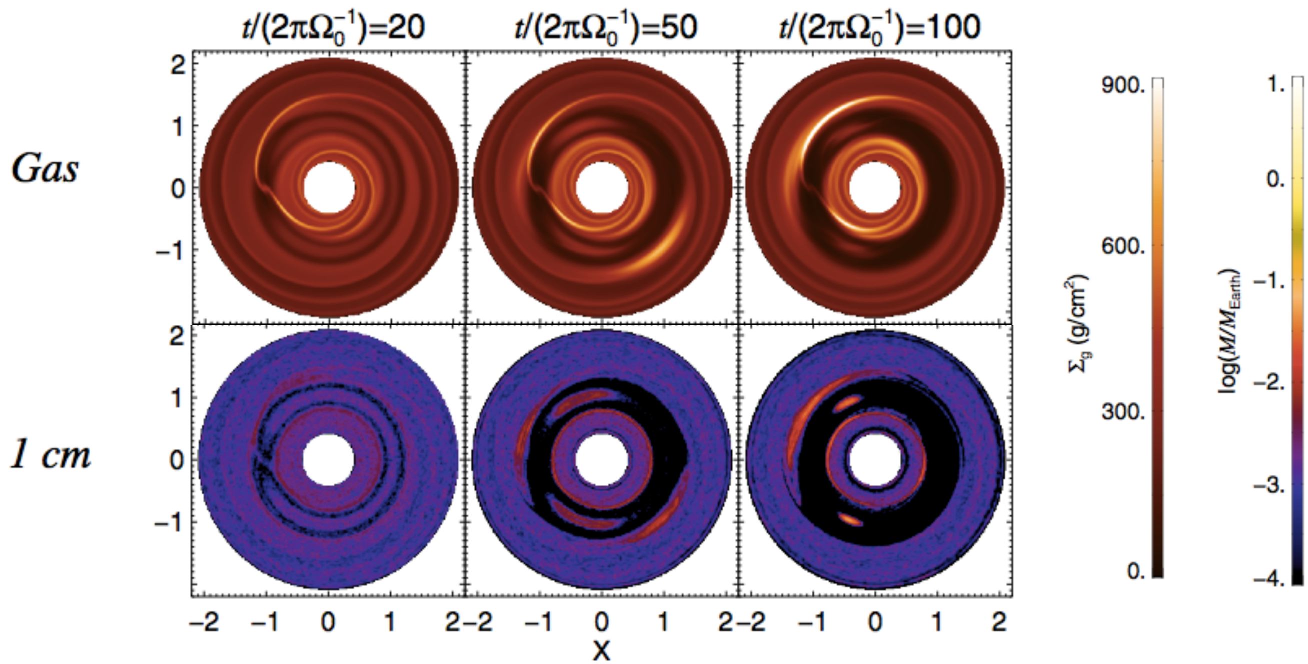

Lyra et al (2009b)

Turbulent "kicks" lead to steady state

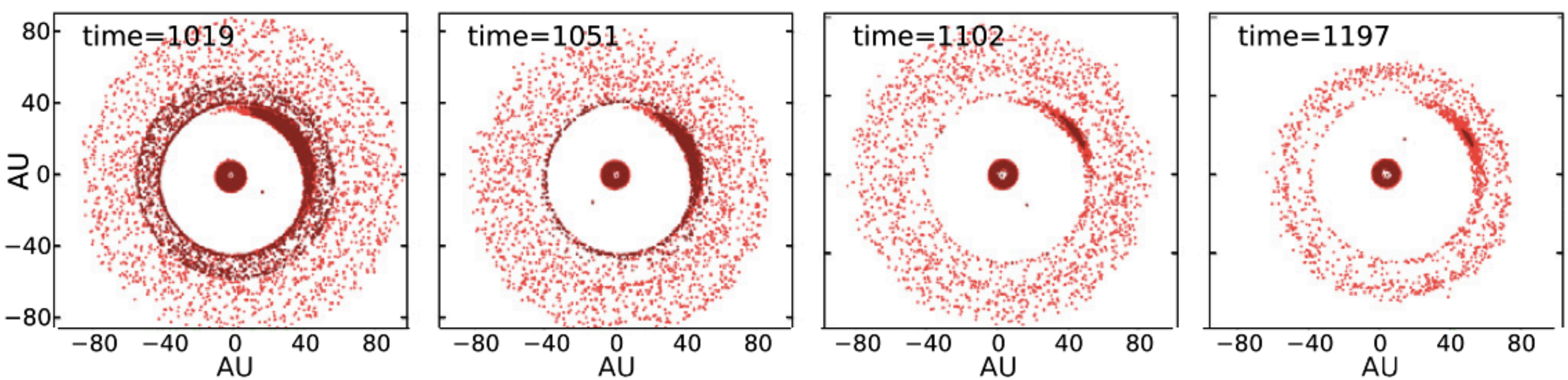

Ataiee et al. (2013)

Drag-Diffusion Equilibrium

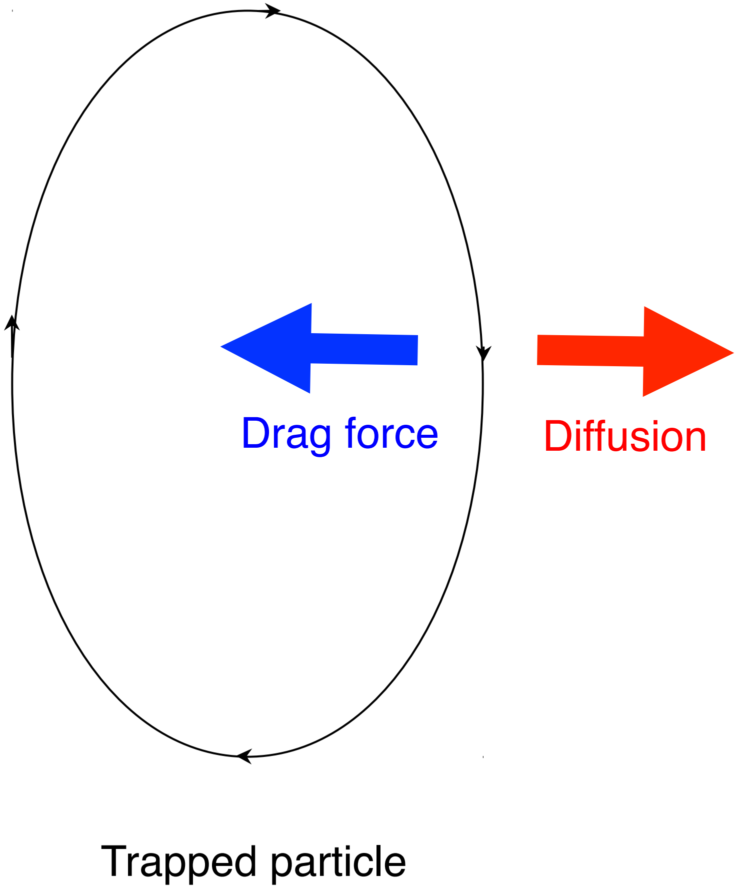

Drag-Diffusion Equilibrium

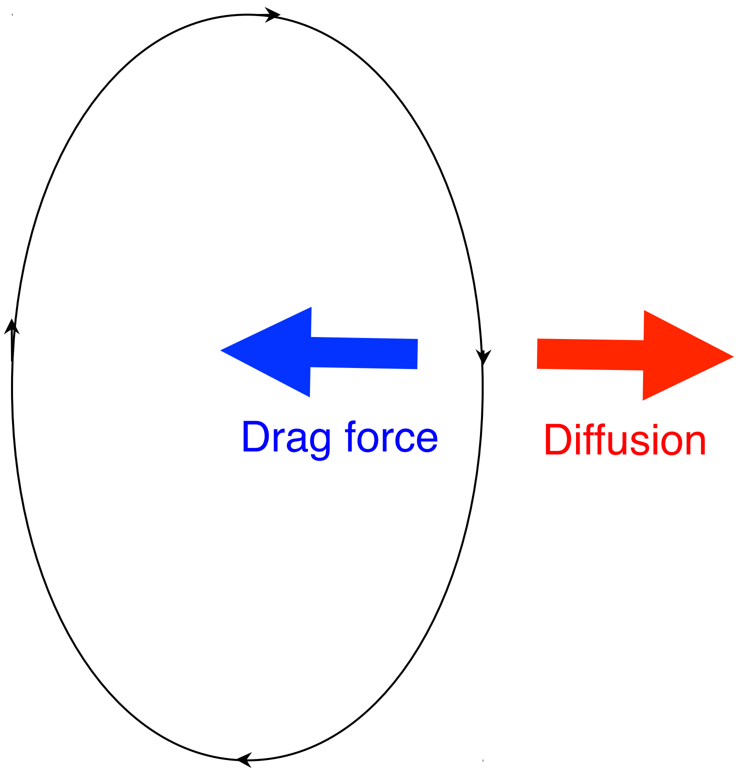

Trapped particle

Dust continuity equation

$$\frac{\partial \rho_d}{\partial t} = \underbrace{-(\boldsymbol{v} \cdot \boldsymbol{\nabla})\rho_d}_{\text{advection}} \underbrace{- \rho_d \boldsymbol{\nabla} \cdot \boldsymbol{v}}_{\text{compression}} + \underbrace{D\nabla^2 \rho_d}_{\text{diffusion}},$$

Drag-Diffusion Equilibrium

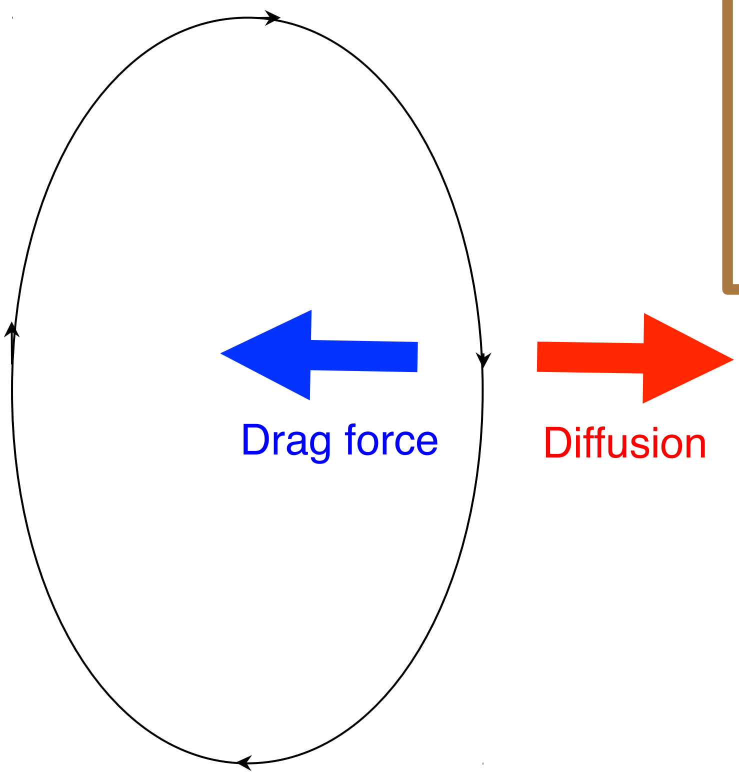

Trapped particle

Steady-state solution

$$\rho_d(a,z) = \varepsilon\rho_0\,(S+1)^{3/2}\,\exp\left\{-\frac{\left[a^2 f^2(\chi)+z^2\right]}{2H^2}(S+1)\right\}$$

Lyra & Lin (2013)

$$S = \frac{St}{\delta}$$

$$\delta = v_{\rm rms}^2/c_s^2,$$

a = vortex semi-minor axis
H = disk scale height (temperature)
χ = vortex aspect ratio
δ = diffusion parameter
St = Stokes number (particle size)
$f(\chi)$ = model-dependent scale function

Analytical solution for dust trapping

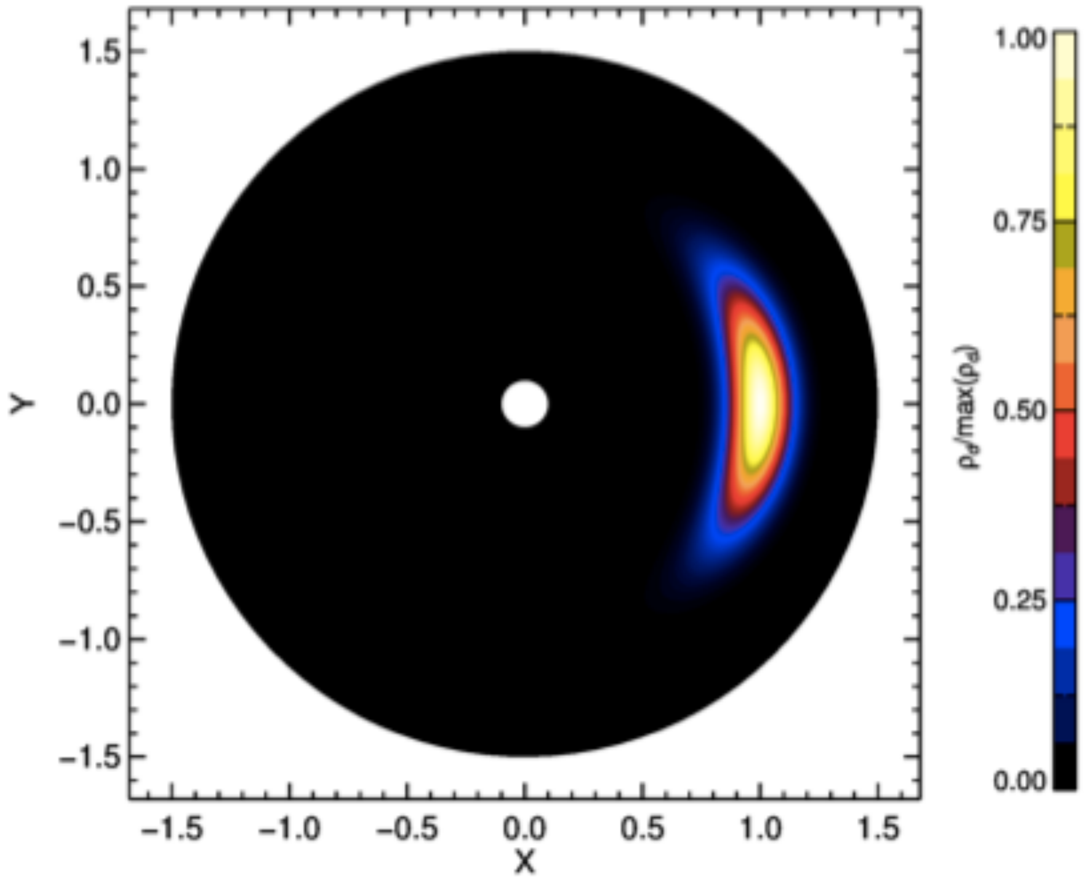

Solution

$$\rho_d(a) = \rho_{d\,\max} \exp\left(-\frac{a^2}{2H_V^2}\right),$$

$$H_V = \frac{H}{f(\chi)}\sqrt{\frac{1}{S+1}}$$

$$S = \frac{St}{\delta}$$

$$\delta = v_{\rm rms}^2 / c_s^2,$$

Solution for

H/r=0.1 χ=4 *S*=1

a	= vortex semi-minor axis
H	= disk scale height (temperature)
χ	= vortex aspect ratio
δ	= diffusion parameter
St	= Stokes number (particle size)
$f(\chi)$	= model-dependent scale function

Lyra & Lin (2013)

Derived quantities

$$\rho_d(a,z) = \varepsilon\rho_0 (S+1)^{3/2} \exp\left\{-\frac{[a^2 f^2(\chi)+z^2]}{2H^2}(S+1)\right\}$$

Lyra & Lin (2013)

Gas distribution

$$\rho_g(a) = \rho_{g\,\max} \exp\left(-\frac{a^2}{2H_g^2}\right),$$

Maximum dust density

$$\rho_{d\,\max} = \varepsilon\,\rho_0\,(S+1)^{3/2}$$

Gas contrast

$$\frac{\rho_{g\,\max}}{\rho_{g\,\min}} = \exp\left[\frac{f^2(\chi)}{2\chi^2\omega_V^2}\right],$$

Dust contrast

$$\frac{\rho_{d\,\max}}{\rho_{d\,\min}} = \frac{\rho_{g\,\max}}{\rho_{g\,\min}} \exp(S),$$

Total trapped mass

$$\int \rho_d(a,z)dV = (2\pi)^{3/2}\,\varepsilon\rho_0\,\chi H H_g^2$$

Vortex size

$$a_s = H(\chi\omega_V)^{-1}$$

H = disk scale height (temperature)
χ = vortex aspect ratio
δ = diffusion parameter
St = Stokes number (particle size)
$f(\chi)$ = model-dependent scale function
ε = dust-to-gas ratio

Applying the model to Oph IRS 48

Observed parameters

Aspect ratio: 3.1

Dust contrast: 130

Temperature: 60K

Trapped mass: 9 M_{Earth}

Derived parameters

S=4.8

Stokes number, St=0.008

$\delta = 0.005$, $v_{rms} = 4\% \ c_s$

Trapped mass: 11 M_{Earth}

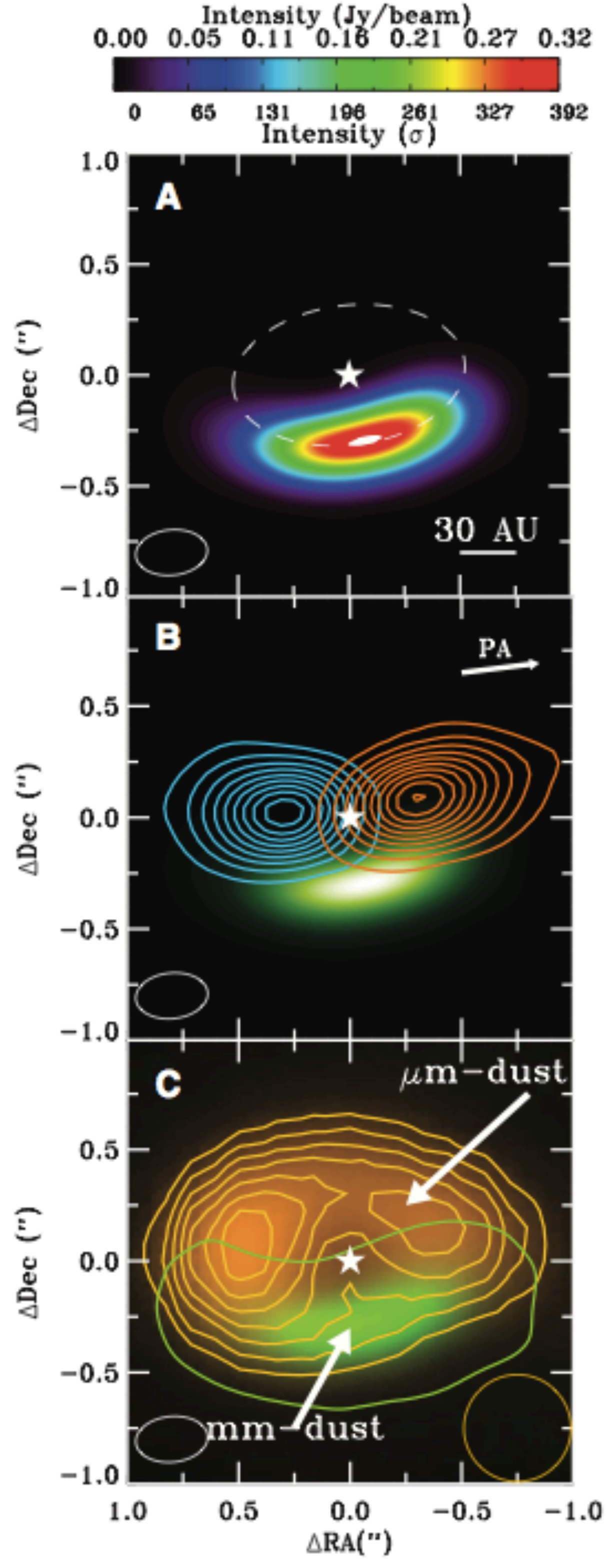

asymmetric mm dust at 63 AU

Gas detection: Keplerian rotation

Micron-sized dust follows gas

Lyra & Lin (2013)

Turbulence in vortex cores

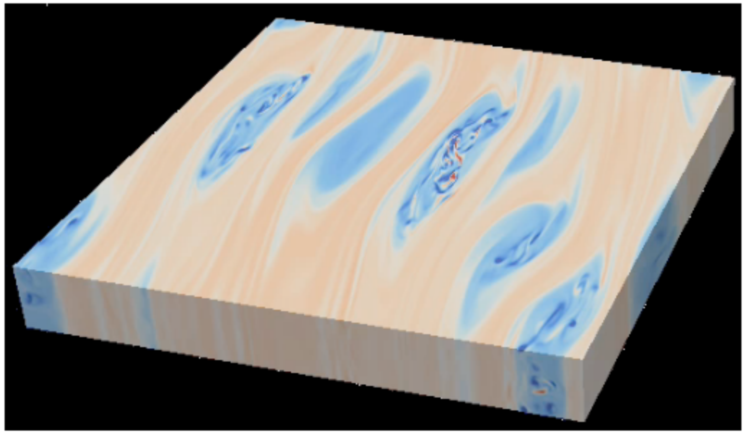

Lesur & Papaloizou (2010)

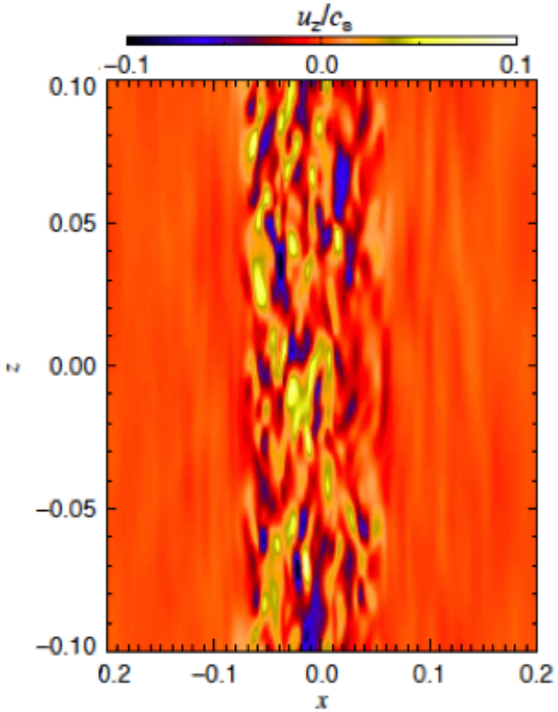

Lyra & Klahr (2011)

Turbulence in vortex cores:

max at ~10% of sound speed
rms at ~3% of sound speed

Conclusions

- Vortices exist in the dead zone only
- Two sustenance modes: Rossby Wave Instability and Convective Overstability
- Vortex-assisted and streaming instability are complementary
- Vortex-trapped dust in drag-diffusion equilibrium explains the observations
- Rossby wave instability may be the culprit of these dust traps
- We're in the era of observational testing/confirmation of our model predictions!!

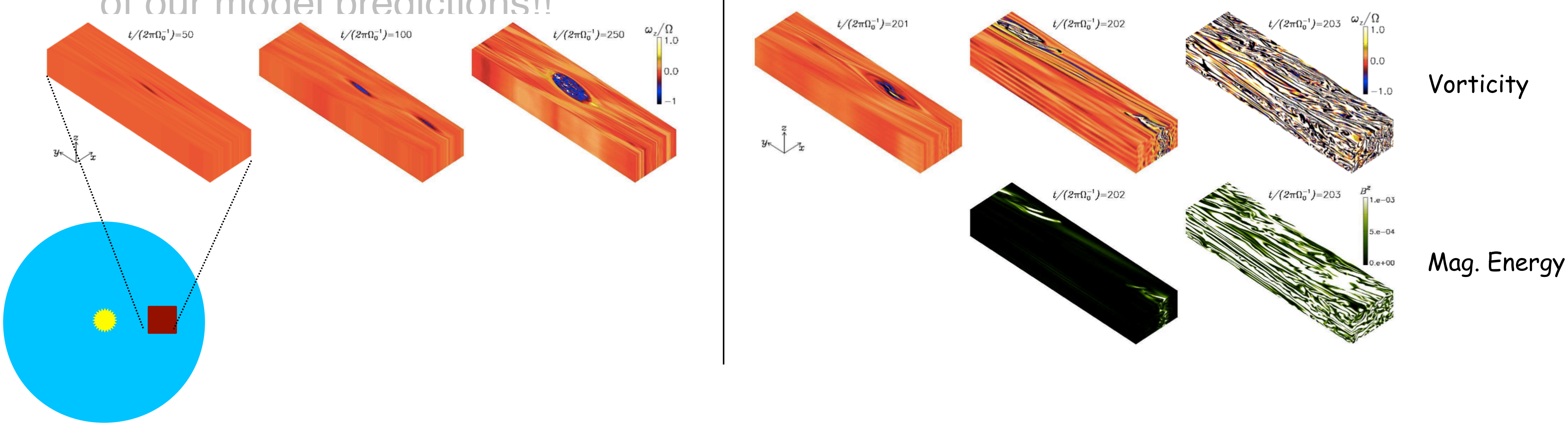

Lyra & Klahr (2011)

Conclusions

- Vortices exist in the dead zone only
- Two sustenance modes: Rossby Wave Instability and Convective Overstability
- Vortex-assisted is a complementary formation mode to streaming instability
- Vortex-trapped dust in drag-diffusion equilibrium explains the observations
- Rossby wave instability may be the culprit of these dust traps
- We're in the era of observational testing/co

Baroclinic instability

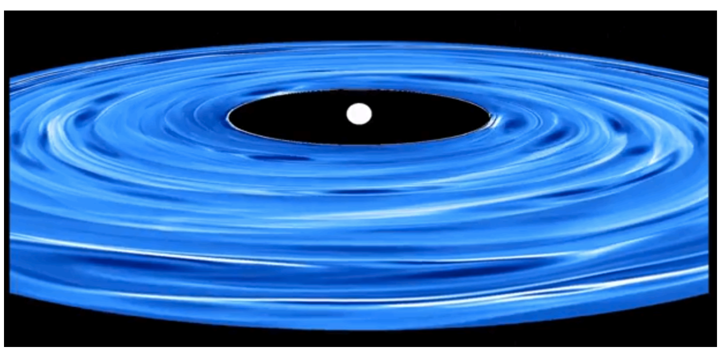

Rossby wave instability

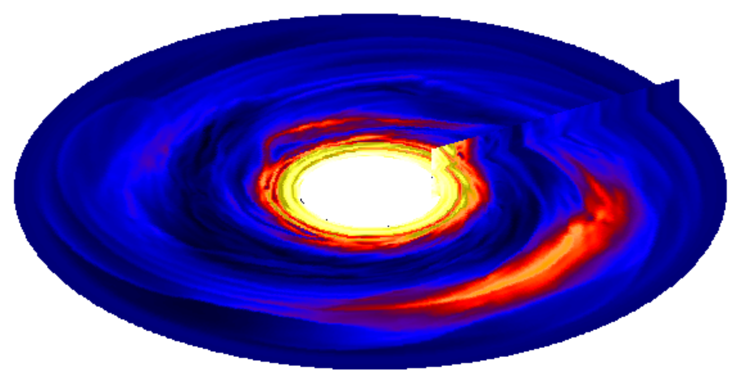

Conclusions

- Vortices exist in the dead zone only
- Two sustenance modes: Rossby Wave Instability and Convective Overstability
- Vortex-assisted and streaming instability are complementary
- Vortex-trapped dust in drag-diffusion equilibrium explains the observations
- Rossby wave instability may be the culprit of these dust traps

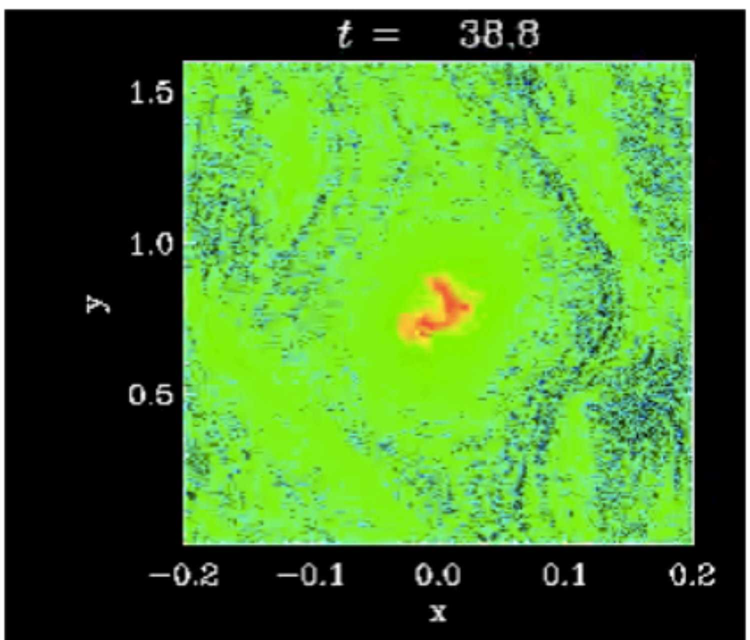

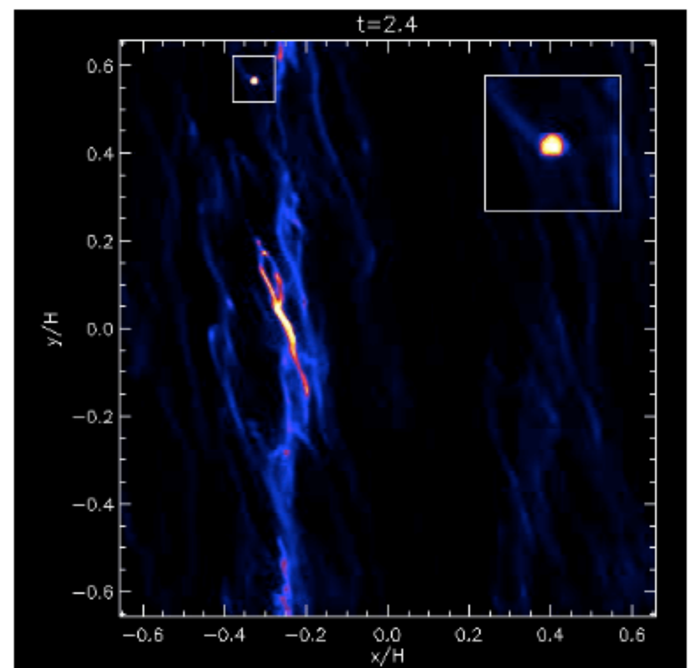

Conclusions

- Vortices exist in the dead zor
- Two sustenance modes: Ros
- Vortex-assisted and streami
- Vortex-trapped dust in drag-diffusion equilibrium explains the observations
- Rossby wave instability may be the culprit of these dust traps
- We're in the era of observational testing/confirmation of our model predictions!!

$$\rho_d(a,z) = \varepsilon\rho_0\,(S+1)^{3/2}\,\exp\left\{-\frac{\left[a^2 f^2(\chi)+z^2\right]}{2H^2}(S+1)\right\}$$

Lyra & Lin (2013)

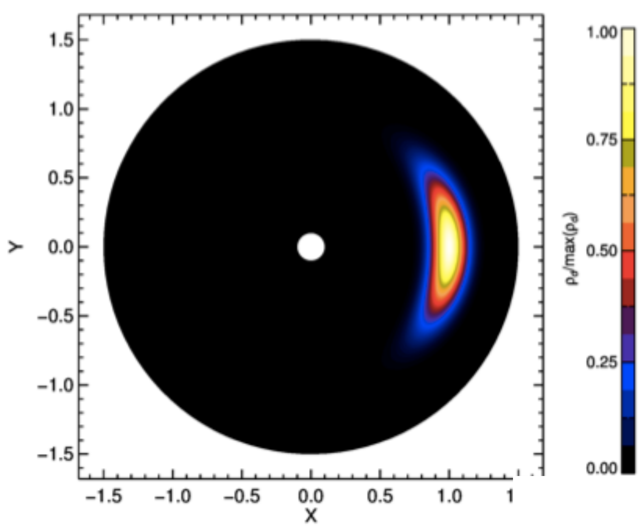

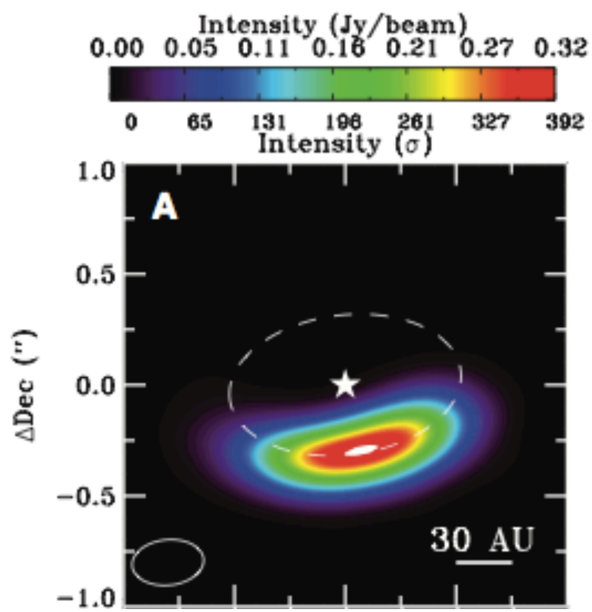

Conclusions

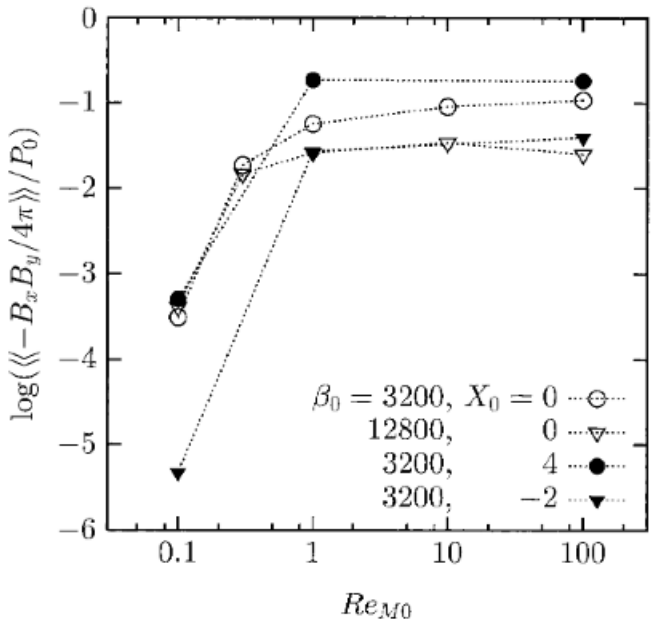

zone only

Rossby Wave Instability and Convective Overstability

mi

ıg-diffusion equilibrium explains the observations

- Rossby wave instability may be the culprit of these dust traps

- We're in the era of observational testing/coı of our model predictions!!

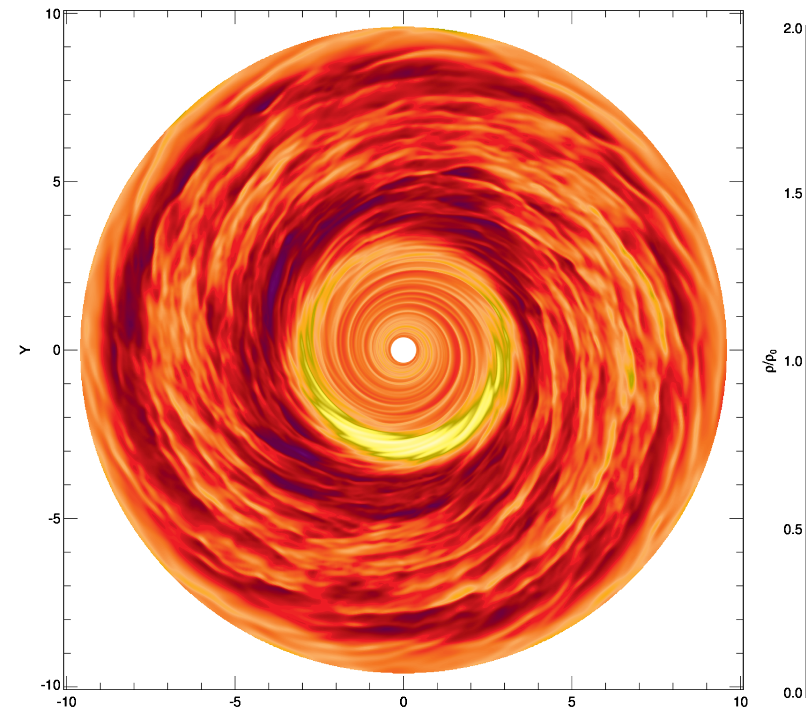

Conclusions

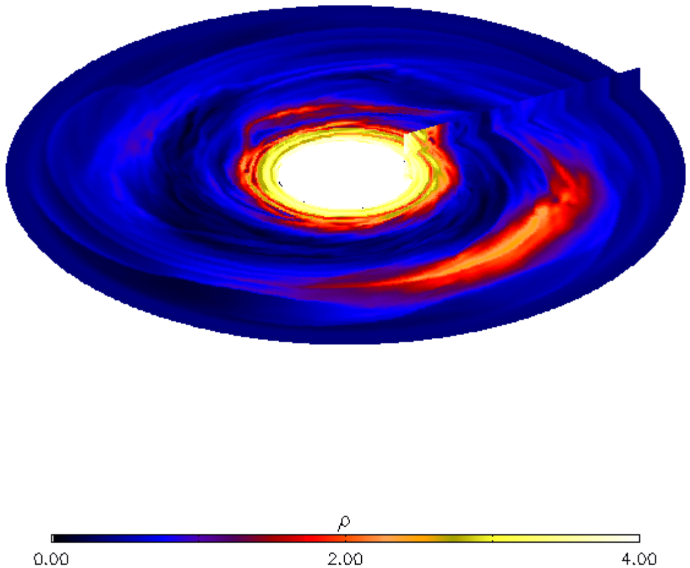

ne only

ssby Wave Insta

i

-diffusion equilibr

be the culprit o

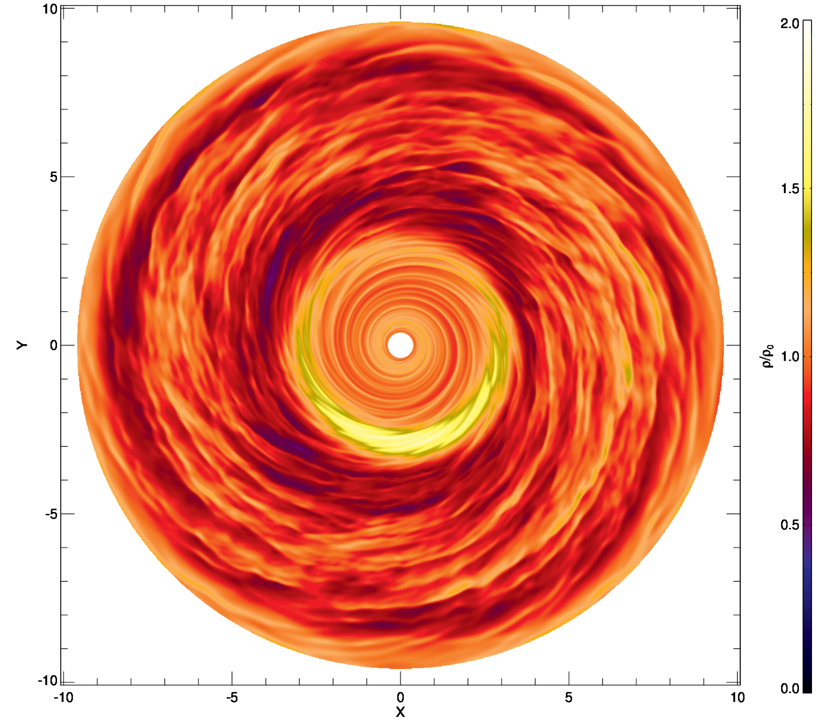

- We're in the era of observational testing/confirmation of our model predictions!!

Future direction

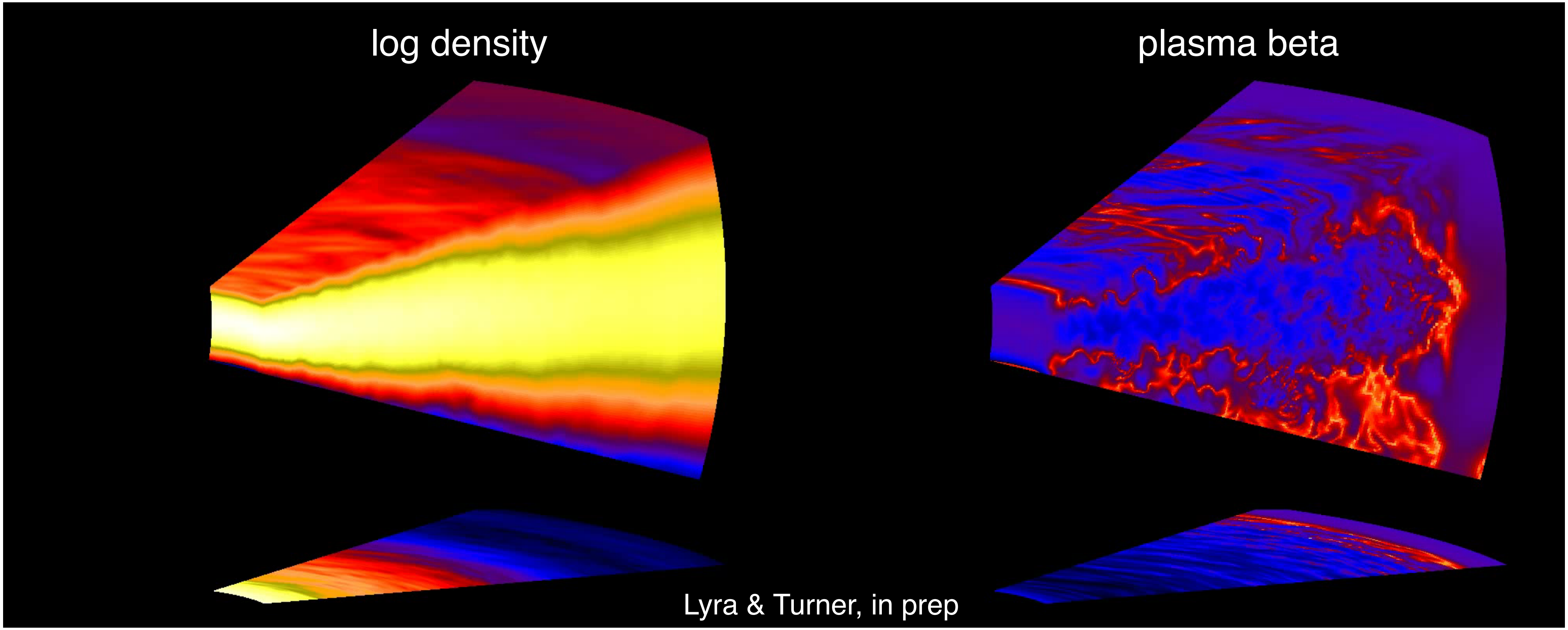

Dynamical resistivity
Particles

Particle gravity

Convergence

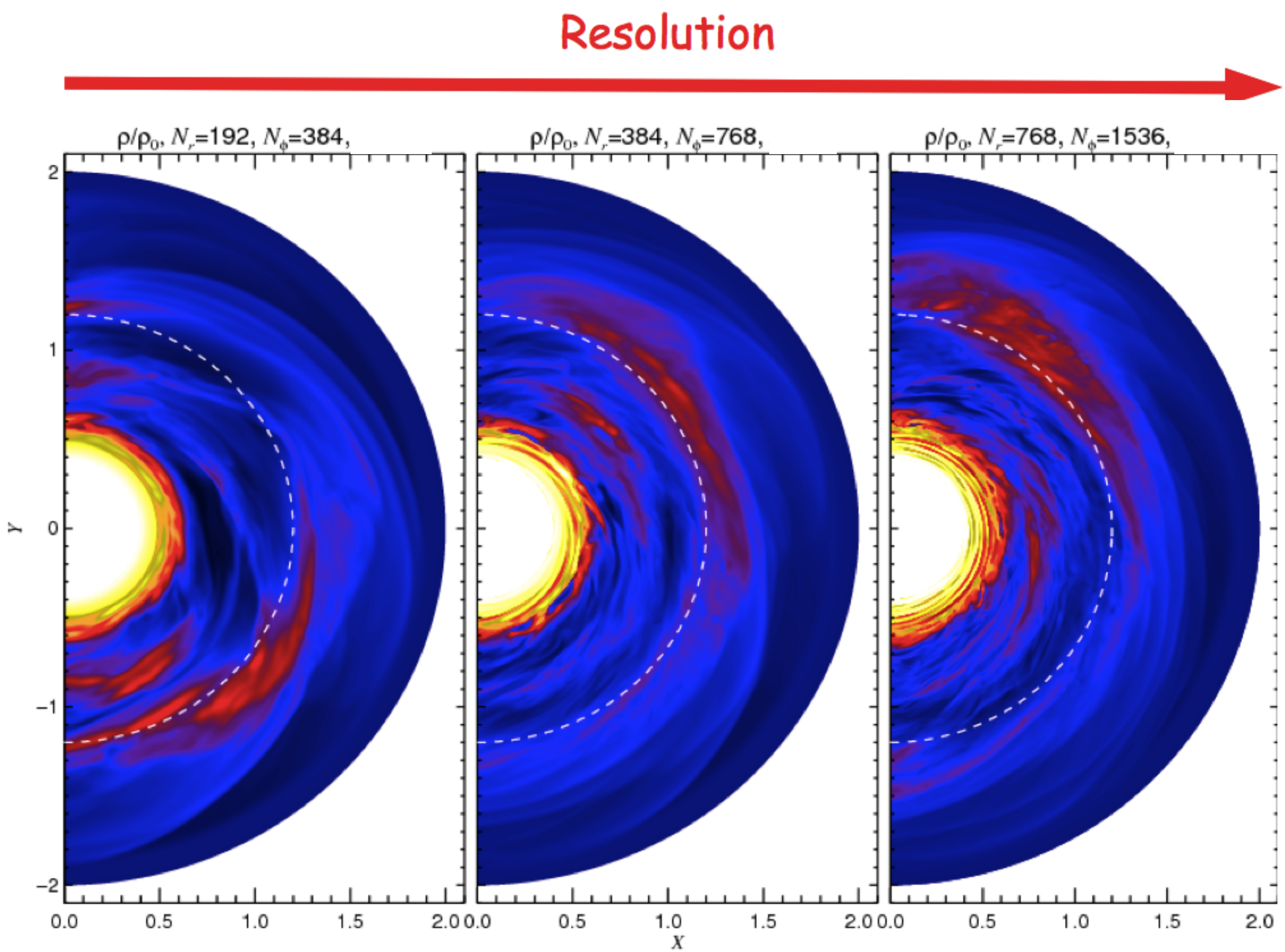

Lyra & Mac Low (2012)

High end computing

The Pencil Code

Brandenburg & Dobler (2002)

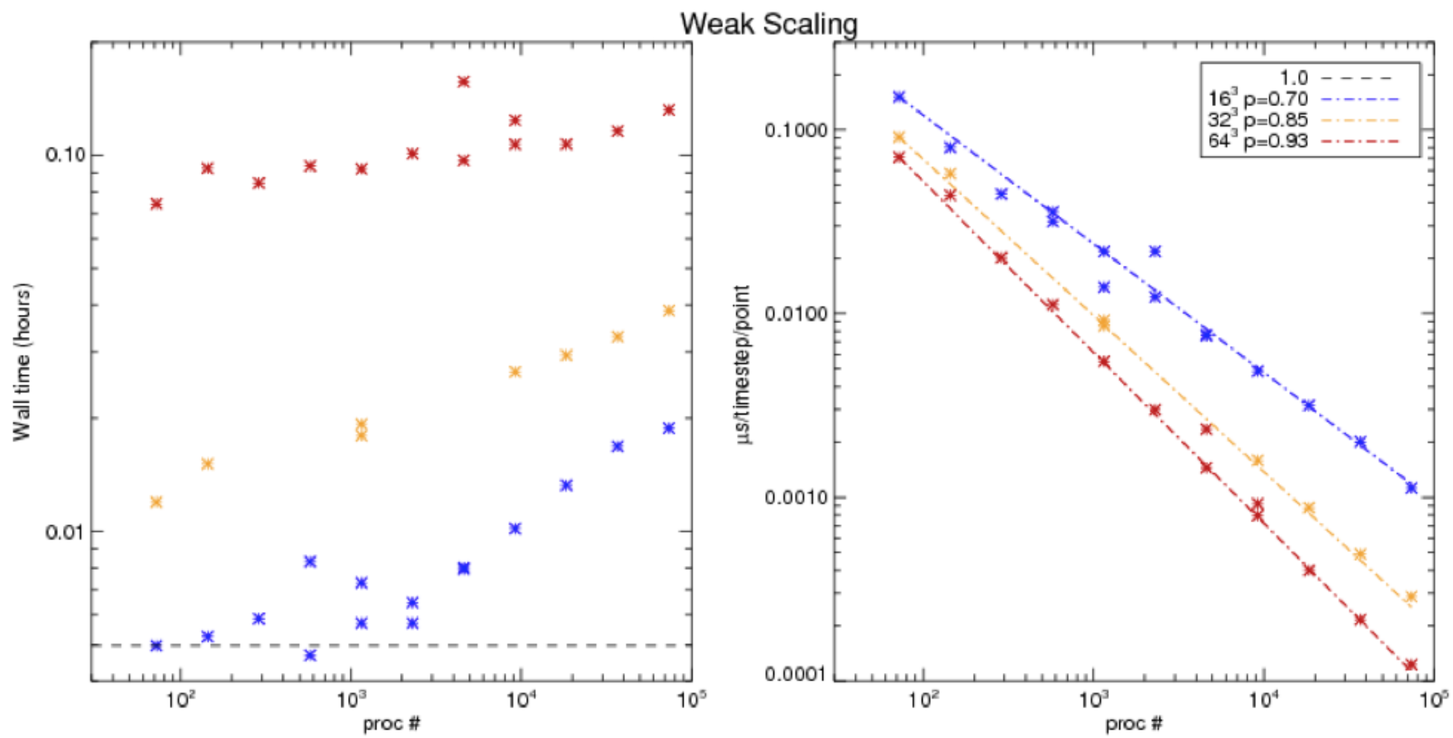

Good scaling up to > 70,000 processors !

(At NICS - Kraken)

A new >100,000 proc supercluster - Stampede

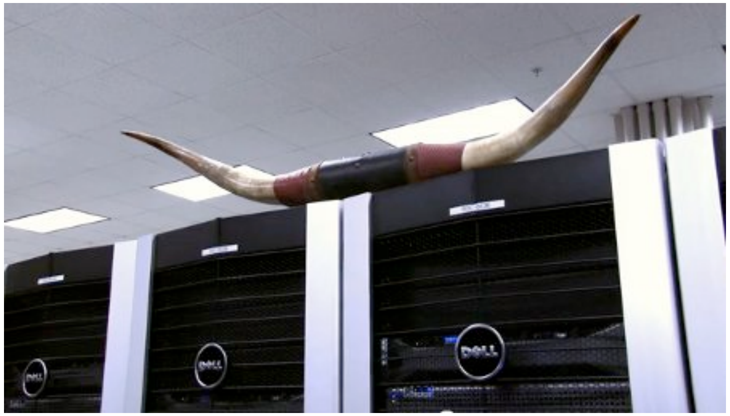

Debris disks – The gas-poor phase

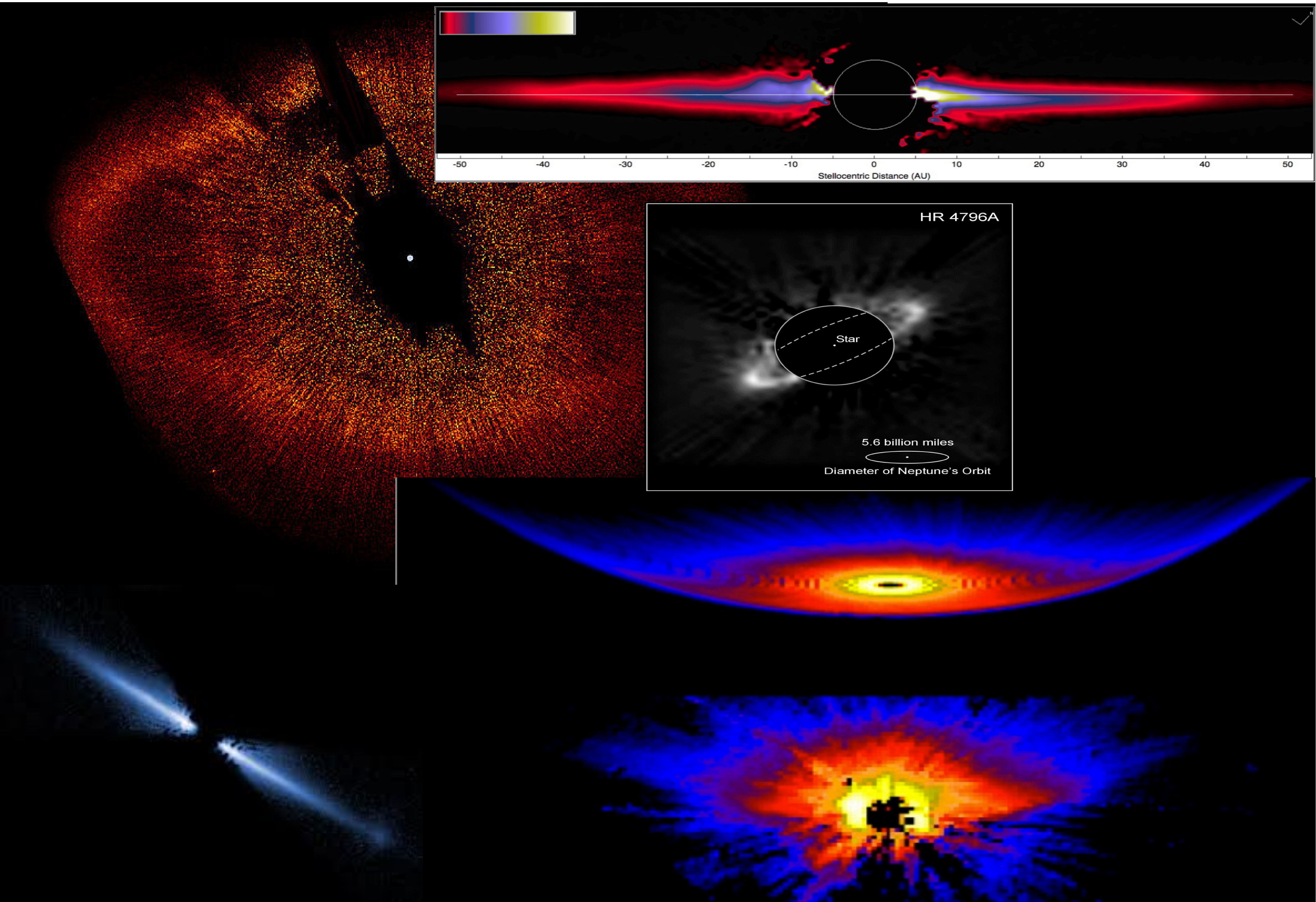

Sharp and eccentric rings in debris disks: Signposts of planets

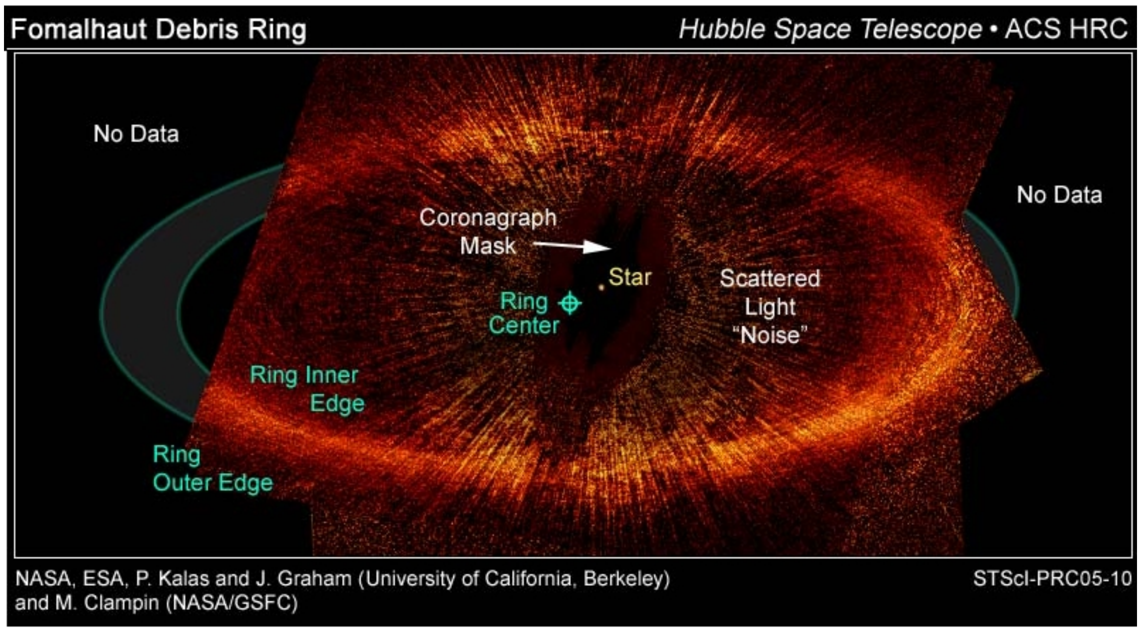

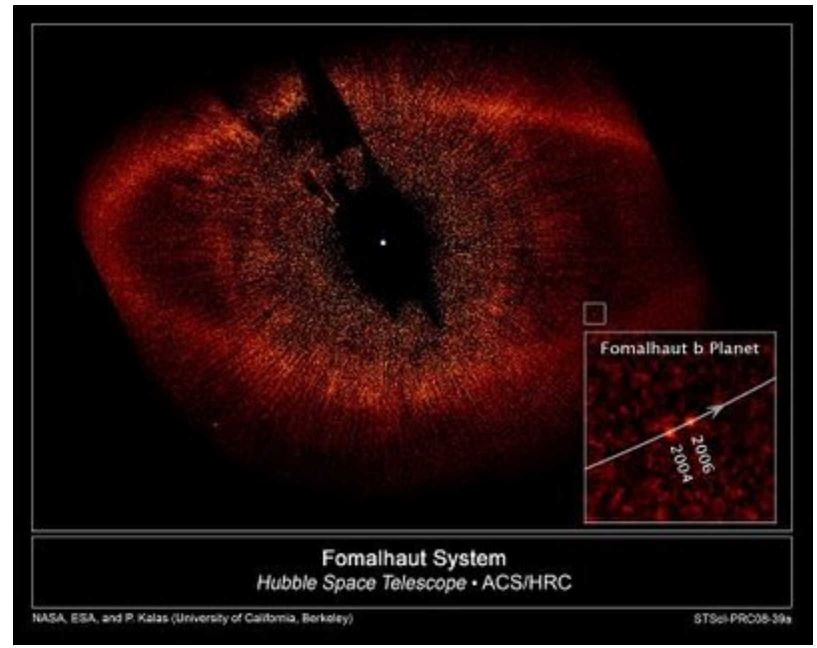

Narrow sharp eccentric ring

Detection of a source quickly heralded as a planet Fomalhaut b

Debris disks are not completely gas-free

Dust

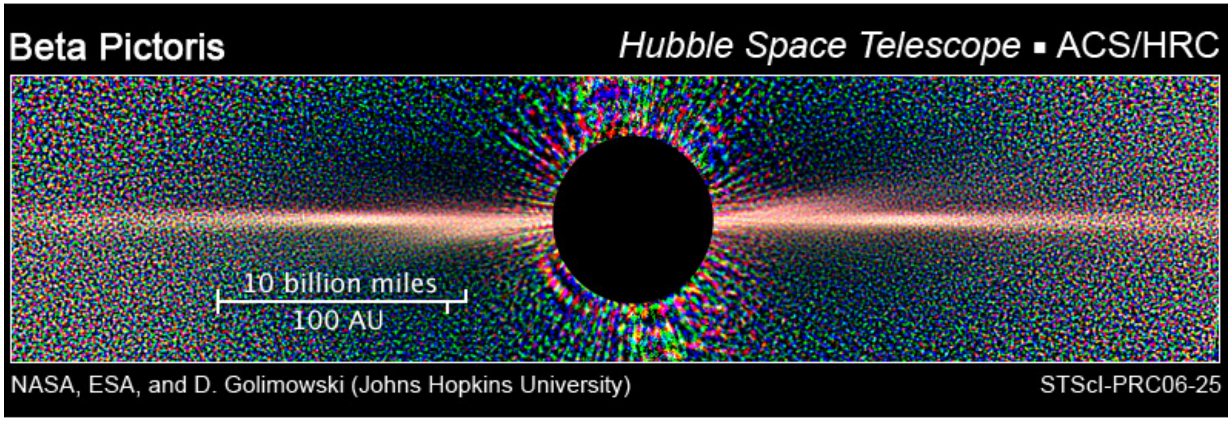

Gas

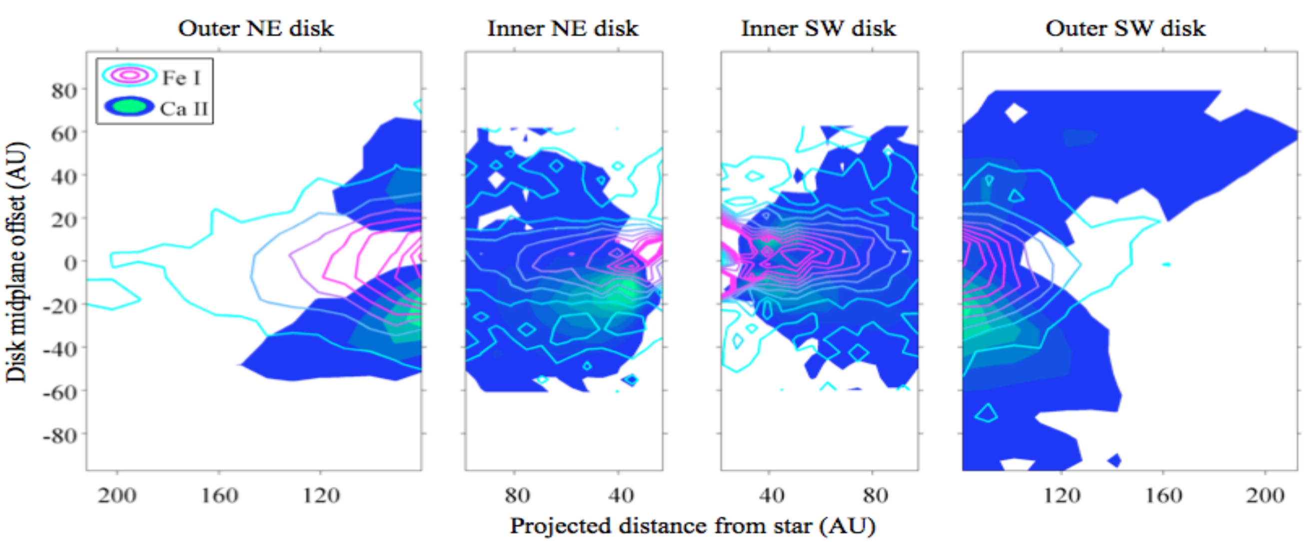

VLT imaging by Nilsson et al. (2012)

Debris disks are

not completely **gas-free**

What is the dynamical effect of this gas?

doi:10.1038/nature12281

Formation of sharp eccentric rings in debris disks with gas but without planets

W. Lyra[1,2,3] & M. Kuchner[4]

'Debris disks' around young stars (analogues of the Kuiper Belt in our Solar System) show a variety of non-trivial structures attributed to planetary perturbations and used to constrain the properties of those planets[1–3]. However, these analyses have largely ignored the fact that some debris disks are found to contain small quantities of gas[4–9], a component that all such disks should contain at some level[10,11]. Several debris disks have been measured with a dust-to-gas ratio of about unity[4–9], at which the effect of hydrodynamics on the structure of the disk cannot be ignored[12,13]. Here we report linear and nonlinear modelling that shows that dust–gas interactions can produce some of the key patterns attributed to planets. We find a robust clumping instability that organizes the dust into narrow, eccentric rings, similar to the Fomalhaut debris disk[14]. The conclusion that such disks might contain planets is not necessarily required to explain these systems.

Disks around young stars seem to pass through an evolutionary phase when the disk is optically thin and the dust-to-gas ratio ε ranges from 0.1 to 10. The nearby stars β Pictoris[5,6,15–17], HD32297 (ref. 7), 49 Ceti (ref. 4) and HD 21997 (ref. 9) all host dust disks resembling ordinary debris disks and also have stable circumstellar gas detected in molecular CO, Na I or other metal lines; the inferred mass of gas ranges from lunar masses to a few Earth masses (Supplementary Information). The gas in

We present simulations of the fully compressible problem, solving for the continuity, Navier–Stokes and energy equations for the gas, and the momentum equation for the dust. Gas and dust interact dynamically through a drag force, and thermally through photoelectric heating. These are parametrized by a dynamical coupling time τ_f and a thermal coupling time τ_T (Supplementary Information). The simulations are performed with the Pencil Code[21–24], which solves the hydrodynamics on a grid. Two numerical models are presented: a three-dimensional box embedded in the disk that co-rotates with the flow at a fixed distance from the star; and a two-dimensional global model of the disk in the inertial frame. In the former the dust is treated as a fluid, with a separate continuity equation. In the latter the dust is represented by discrete particles with position and velocities that are independent of the grid.

We perform a stability analysis of the linearized system of equations that should help interpret the results of the simulations (Supplementary Information). We plot in Fig. 1a–c the three solutions that show linear growth, as functions of ε and $n = kH$, where k is the radial wavenumber and H is the gas scale height ($H = c_s/\sqrt{\gamma}\Omega_K$, where c_s is the sound speed, Ω_K the Keplerian rotation frequency and γ the adiabatic index). The friction time τ_f is assumed to be equal to $1/\Omega_K$. The left and middle panels show the growth and damping rates. The

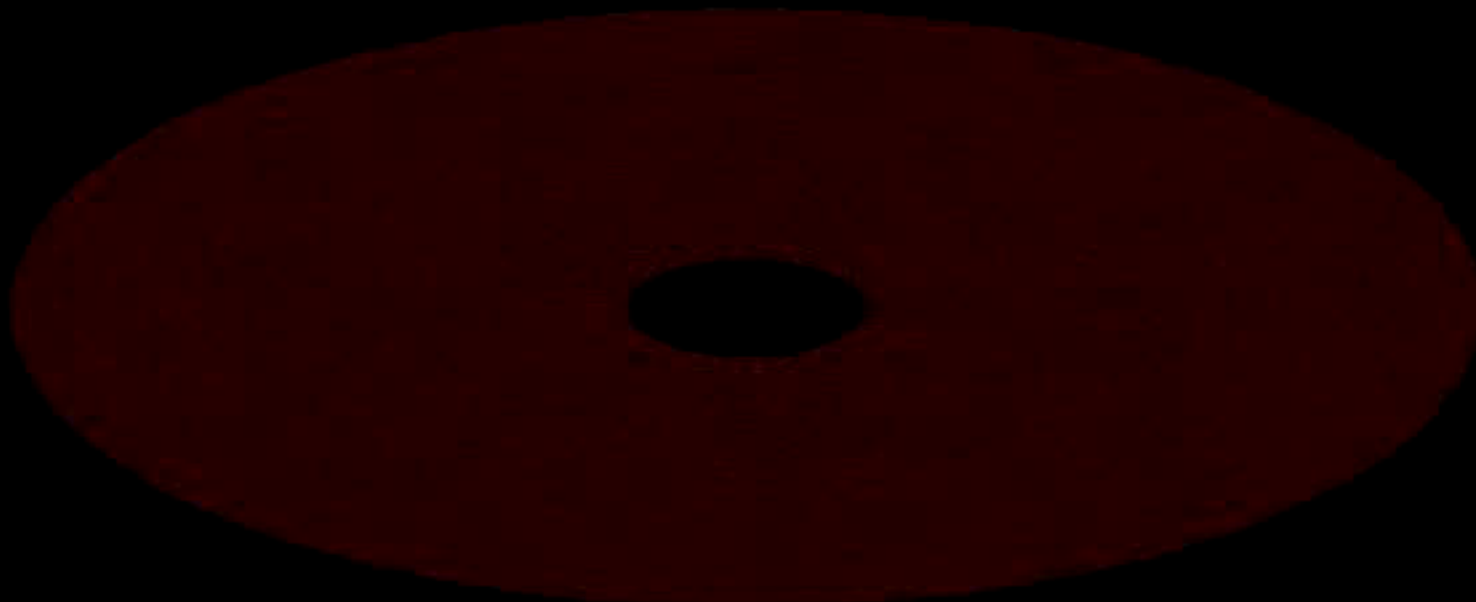

Lyra & Kuchner (2013, Nature, 499, 184)

Particles move toward pressure maxima

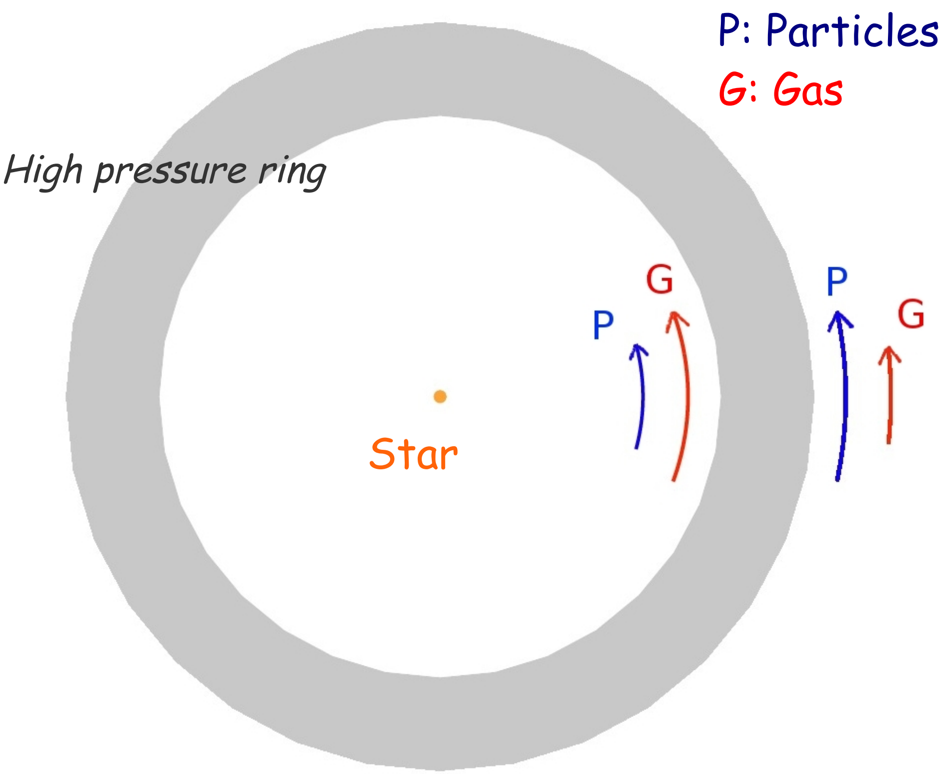

Adapted from Whipple (1972)

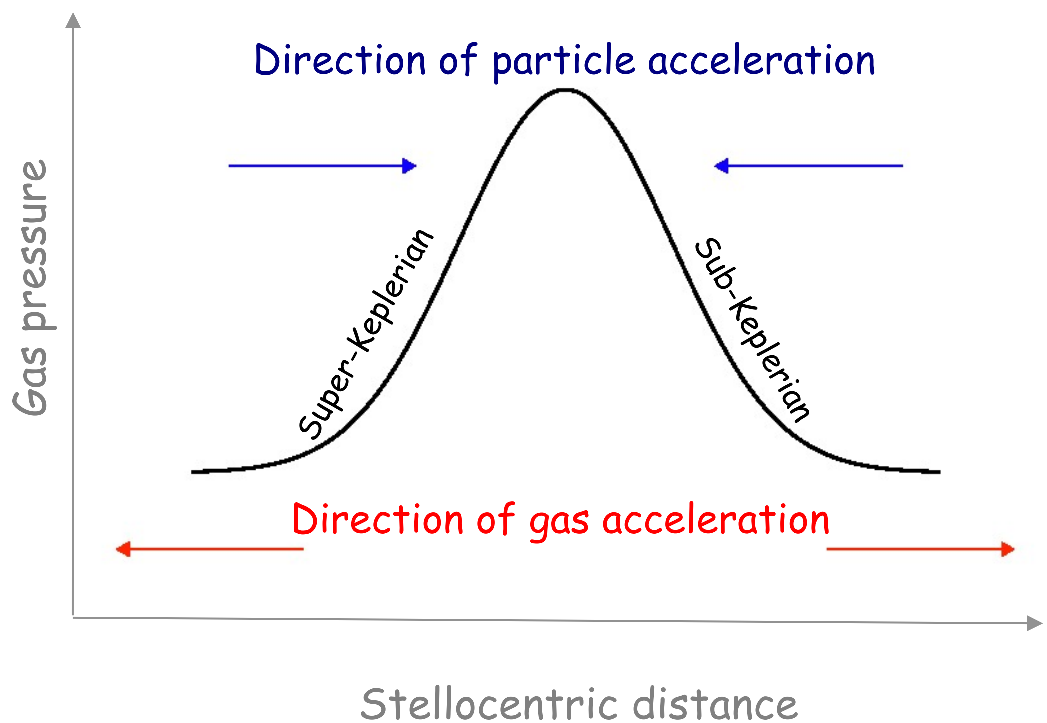

Photoelectric heating

In optically thin debris disks,
the **dust** is the **main heating agent** for the gas.

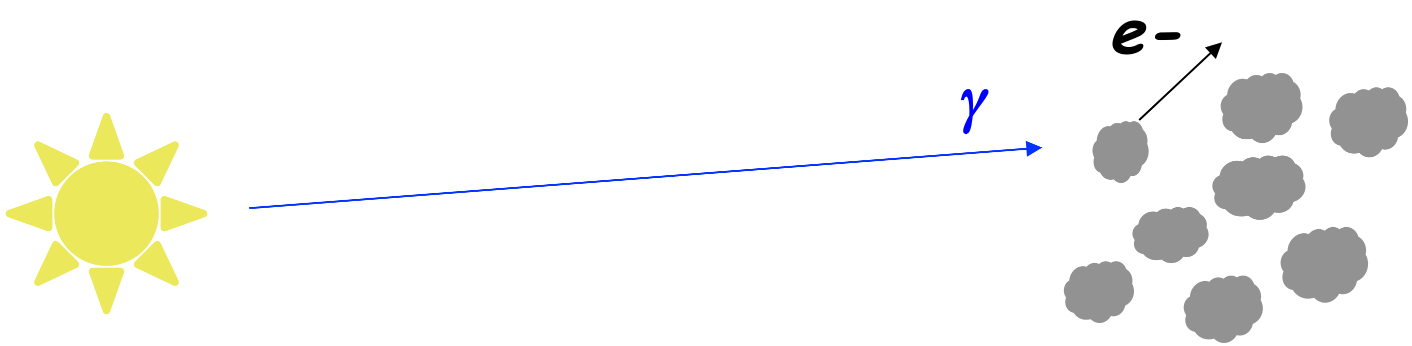

Dust intercepts starlight directly,
emits electron, that heats the gas.

Gas is photoelectrically heated by the dust

Runaway process: instability

Dust heats gas

Heated gas = high pressure region

High pressure concentrates dust

Runaway process: instability

Dust heats gas

Heated gas = high pressure region

High pressure concentrates dust

Linear Analysis

Dust

$$D_w \Sigma_d = -\Sigma_d \nabla \cdot \boldsymbol{w}$$

$$D_w w_x = 2\Omega w_y - \frac{1}{\tau_f}(w_x - u_x)$$

$$D_w w_y = -\frac{1}{2}\Omega w_x - \frac{1}{\tau_f}(v_y - u_y)$$

Gas

$$D_u \Sigma_g = -\Sigma_g \nabla \cdot \boldsymbol{u}$$

$$D_u u_x = 2\Omega u_y - \frac{1}{\Sigma_g}\frac{\partial P}{\partial x} - \frac{\epsilon}{\tau_f}(u_x - w_x)$$

$$D_u u_y = -\frac{1}{2}\Omega u_x - \frac{1}{\Sigma_g}\frac{\partial P}{\partial y} - \frac{\epsilon}{\tau_f}(u_y - w_y)$$

$$\lim_{\tau_T \to 0} P = c_v(\gamma - 1) T_0 \Sigma_g \Sigma_d / \Sigma_0$$

$$\psi = \psi_0 + \psi'$$

$$\psi' = \hat{\psi}\exp(ikx + st)$$

Dispersion relation

$$A\omega^5 + B\omega^4 + C\omega^3 + D\omega^2 + E\omega + F = 0$$

$$\begin{aligned}
A &= 1\\
B &= 2\epsilon + 2\\
C &= \epsilon^2 + \epsilon(n^2+2) + 3\\
D &= \epsilon^2 n^2 + \epsilon(3n^2+2) + 2\\
E &= \epsilon^2(2n^2+1) + \epsilon(3n^2+2) + 2\\
F &= \epsilon^2 n^2 - \epsilon n^2
\end{aligned}$$

$\epsilon = \Sigma_d / \Sigma_g$ $\quad n = kH$ $\quad \omega = s/\Omega$

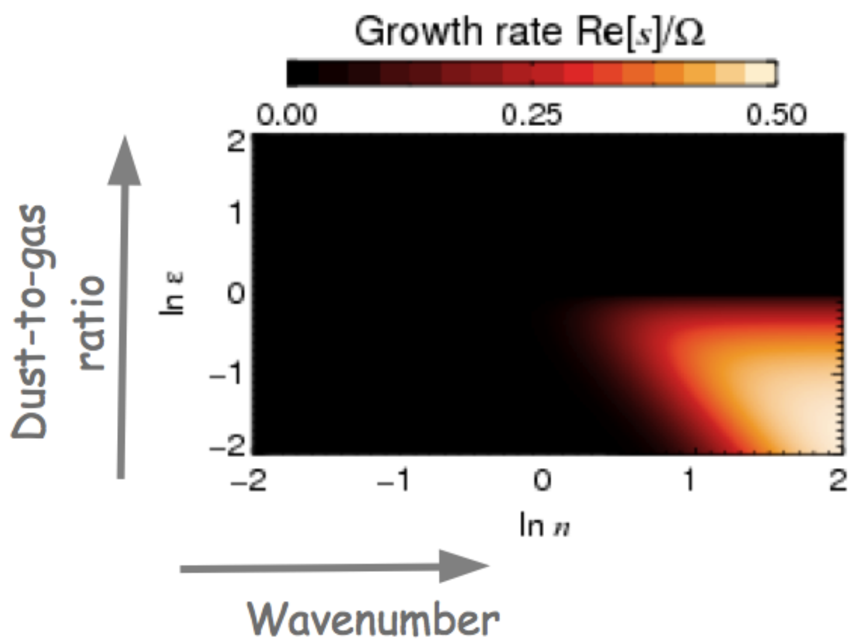

Solutions

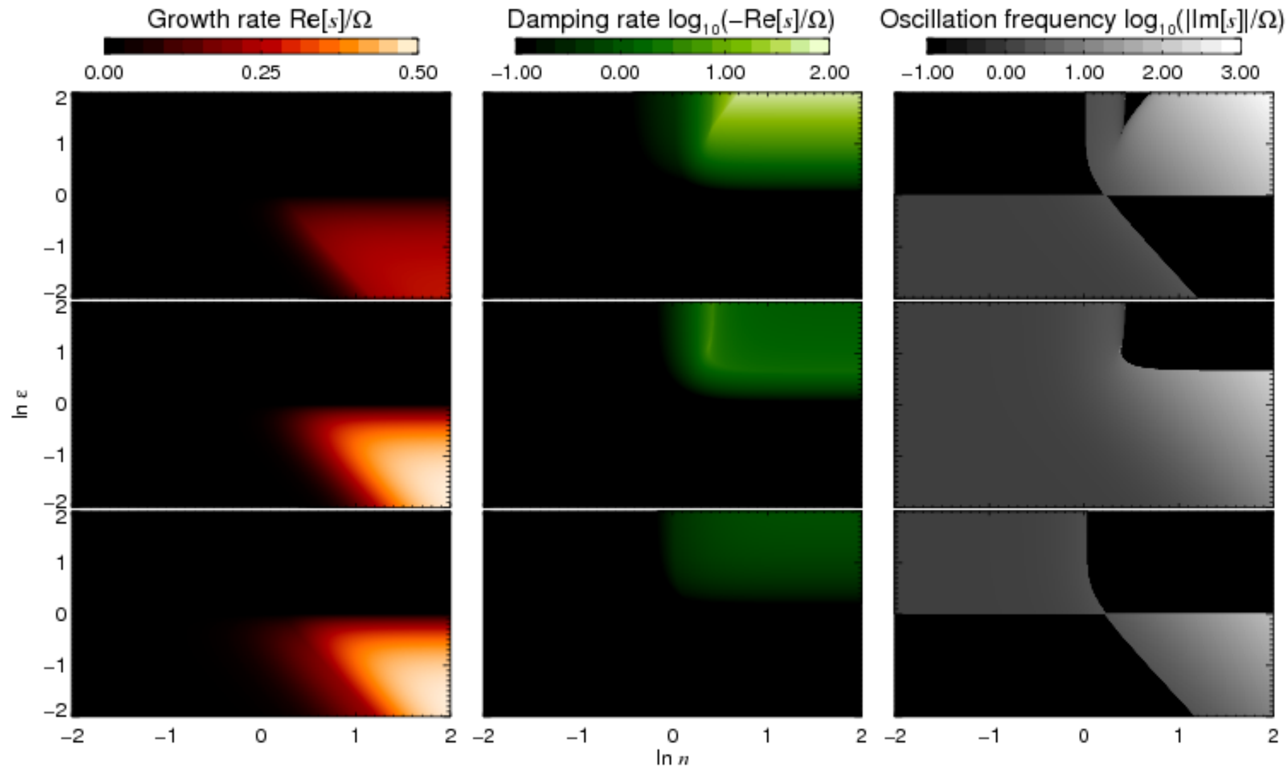

The dispersion relation is a 5[th] order polynomium, so there are five roots!

Dispersion relation

$$A\omega^5 + B\omega^4 + C\omega^3 + D\omega^2 + E\omega + F = 0$$

$$A = 1$$
$$B = 2\epsilon + 2$$
$$C = \epsilon^2 + \epsilon(n^2+2) + 3$$
$$D = \epsilon^2 n^2 + \epsilon(3n^2+2) + 2$$
$$E = \epsilon^2(2n^2+1) + \epsilon(3n^2+2) + 2$$
$$F = \epsilon^2 n^2 - \epsilon n^2$$

$\epsilon = \Sigma_d / \Sigma_g$ $\qquad n = kH$ $\qquad \omega = s/\Omega$

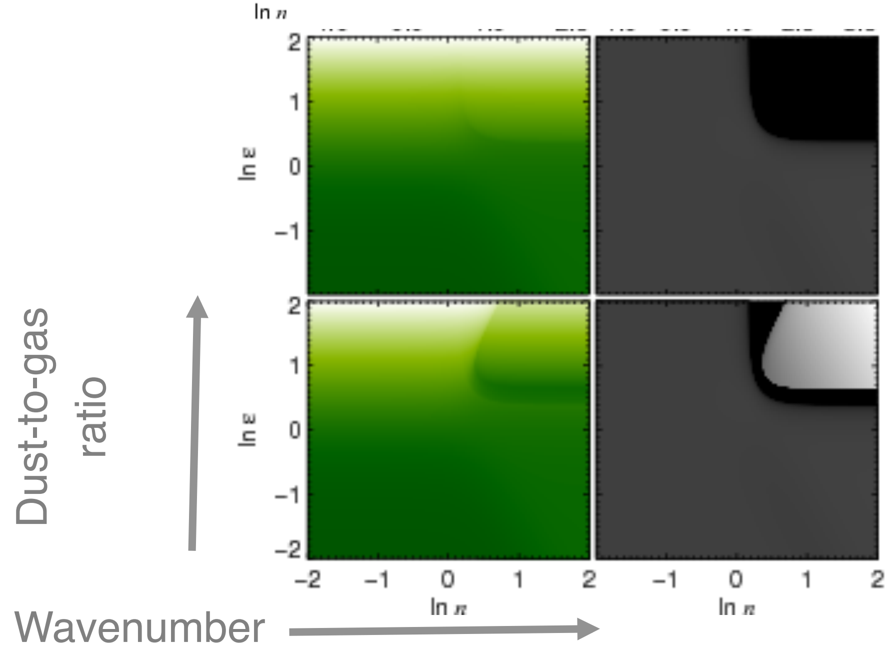

Solutions

Instability

Overstability

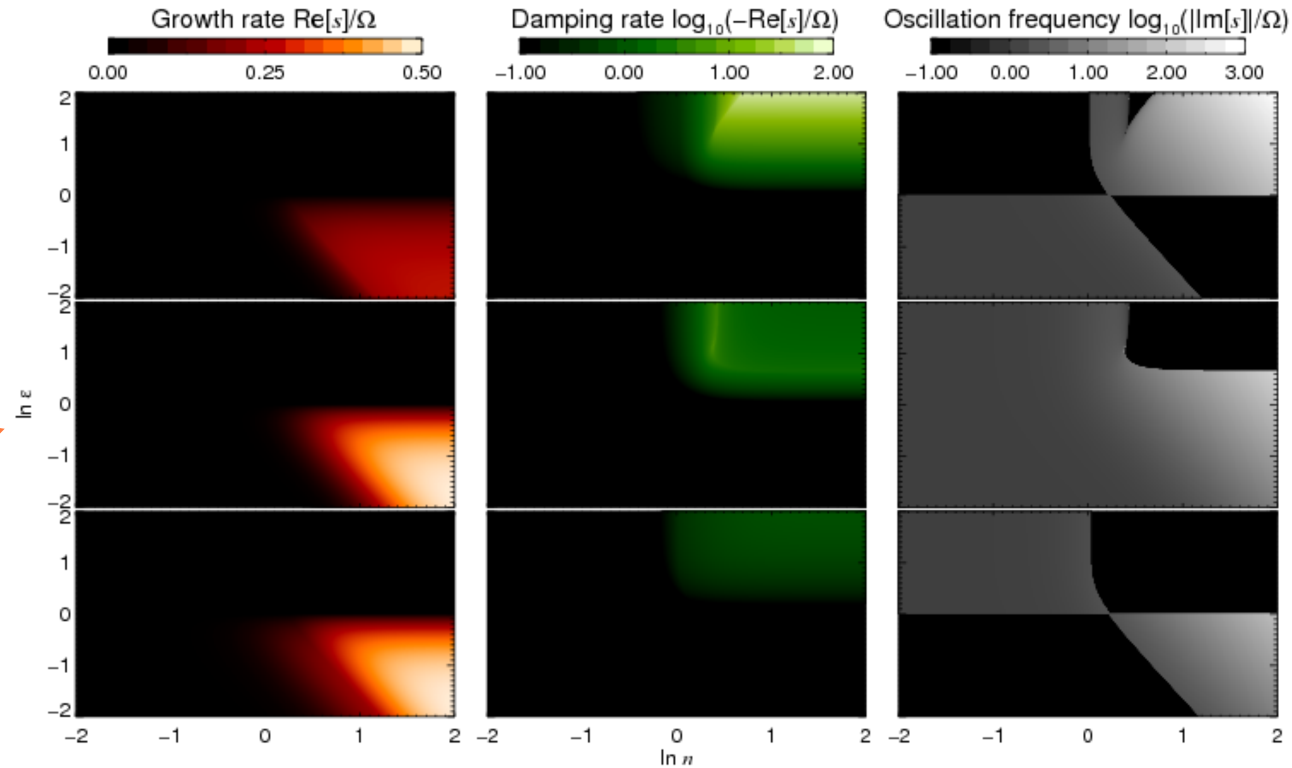

Damped and free Oscillations

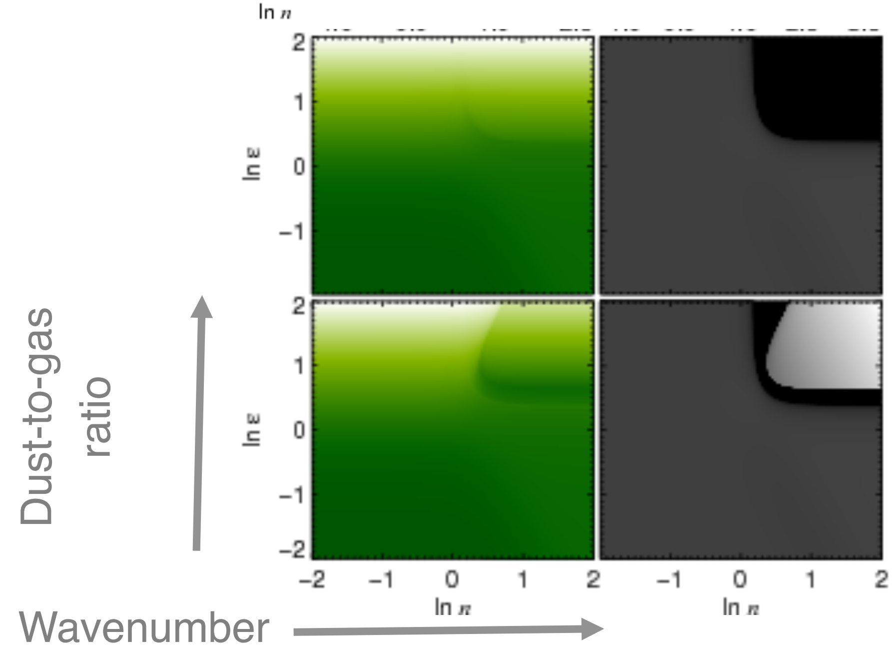

Dispersion relation

$$A\omega^5 + B\omega^4 + C\omega^3 + D\omega^2 + E\omega + F = 0$$

$$
\begin{aligned}
A &= 1 \\
B &= 2\epsilon + 2 \\
C &= \epsilon^2 + \epsilon(n^2+2) + 3 \\
D &= \epsilon^2 n^2 + \epsilon(3n^2+2) + 2 \\
E &= \epsilon^2(2n^2+1) + \epsilon(3n^2+2) + 2 \\
F &= \epsilon^2 n^2 - \epsilon n^2
\end{aligned}
$$

$\epsilon = \Sigma_d / \Sigma_g$ $\quad n = kH \quad$ $\omega = s/\Omega$

Solutions

Instability

Overstability

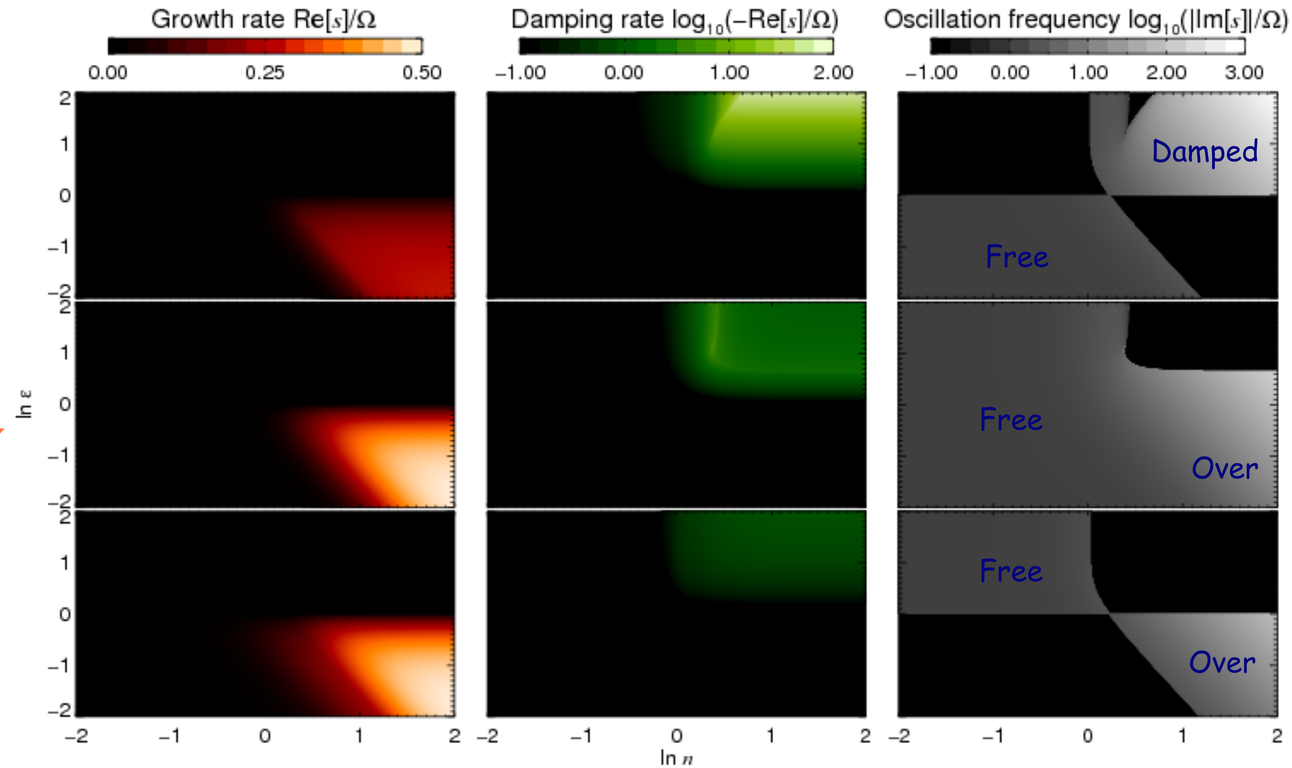

Damped and free Oscillations

Dispersion relation

$$A\omega^5 + B\omega^4 + C\omega^3 + D\omega^2 + E\omega + F = 0$$

$$A = 1$$
$$B = 2\epsilon + 2$$
$$C = \epsilon^2 + \epsilon(n^2 + 2) + 3$$
$$D = \epsilon^2 n^2 + \epsilon(3n^2 + 2) + 2$$
$$E = \epsilon^2(2n^2 + 1) + \epsilon(3n^2 + 2) + 2$$
$$F = \epsilon^2 n^2 - \epsilon n^2$$

$\epsilon = \Sigma_d / \Sigma_g \qquad n = kH \qquad \omega = s/\Omega$

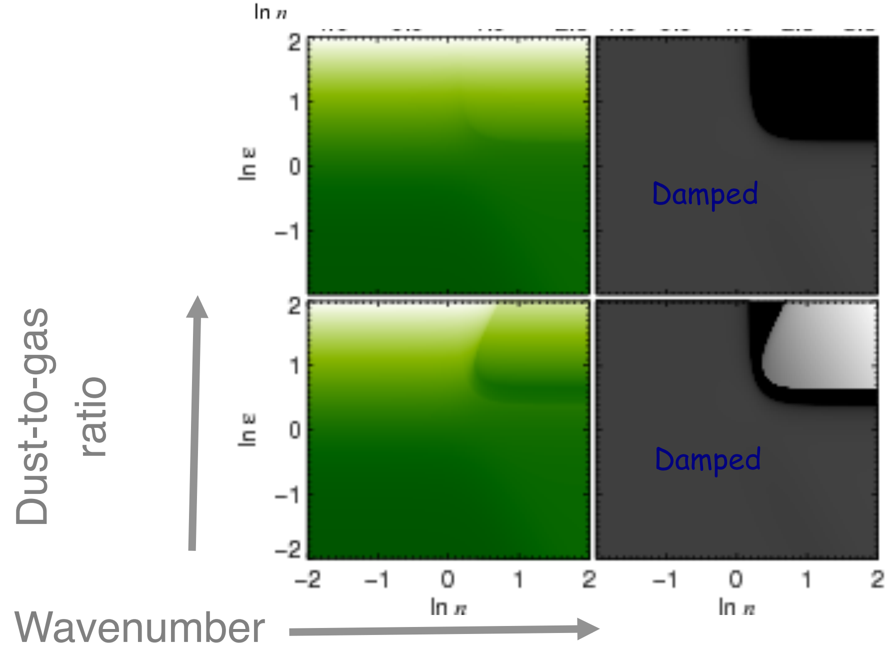

Oscillations

Low Reynolds number *High Reynolds number*

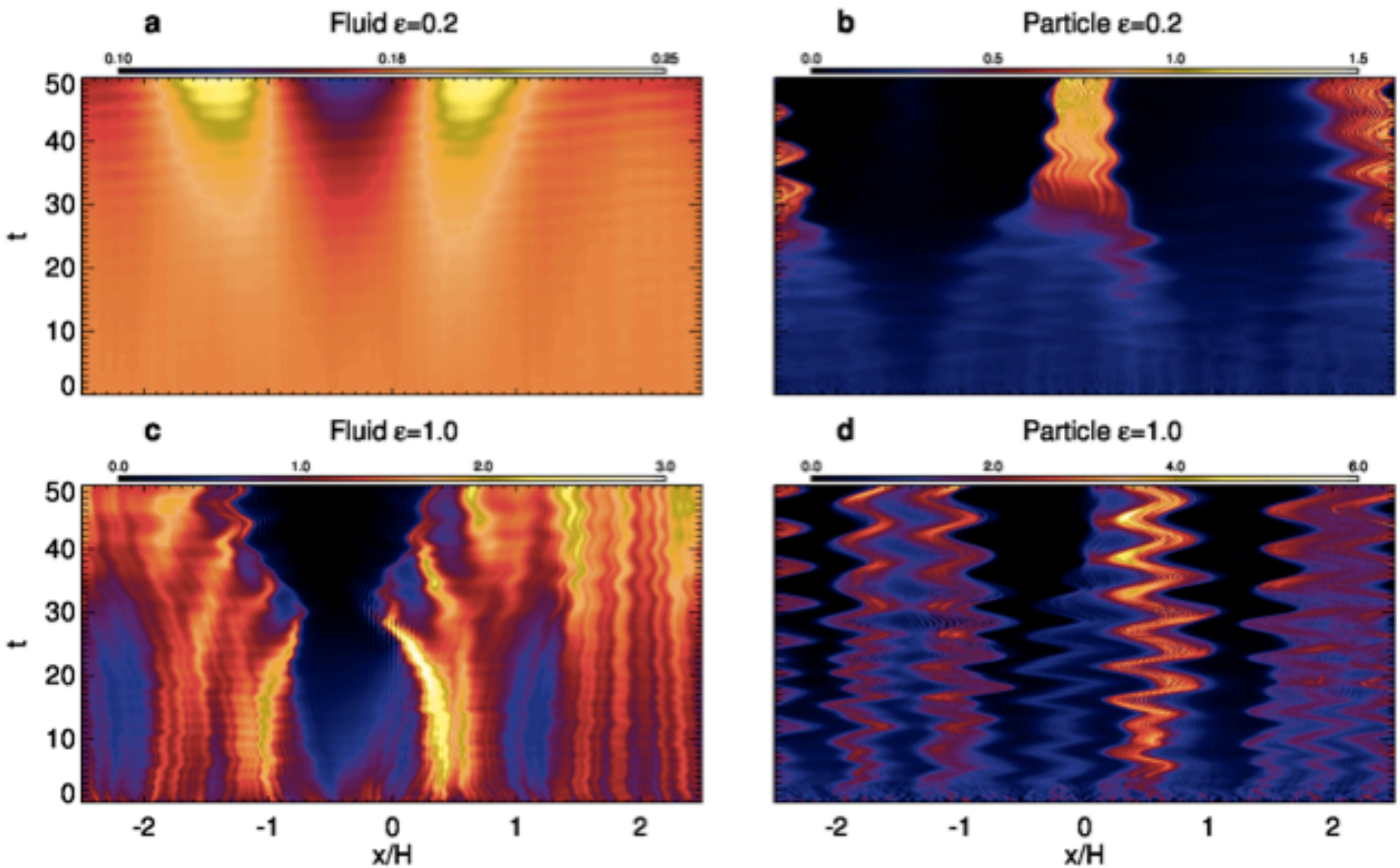

Epicyclic oscillations

clear at high Reynolds numbers!

The model in r-ϕ: Eccentric rings

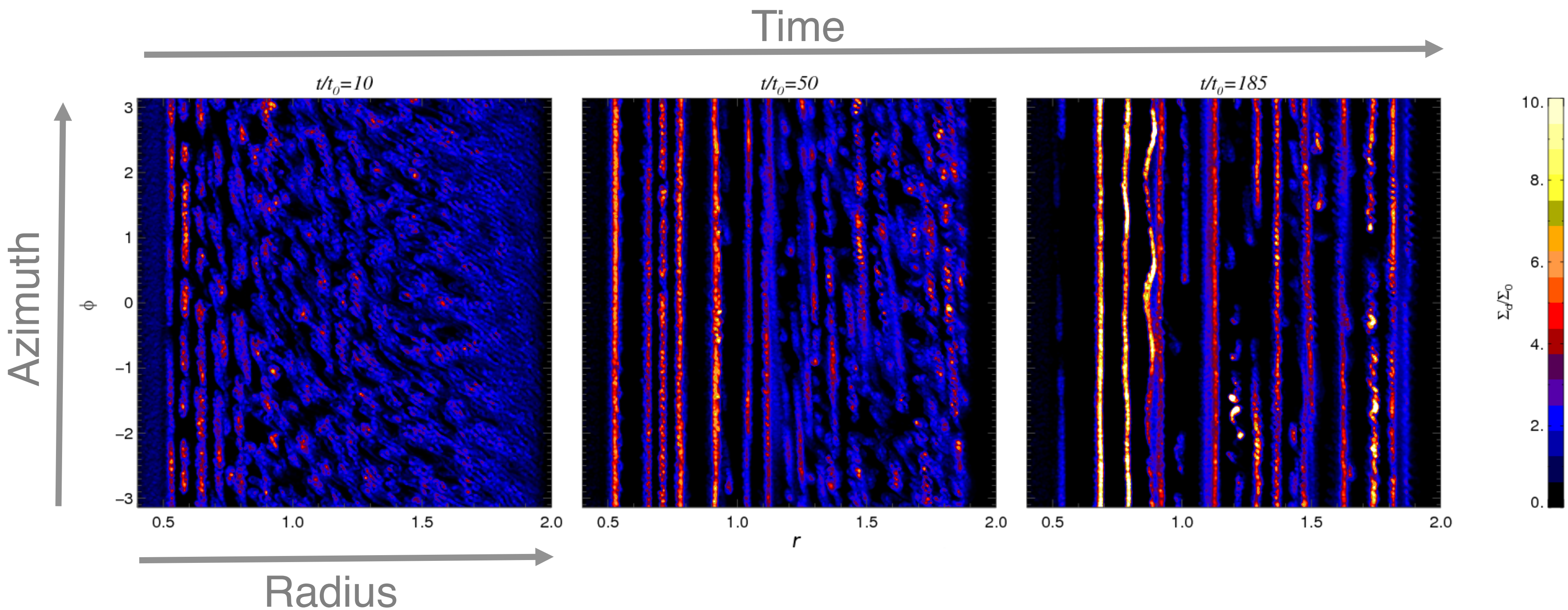

Epicyclic oscillations

make the ring appear ***eccentric !!!***

Ring Offset

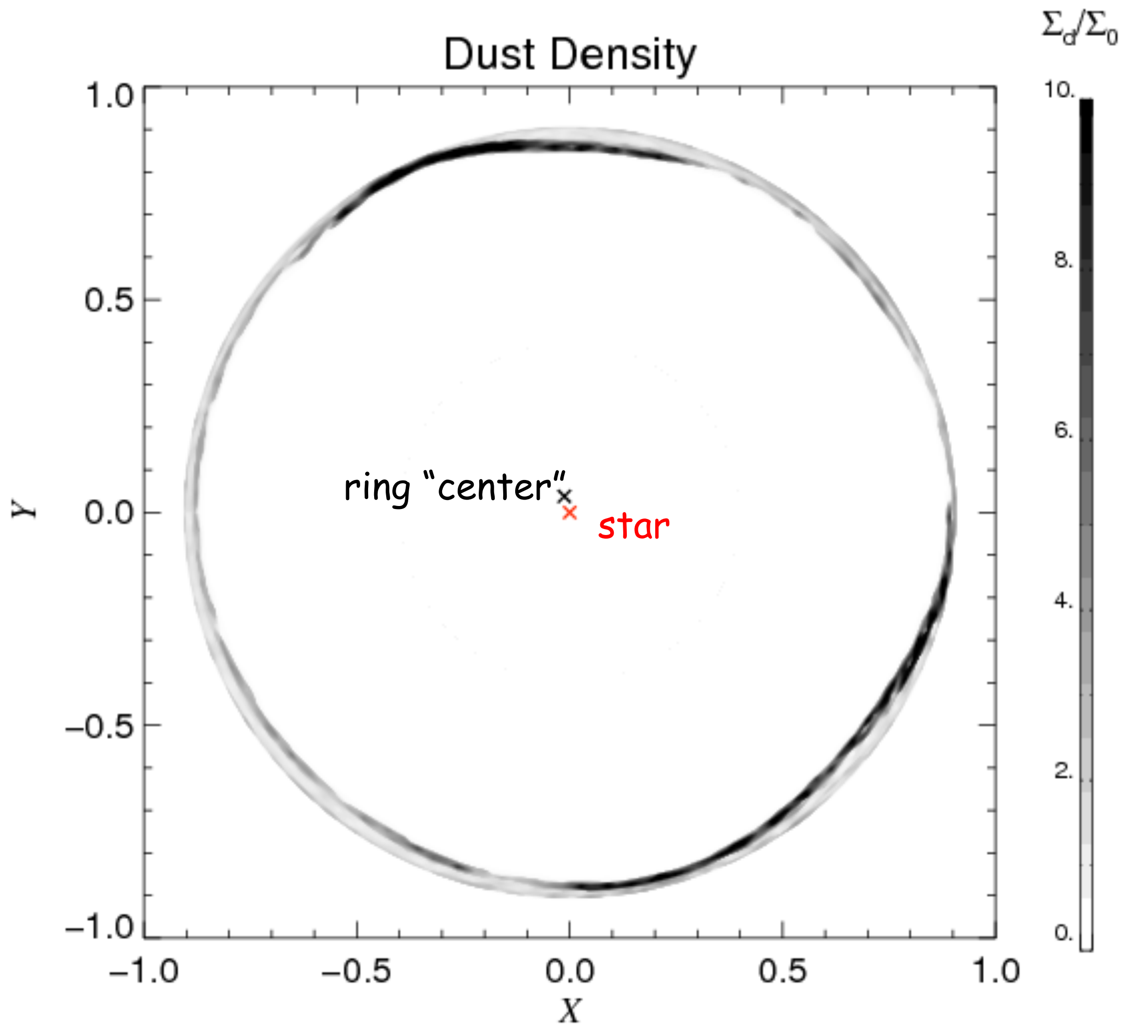

Eccentricity e=0.04

Conclusions

There is a robust ring-forming

photoelectric instability

in optically thin gas-dust disks

Reproduces gross properties of observed systems

(rings, sharp edges, eccentricity)

Maximum for gas-to-dust ratio ~ 5

(probably more applicable to transitional disks
and gas-rich debris disks such as 49 Ceti)

Future work:

3D turbulence, Radiation forces, Collisions….

…. (suggestions?)

Europa

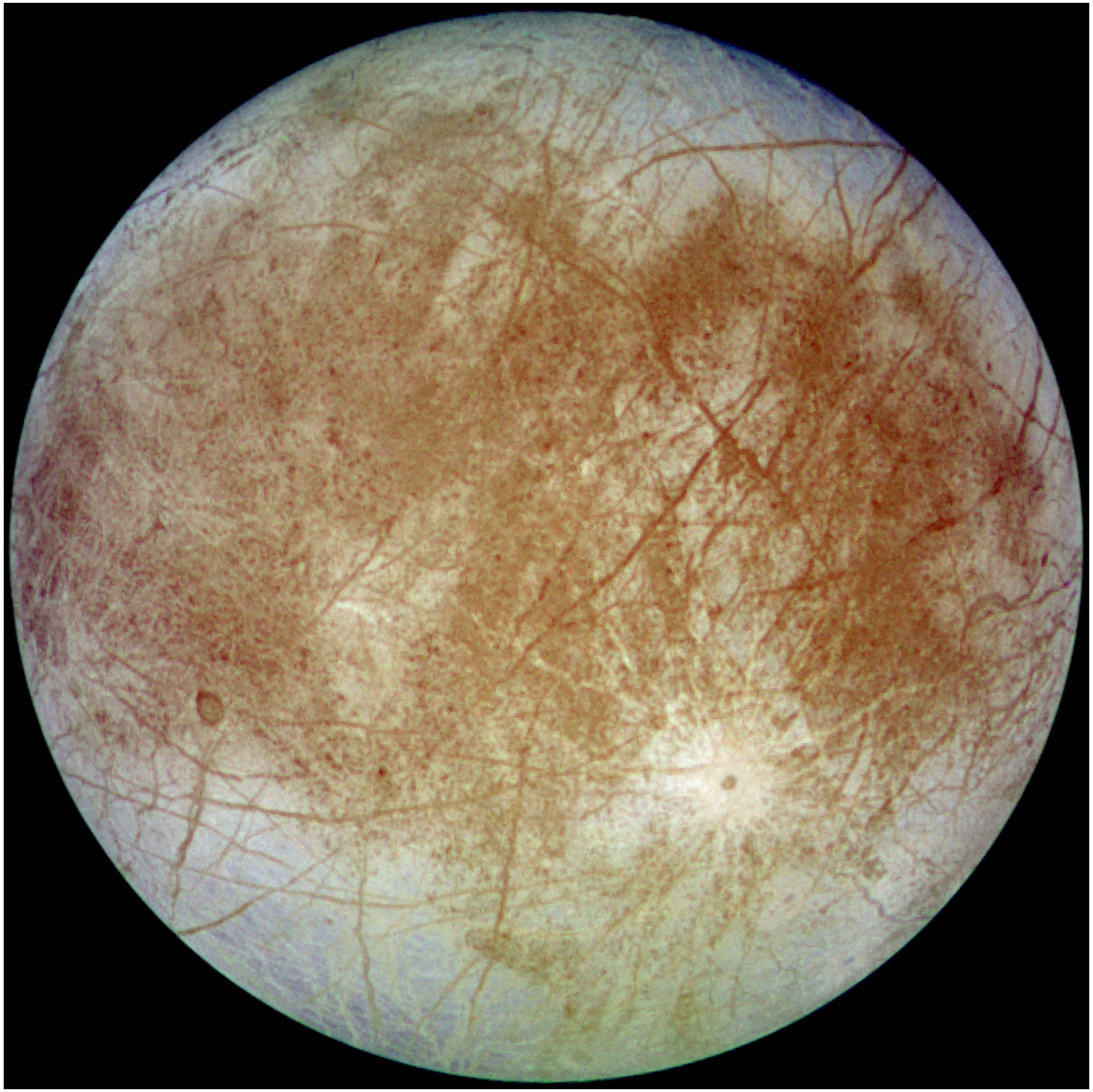

Europa: ocean-bearing moon

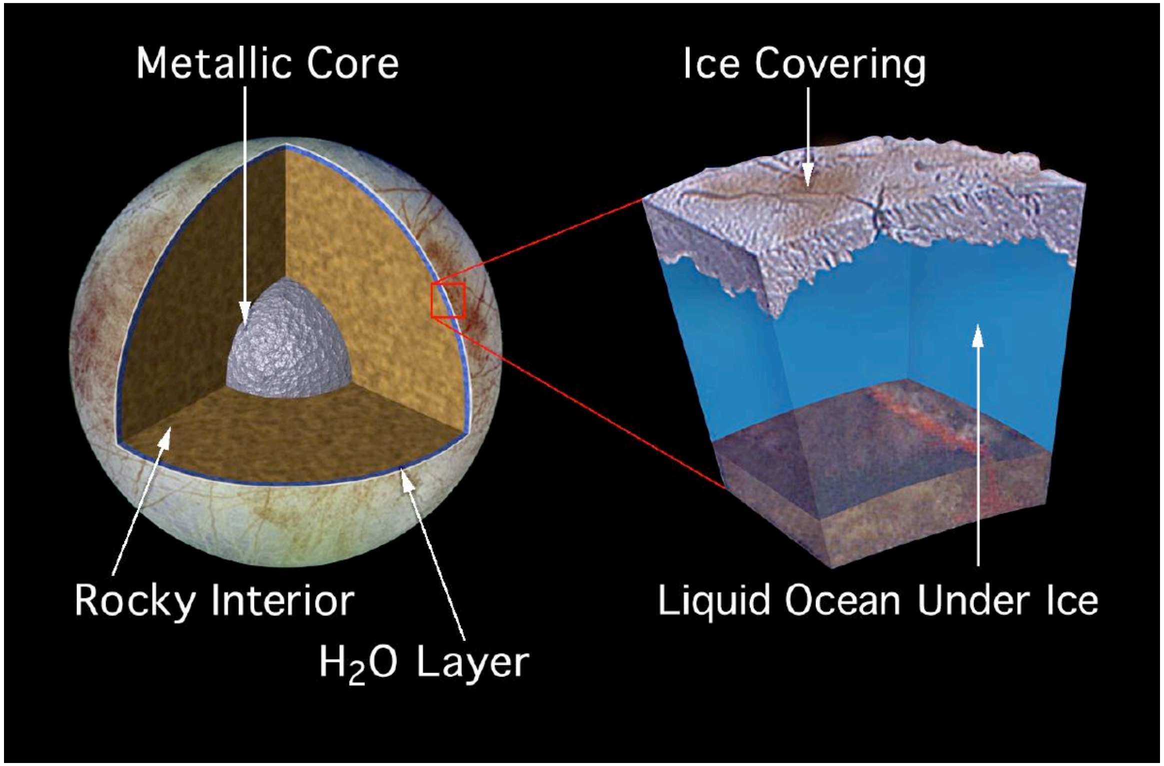

Induced magnetic field

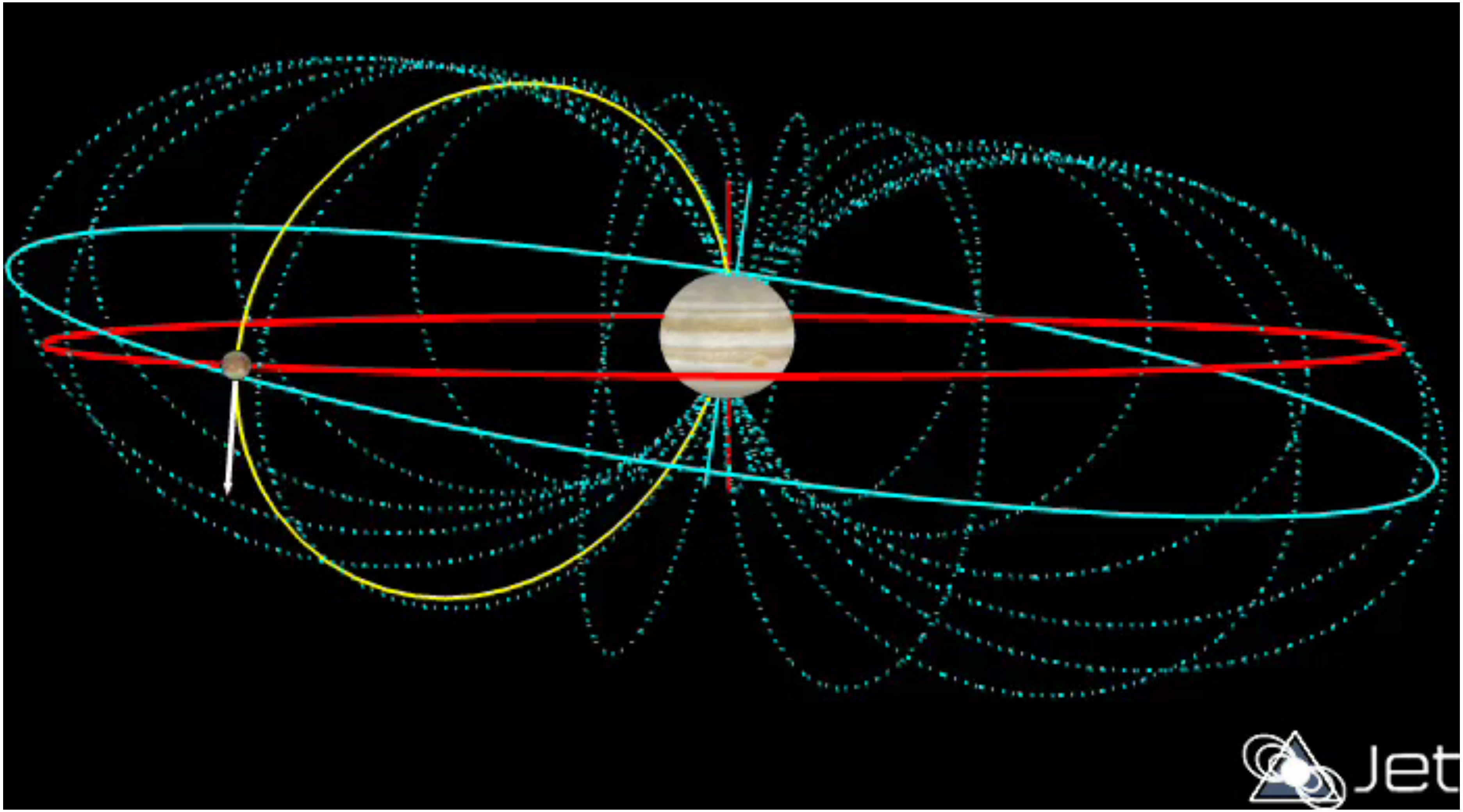

Europa Clipper

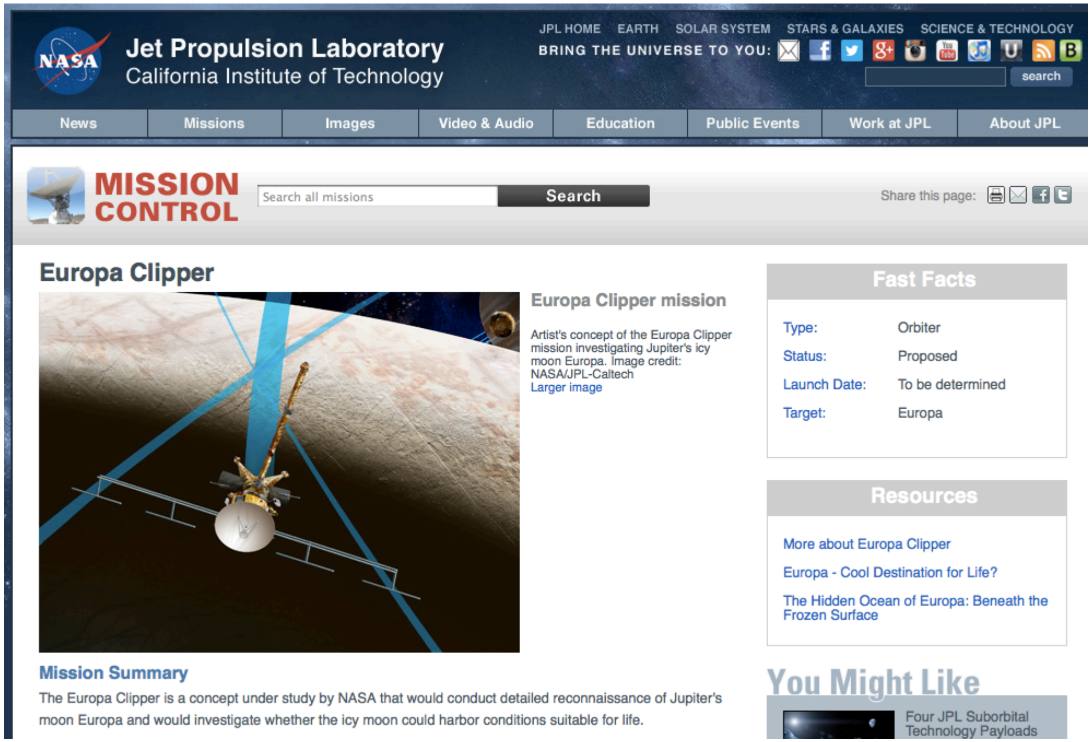

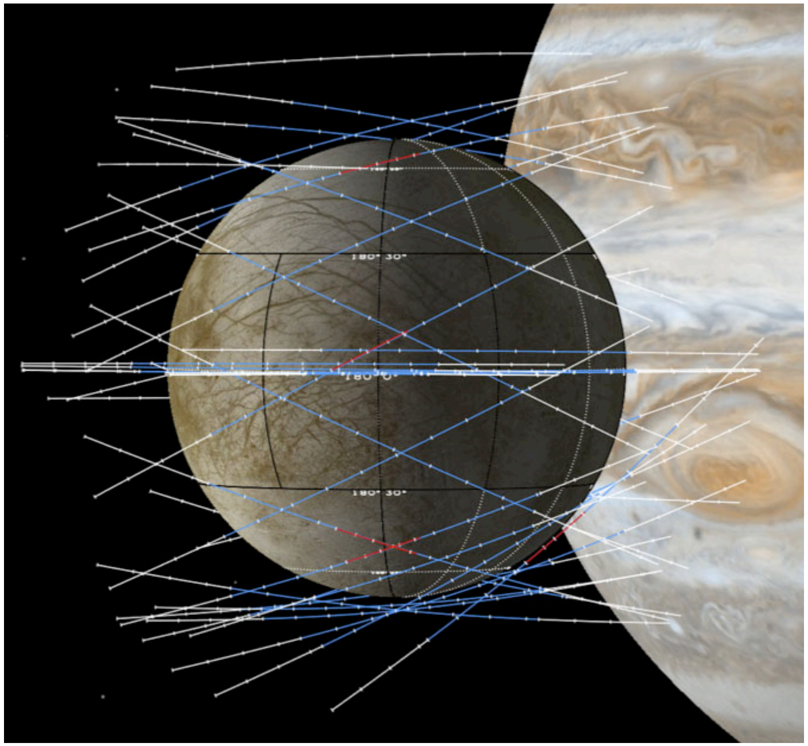

Reconnaissance: 45 flybys, as low as 25km

Radar to determine ice's thickness

High resolution camera

Identify future landing sites

Ice Convection: Statement of the Problem

Dynamical equations

$$\frac{\partial}{\partial x_j}\sigma_{\mathbf{ij}} - \nabla p + (RaT)\mathbf{z} = 0,$$

$$\frac{\partial T}{\partial t} + \mathbf{u}\cdot\nabla T = \nabla^2 T + q',$$

$$\nabla \cdot \mathbf{u} = 0.$$

Ice Rheology

$$\dot{\varepsilon}_{ij} = \tfrac{1}{2}\left(\frac{\partial u_i}{\partial x_j} + \frac{\partial u_j}{\partial x_i}\right).$$

$$\dot{\varepsilon}_{ij} = A^{-1}\sigma^{n-1}\sigma_{ij} \quad \text{or} \quad \sigma_{ij} = A^{1/n}\dot{\varepsilon}^{(1-n)/n}\dot{\varepsilon}_{ij},$$

$$\eta = \frac{\sigma_{ij}}{2\dot{\varepsilon}_{ij}} = \tfrac{1}{2}\sigma^{1-n} = \tfrac{1}{2}\dot{\varepsilon}^{(1-n)/n}.$$

Parameters

$$Ra = \frac{\rho g \alpha \Delta T d^3}{\kappa \eta_0},$$ *Rayleigh number*

$$q = \frac{\epsilon_0^2 \omega^2 \eta}{2\left[1 + \frac{\omega^2 \eta^2}{\mu^2}\right]}.$$ *Tidal heating*

State of the art

3. Coupled thermal convection with tidal dissipation

Next, we perform fully coupled numerical simulations of thermal convection and tidal heating that we self-consistently calculate from the time-evolving temperature structure. We again adopt 2D cartesian (rectangular) geometry, with the dimensions in this case representing horizontal position *x* and height *z*. Cartesian geometry is appropriate for regional studies of Europa's ice shell because Europa's ice-shell thickness is much smaller than its radius. We neglect inertia and adopt the Boussinesq approximation. We use the finite-element code ConMan (King et al., 1990) to solve the dimensionless equations of momentum, continuity, and energy, respectively given by

$$\frac{\partial \sigma_{ij}}{\partial x_j} + Ra\,\theta k_i = 0 \quad (3)$$

$$\frac{\partial u_i}{\partial x_i} = 0 \quad (4)$$

$$\frac{\partial \theta}{\partial t} + u_i \frac{\partial \theta}{\partial x_i} = \frac{\partial^2 \theta}{\partial x_i^2} + q' \quad (5)$$

Icarus 207 (2010) 834–844

Contents lists available at ScienceDirect

Icarus

journal homepage: www.elsevier.com/locate/icarus

Coupled convection and tidal dissipation in Europa's ice shell

Lijie Han [a,*], Adam P. Showman [b]

[a] Planetary Science Institute, 1700 E. Fort Lowell, Suite 106, Tucson, AZ 85719, USA
[b] Department of Planetary Sciences, Lunar and Planetary Laboratory, University of Arizona, Tucson, AZ 85721, USA

ARTICLE INFO

Article history:
Received 13 May 2009
Revised 29 October 2009
Accepted 22 December 2009
Available online 6 January 2010

ABSTRACT

We performed 2D numerical simulations of oscillatory tidal flexing to study the interrelationship between tidal dissipation (calculated using the Maxwell model) and a heterogeneous temperature structure in Europa's ice shell. Our 2D simulations show that, if the temperature is spatially uniform, the tidal dissipation rate peaks when the Maxwell time is close to the tidal period, consistent with previous stud-

Han and Showman (2010)

2D, Resolution 100x100

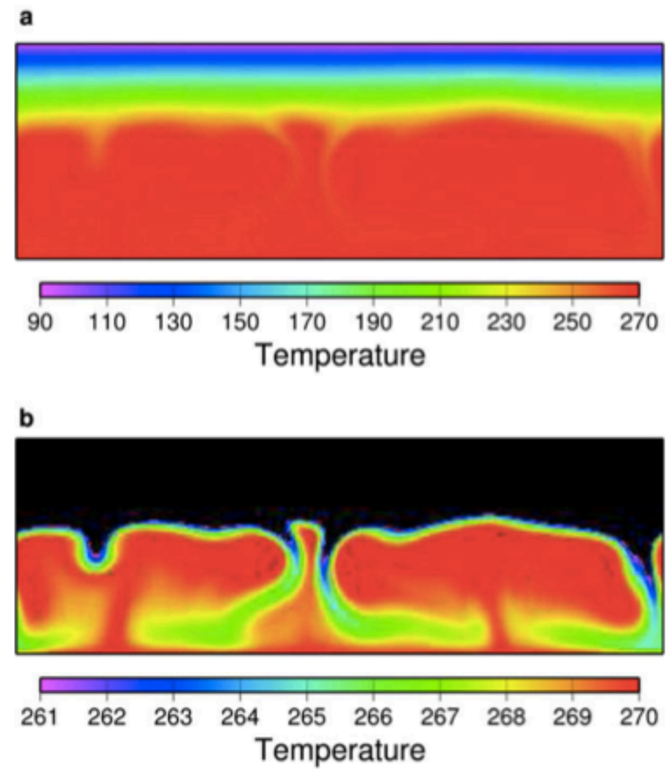

Fig. 5. Temperature distribution from a fully coupled ConMan/Tekton model of thermal convection and oscillatory tidal flexing. The model implements a domain-averaged tidal-flexing amplitude of 1.25×10^{-5} and tidal period of 3.5 days. The thickness of the ice shell is 15 km, and the Rayleigh number is 1.81×10^7. Top: temperature range of 90–270 K. Bottom: temperature range of 260–270 K.

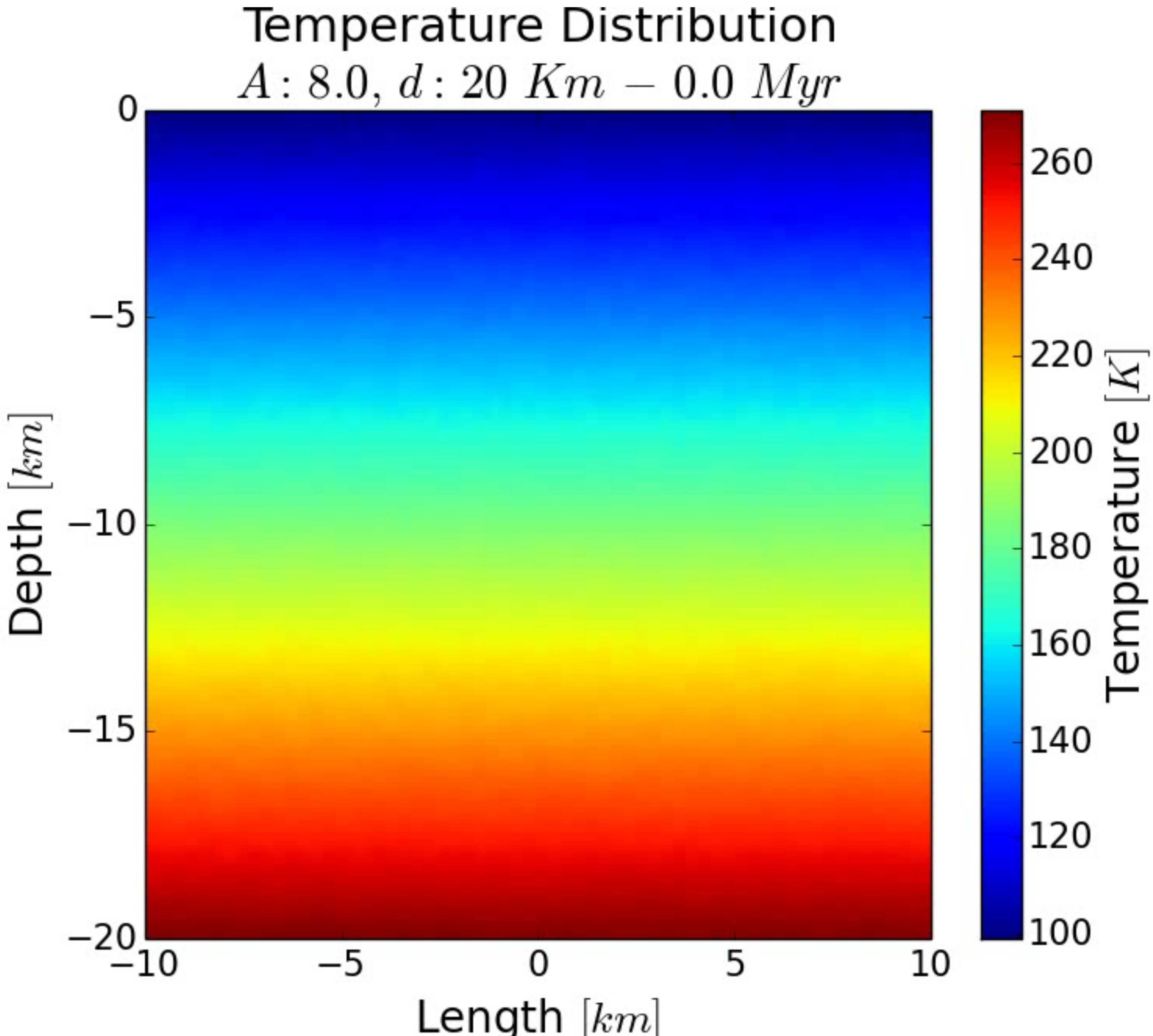

Temperature Distribution
$A: 8.0,\ d: 20\ Km - 0.0\ Myr$
Depth $[km]$
Length $[km]$
Temperature $[K]$
0
−5
−10
−15
−20
−10
−5
0
5
10
260
240
220
200
180
160
140
120
100

Temperature structure and terrain morphology

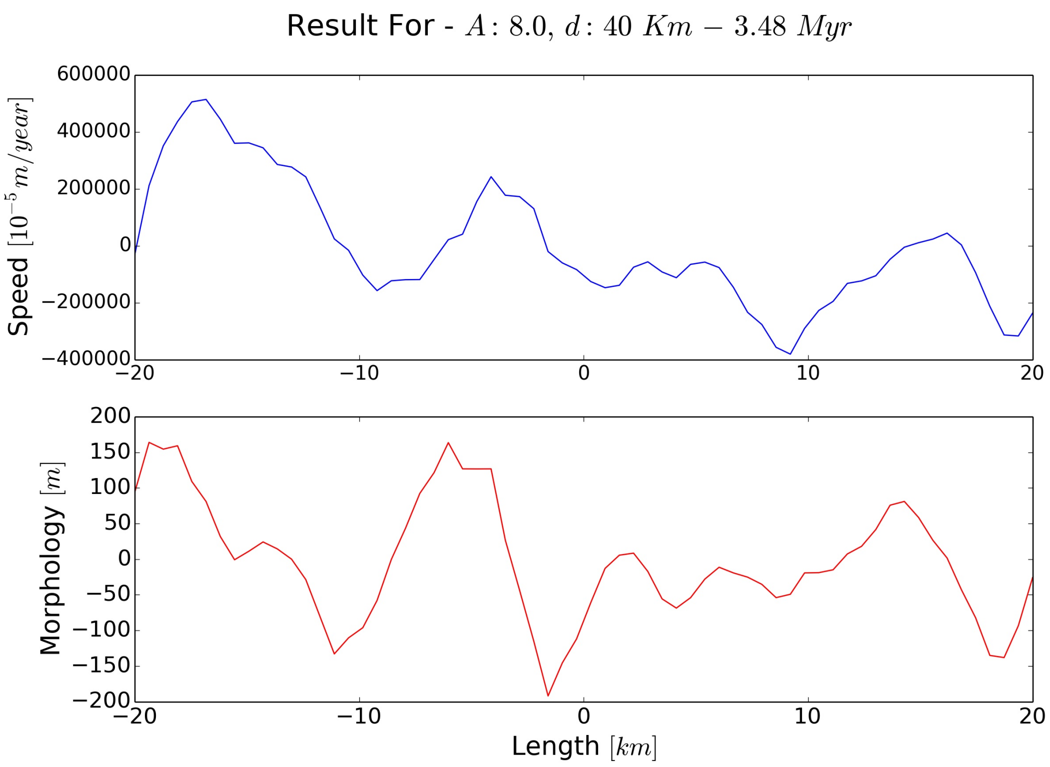

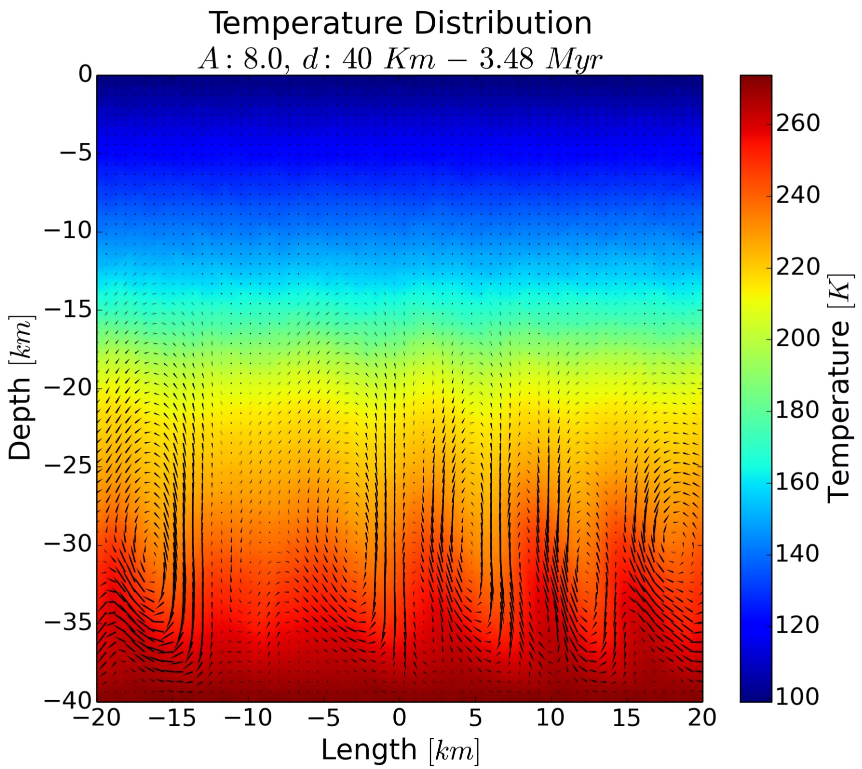

To be done:

- Consider more realistic equation of state for the ice.
- Include melting/freezing and different grain size.
- Code 3D model.